

REFLECTION AND REFRACTION OF ACOUSTIC
WAVES AT A PLANE INTERFACE

By

HAMZAH ABDULGADER ALMOGHRABI

Bachelor of Science

University of Petroleum and Minerals

Dehran, Saudi Arabia

1977

Submitted to the Faculty of the Graduate College
of the Oklahoma State University
in partial fulfillment of the requirements
for the Degree of
MASTER OF SCIENCE
July, 1983

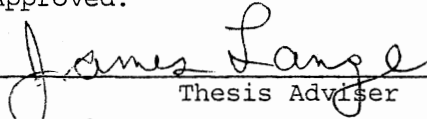


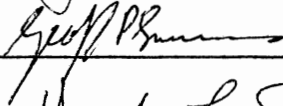
بِسْمِ اللَّهِ الرَّحْمَنِ الرَّحِيمِ

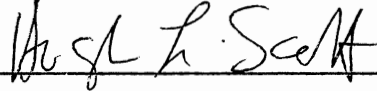
In the name of Allah, the Most Gracious, the Most Merciful

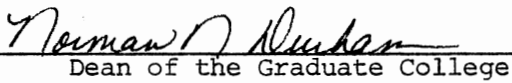
REFLECTION AND REFRACTION OF ACOUSTIC
WAVES AT A PLANE INTERFACE

Thesis Approved:


Thesis Adviser






Dean of the Graduate College

ACKNOWLEDGMENTS

The author wishes to express sincere appreciation to his major advisor, Dr. James N. Lange, for his interest, assistance and guidance throughout the course of this work.

Additional thanks is extended to Dr. Earl Lafon, Department of Physics, for his assistance in computer work. Also gratitude is extended to Dr. G. P. Summers and Dr. Larry Scott for serving on my Master's Committee. A note of thanks is given to Mrs. Janet Sallee for her excellent typing of the manuscript.

Finally, special appreciation is expressed to my parents, my wife Nahera, my two daughters Ibtehel and Shima, and my son Moath, for their sacrifices and patience.

TABLE OF CONTENTS

Chapter	Page
I. INTRODUCTION.	1
Statement of the Problem	3
Importance of the Study.	3
Procedure of the Study	4
Limitation of the Study.	6
Review of Related Literature	7
II. THEORY OF ELASTICITY.	10
Stress	10
Strain	11
Hooke's Law.	16
Wave Equation.	17
Bounded Medium and Boundary Conditions	23
General Solution for the Reflection and Refraction of Plane Waves at an Interface	24
Boundary Conditions.	33
Continuity of Tangential Displacement u	33
Continuity of Vertical Displacement w	34
Continuity of Tangential Stress	34
Continuity of Normal Stress at z	35
Partitioning of Energy.	38
III. MODE CONVERSION DUE TO AN INCIDENT 'P-WAVE' AT A PLANE INTERFACE	44
Solid/Vacuum Interface	45
Reflected "P-Wave" Vanishes.	50
Liquid/Liquid Interface.	50
Boundary Conditions	50
Liquid/Solid Interface.	55
Solid/Liquid Interface.	65
Solid/Solid Interface	68
IV. TOTAL REFLECTION.	74
V. DIRECTIVITY OF REFLECTED AND TRANSMITTED WAVES.	95
General Comments on the Directivity of Reflected and Transmitted Waves.	105
VI. SEISMIC DATA GATHERING METHOD AND CDP ANALYSIS.	133

Chapter	Page
The Normal Moveout Correction.	136
Cancellation of Multiple Reflections by CDP Process-	
ing.	140
Acoustic Impedance and CDP Gathers	147
VII. SUMMARY AND CONCLUSIONS	160
Suggestions for Further Study.	162
A SELECTED BIBLIOGRAPHY	164
APPENDIX A - ORTHOGONAL EXPANSION	166
APPENDIX B - LEGENDRE POLYNOMIALS	169
APPENDIX C - ASSOCIATED LEGENDRE FUNCTIONS.	170
APPENDIX D - SYMBOLS.	172

TABLE

Table	Page
I. Elastic Properties of Rocks and Fluids.	96

LIST OF FIGURES

Figure	Page
1. Components of Stress on a Small Rectangular Parallelepiped.	12
2. Strain Analysis in Two Dimensions	13
3. Reflection and Refraction of Incident P-Wave at an Interface of Two Elastic Solids.	25
4. Phase Velocity Along the Interface of Mode Converted Waves.	31
5. Reflection of Incident P-Wave at Free Surface of Elastic Solid	46
6. Reflection and Refraction of Incident P-Wave at Liquid/Liquid Interface.	51
7. Reflection and Refraction of Incident P-Wave at Liquid/Solid Interface	56
8. Reflection and Refraction of Incident P-Wave at Solid/Liquid Interface.	66
9. Reflected, Transmitted, and Mode Converted Waves Due to an Incident P-Wave at Solid/Solid Interface.	69
10. Phase Velocity of the Transmitted P-Wave for Incident P-Wave With a Lower Velocity ($\alpha < \alpha'$)	75
11. Critical Reflections for an Incident P-Wave at Solid/Solid Interface	77
12. Critical Reflections for an Incident S-Wave at Solid/Solid Interface	79
13. Phase Velocity of the P-Wave for an Incident S-Wave	83
14. P-Wave Skin Depth Dependence on the Incident Angle of S-Wave at Free Solid Interface.	85
15. Transmitted P-Wave Due to an Incident P-Wave at Liquid/Liquid Interface Beyond the Critical Angle.	87
16. Phase Velocity of the Transmitted S-Wave for an Incident P-Wave With $\alpha < \beta'$	90

Figure	Page
17. Reflection and Refraction of Incident P-Wave at Solid/ Liquid Interface Beyond the Critical Angle $\theta_p^{(cp)}$	91
18. Phase Angle of Reflected P-Wave for an Incident P-Wave on Sandstone/Limestone Interface	93
19. Phase Angle of Reflected S-Wave for an Incident P-Wave on Sandstone/Limestone Interface	94
20. Polar Directivity of Reflected P- and S-Waves for an Inci- dent P-Wave on (A) Sandstone/Vacuum Interface and (B) Liquid/Vacuum Interface	107
21. Polar Directivity of Reflected and Transmitted P-Wave for an Incident P-Wave on (A) Air/Sandstone Interface and (B) Sandstone/Air Interface	108
22. Polar Directivity of Reflected and Transmitted S-Wave for an Incident P-Wave on (A) Air-Sandstone Interface and (B) Sandstone/Air Interface	109
23. Polar Directivity of Reflected and Transmitted P-Wave for an Incident P-Wave on (A) Water/Air Interface and (B) Air-Water Interface	110
24. Polar Directivity of Reflected and Transmitted P-Wave for an Incident P-Wave on (A) Water/Oil Interface and (B) Oil-Water Interface	111
25. Polar Directivity of Reflected and Transmitted P-Wave for an Incident P-Wave on (A) Water/Mercury Interface and (B) Mercury/Water Interface	112
26. Polar Directivity of Reflected and Transmitted P-Wave for an Incident P-Wave on (A) Water/Sandstone Interface and (B) Sandstone/Water Interface	113
27. Polar Directivity of Reflected and Transmitted S-Wave for an Incident P-Wave on (A) Water/Sandstone Interface and (B) Sandstone/Water Interface	114
28. Polar Directivity of Reflected and Transmitted P-Wave for an Incident P-Wave on (A) Water/Limestone Interface and (B) Limestone/Water Interface	115
29. Polar Directivity of Reflected and Transmitted S-Wave for an Incident P-Wave on (A) Water/Limestone Interface and (B) Limestone/Water Interface	116
30. Polar Directivity of Reflected and Transmitted P-Wave for an Incident P-Wave on (A) Water/Shale Interface and (B) Shale/Water Interface	117

Figure	Page
31. Polar Directivity of Reflected and Transmitted S-Wave for an Incident P-Wave on (A) Water/Shale Interface and (B) Shale/Water Interface.	118
32. Polar Directivity of Reflected and Transmitted P-Wave for an Incident P-Wave on (A) Sandstone/Limestone Interface and (B) Limestone/Sandstone Interface.	119
33. Polar Directivity of Reflected and Transmitted S-Wave for an Incident P-Wave on (A) Sandstone/Limestone Interface and (B) Limestone/Sandstone Interface.	120
34. Polar Directivity of Reflected and Transmitted P-Wave for an Incident P-Wave on (A) Sandstone/Shale Interface and (B) Shale/Sandstone Interface.	121
35. Polar Directivity of Reflected and Transmitted S-Wave for an Incident P-Wave on (A) Sandstone/Shale Interface and (B) Shale/Sandstone Interface.	122
36. Polar Directivity of Reflected and Transmitted P-Wave for an Incident P-Wave on (A) Sandstone/Granite Interface and (B) Granite/Sandstone Interface.	123
37. Polar Directivity of Reflected and Transmitted S-Wave for an Incident P-Wave on (A) Sandstone/Granite Interface and (B) Granite/Sandstone Interface.	124
38. Polar Directivity of Reflected and Transmitted P-Wave for an Incident P-Wave on (A) Sandstone/Basalt Interface and (B) Basalt/Sandstone Interface	125
39. Polar Directivity of Reflected and Transmitted S-Wave for an Incident P-Wave on (A) Sandstone/Basalt Interface and (B) Basalt/Sandstone Interface	126
40. Polar Directivity of Reflected and Transmitted P-Wave for an Incident P-Wave on (A) Sandstone/Calcite Interface and (B) Calcite/Sandstone Interface.	127
41. Polar Directivity of Reflected and Transmitted S-Wave for an Incident P-Wave on (A) Sandstone/Calcite Interface and (B) Calcite/Sandstone Interface.	128
42. Polar Directivity of Reflected and Transmitted P-Wave for an Incident P-Wave on (A) Sandstone (Wet)/Limestone Interface and (B) Limestone/Sandstone (Wet) Interface. .	129
43. Polar Directivity of Reflected and Transmitted S-Wave for an Incident P-Wave on (A) Sandstone (Wet)/Limestone Interface and (B) Limestone/Sandstone (Wet) Interface. .	130

Figure	Page
44. Polar Directivity of Reflected and Transmitted P-Wave for an Incident P-Wave on (A) Sandstone (Wet)/Shale Interface and (B) Shale/Sandstone (Wet) Interface.	131
45. Polar Directivity of Reflected and Transmitted S-Wave for an Incident P-Wave on (A) Sandstone (Wet)/Shale Interface and (B) Shale/Sandstone (Wet) Interface.	132
46. Common-Depth-Point Shooting	135
47. Traveltime Curve for Horizontal Reflector	137
48. Cancellation of Multiple Reflections by CDP Processing. .	141
49. Geophone Response to Reflected P-Wave	144
50. Geophone Response to Reflected S-Wave	146
51. Hydrophone Response to Reflected P-Wave	148
52. Hydrophone Response of a Reflected P-Wave From Air/Sandstone Interface	149
53. Hydrophone Response of a Reflected P-Wave From Water/Sandstone Interface	151
54. Hydrophone Response of a Reflected P-Wave From Water/Limestone Interface	152
55. Hydrophone Response of a Reflected P-Wave From Water/Shale Interface	153
56. Geophone Response of a Reflected P-Wave for an Incident P-Wave on (A) Sandstone/Limestone Interface and (B) Limestone/Sandstone Interface	154
57. Geophone Response of a Reflected S-Wave for an Incident P-Wave on (A) Sandstone/Limestone Interface and (B) Limestone/Sandstone Interface	155
58. Geophone Response of a Reflected P-Wave for an Incident P-Wave on (A) Sandstone/Shale Interface and (B) Shale/Sandstone Interface	156
59. Geophone Response of a Reflected S-Wave for an Incident P-Wave on (A) Sandstone/Shale Interface and (B) Shale/Sandstone Interface	157
60. Geophone Response of a Reflected P-Wave for an Incident P-Wave on (A) Limestone/Shale Interface and (B) Shale/Limestone Interface	158

Figure	Page
61. Geophone Response of a Reflected S-Wave for an Incident P-Wave on (A) Limestone/Shale Interface and (B) Shale/Limestone Interface.	159

CHAPTER I

INTRODUCTION

The most important geophysical technique used for petroleum exploration is the seismic method. This is due to the fact that it has high accuracy, high resolution, and deep penetration. Although the seismic method has some applications in other fields such as civil engineering and radar technology, its most extensive use has been in oil and gas exploration.

Exploration seismology is a by-product of earthquake seismology. During an earthquake sound waves travel outward from the fracture surface and recorded at various sites using seismometers. This data is then analyzed to provide some information about the elastic properties of the rock through which the sound waves travel.

The basic technique of exploration seismology is essentially the same as the one used in earthquake seismology. It consists of generating controlled waves (by dynamites, mechanical impact or vibration) and measuring the time needed for the waves to travel from the source to an array of geophones which detect vertical or horizontal ground motion. The data are usually recorded on magnetic tape and processed by computer in order to eliminate the noise and extract the desired information.

Seismic technique falls into two different categories:

1. Reflection Seismology, which is the most widely used method in geophysical prospecting techniques, deals with generating elastic waves

and making surface measurements on the waves that are reflected from interfaces between formations having different physical properties. Later these measurements are interpreted to give some information about the depths of the reflecting beds and the structural features of the subsurface formations. Thus with reflection methods one can locate and map some features of interest such as anticlines, faults, salt domes, and reefs which are generally associated with the accumulation of oil and gas.

In reflection seismology, the reflections are recorded by seismometers which are laid along the ground at distances from the source that are generally small compared with the depth of the bed. These seismometers are either geophones which are responsive to ground motion or hydrophones which are responsive to water pressure.

2. Refraction Seismology--it deals with the case where the detectors of seismic waves are at a large distance from the source compared to the depth of the layer to be mapped. The refracted waves must thus travel large horizontal distances through the earth. The times of flight give some information about the velocity and depth of the subsurface formations along which they propagate.

This method has some advantages. It can cover a given area in a shorter time and more economically than with the reflection method. It is particularly suitable to determine the shape and depth of some sedimentary basin if it has a lower speed than the basement formation.

In spite of these advantages, it is not employed as much as the refraction method in oil exploration. This is probably due to the greater amounts of dynamite needed for field operations, and the lower precision in the information of the structural features of the subsur-

face formations.

Statement of the Problem

So far the reflection method has not been used for direct petroleum exploration, but instead limited to the mapping of structural features or stratigraphic conditions favorable for the accumulation of oil or gas.

On the other hand the technique that has been used for direct indication for the presence of hydrocarbons is the drilling process and testing the core samples.

Using seismic reflection method for direct detection of hydrocarbons has not been achieved yet. So, our problem is to relate the reflection amplitudes to the acoustic impedance of the buried interfaces. Knowing the physical properties (velocity and density) of the stratum will help in locating oil or gas.

In this study the concern will be with reflection and refraction of plane waves incident on plane interfaces. The solution of a boundary value problem of an incident plane wave at some interface is obtained. Then the angular dependence of all reflected and transmitted waves is found. All possible cases of interfaces are taken, that is solid/vacuum, liquid/liquid, liquid/solid, and solid/solid interfaces.

Importance of the Study

Most of the seismic work that has been done deals with normal incidence only and with one type of elastic wave, which is the longitudinal or pressure wave. In the present study, I will be dealing with oblique incidence as well and with both types of elastic waves which would be

generated at the boundary interface due to mode conversion. This occurs with either type of elastic wave; pressure (p) wave or shear (s) wave.

Knowing the reflected and transmitted amplitudes of the p-wave and s-wave will give information about the elastic properties of the subsurface formation. This would add a new dimension in geophysics prospecting, to have an idea not only about the structure of the bedrock but also about some physical parameters such as velocity and density.

This method can be applied to Common Depth Point analysis as described in Chapter VI, and utilize the information given about the relative amplitudes of the reflected waves as a direct indication of the relative speeds and densities of strata about the reflecting surface.

Due to the high directivity of the reflected s-wave some analysis of its amplitude can be done more economically than the analysis needed for the reflected p-wave. The p-wave and s-waves are easily separated due the considerable difference in their speeds of propagation.

Procedure of the Study

The writer will start with some theoretical background for the subject which is the theory of elasticity, then the wave equation is derived for the pressure wave and shear wave. These are two independent elastic waves which propagate with different velocities and are governed by the elastic properties of the medium. In Chapter II the theoretical boundary value problem is solved for the most general case of two solids. Then mode conversion is discussed in Chapter III, where one type of wave incident on a discontinuity will generate the other type of wave in order to satisfy the boundary conditions.

Different cases are taken of solid/vacuum, liquid/liquid, liquid/

solid, and solid/solid interfaces, and all data used represent familiar rocks and fluids.

In Chapter III we limited our discussion to the non-critical situations. The solutions are found by using numerical analysis to solve four equations and four unknowns (or less for simpler cases). Normal and grazing incidence are solved algebraically to avoid any singularity. After solving for the amplitudes, some modified factors are introduced to get the square root of the normal energy flux. The physical requirement of conservation of normal energy flux is used as a check for our results.

In Chapter IV critical angles are discussed thoroughly, and the associated sharp discontinuities in reflected, mode converted, and transmitted amplitudes. At and beyond critical angles the z-component of the wave vector k of the transmitted wave becomes imaginary, so that will lead to an exponential decay of the amplitude as a function of the distance from the interface. This transmitted wave propagates parallel to the interface with a phase velocity that is determined by the incident wave velocity and the angle of incidence and it does not transfer any energy across the barrier.

In Chapter V results from Chapter III, and Chapter IV for critical and non-critical situations are presented in polar form which shows the angular dependence of the reflected and transmitted pressure and shear waves. These plots have very definite features which reflect the dependence on the relative acoustic parameters (velocity and density) of the reflecting interface.

Some application of our results on Common Depth Point data evaluation is discussed in Chapter VI. Useful information about the relative

amplitudes from offshore and onshore measurements is explained and how we can use that as a direct measure of the relative velocity or density especially for the case when there are sharp discontinuities in the reflection amplitudes due to critical angles.

An attempt for expanding the relative reflected amplitudes in terms of some orthonormal set is illustrated in Appendix A where we used three different sets of orthogonal functions; these are Legendre, Associated Legendre, and Sinusoidal Functions.

Using the first few terms the approximation was good enough for smooth reflections, but for the case when we have sharp discontinuities more terms are needed, or may be some other set of orthogonal functions.

Finally, some suggestions for further investigations are discussed.

Limitation of the Study

In our study we assumed plane interfaces, but in reality one hardly can find such regular interfaces, especially for a large region of field measurements. Some regions of uniform depositions of sediments such as those at the bottom of the ocean can be approximated as plane interfaces.

Also, we assumed flat interfaces, but some interfaces are inclined, so that will affect the magnitude of the reflections and hence the location of maximum reflection points.

We have limited our analyses to primary reflections, but it can be extended for multiple reflections where we have to use the idea of successive image points to give the right reflections.

As far as the speed is concerned we assumed an isotropic medium, and hence the speed is equal in all directions, but in reality there is a measurable difference in the speed along the bedding planes from that

normal to them. Also there is some frequency dependent in the velocity that we haven't put into consideration.

The attenuation effect of the amplitudes from energy loss due to internal friction is not considered, but this effect is reduced since we are dealing with relative amplitudes, and all reflected amplitudes have nearly suffered from the same attenuation.

Finally, even though our results are obtained for all range of angles (normal to grazing incidence), but when they are applied to CDP (Common Depth Point) analysis the relative amplitudes are plotted for a limited range of angles; that is from normal incidence to about 30° (angles are measured from horizontal). Practically taking all range of angles is impossible, because at grazing incidence some detectors have to be at infinite in order to respond to the reflected p-wave.

Review of Related Literature

Energy densities of seismic waves reflected and refracted at an interface of two elastic media has been studied by various authors, such as Knott (11), Stoneley (9), Muskat and Meres (16), Ergin (3), and Koe-foeld (12).

C. G. Knott (11) derived formulas for the reflection coefficients for plane waves incident on a boundary between two elastic media, permitting their values to be computed when the elastic constants of the media are known. He considered the cases of: solid-air, solid-water, and solid-solid interfaces.

R. Stoneley (19) concentrated on the dissipated energy, at a discontinuity, due to internal viscosity and on the existence of surface waves analogous to Rayleigh and Love waves.

M. Muskat and M. W. Meres (16) computed the reflection and transmission coefficients for the elastic waves due to an incident p-wave or s-wave for a range of densities and longitudinal velocities ratio. Their analysis was limited to the assumption that in both media the Poisson ratio was equal to 0.25, and that the angle of incidence did not exceed 30° .

Kazim Ergin (3) investigated the energy ratios of the seismic waves reflected and refracted at a rock-water boundary. He has determined the angles (if any) that lead to the extreme values of energy, and the dependence of these angles on the elastic constants of the media involved.

O. Koefoeld (12) calculated the reflection coefficients of plane longitudinal waves incident at oblique angles on boundary planes between elastic media. He discussed the effect of Poisson's ratios of rock strata on the reflection coefficients.

When the angle of the incidence exceeds a certain value (the critical angle), the phenomena of total reflection occurs. Such a phenomena has been a subject of many papers.

Among these papers F. G. Friedlander (5) considered the reflection and refraction of transverse plane waves, at an interface parallel to the direction of polarization. The incident wave is of arbitrary shape and the angle of incidence is allowed to exceed the critical angle.

J. N. Goodier and R. E. Bishop (7) discussed the critical reflections of elastic waves at free surfaces. By applying suitable limiting processes, they were able to obtain the wave motion of a p-wave or an s-wave incident at grazing incidence.

B. Gutenberg (8) applied the method for calculating the amplitudes

for bodily waves in earthquakes to the study of amplitude of longitudinal waves produced by an artificial explosion. He related the discontinuity in the energy of the reflected longitudinal wave to the critical refraction angle.

C. Y. Fu (6) discussed the complex behavior of the reflected and refracted amplitudes beyond critical angles, and their analogy to Rayleigh wave. He, also, derived the equations for the reflected and refracted amplitudes due to an incident dilational or distortional wave at the interface of two semi-infinite media.

As far as using the reflection method in the field W. Harry Mayne (15) described some technique for multiple coverage of the subsurface. He assumed an average velocity that increases with depth, and he has arranged the detectors spreads and the shotpoints so that when the channels which have a common reflection point are combined or stacked a minimum ratio of noise to signal is obtained.

C. S. Clay and H. Menell (2) made some comparison between the measured and calculated amplitudes of two seismic events which have traveled through a two layer seismic model, and they found that the relative amplitudes of the reflected waves are in agreement to the calculation based on reflection theory of plane waves with correction for the $\frac{1}{r}$ spherical divergence of the amplitude.

CHAPTER II

THEORY OF ELASTICITY

The seismic method uses waves propagating through the earth to obtain information about subsurface geological structure, propagation of the wave causes a local disturbance of the particles of the medium. The deformation due to the wave is determined by the elastic properties of the medium and the type of wave.

Elasticity is a measure of the ability of some substance to resist any deformation in size or shape (size only in case of fluids) to some applied external force. This reaction is due to some internal forces which exist whenever the body is distorted from an equilibrium configuration. The theory of elasticity relates the deformation of the body in shape or size to the applied forces. The elasticity is the proportionality constant between the applied force (stress) and the resulting deformation (strain).

Stress

Stress is defined as the force per unit area. It is normal if the applied force is normal to the area, and it is tangential stress if the force is tangential to the area. Any other stress can be resolved into normal and tangential components.

Consider an infinitesimal rectangular parallelepiped inside the stressed body with three sides along three mutually perpendicular axes

Ox, Oy, Oz. There are stresses acting on each of the six faces which can be resolved into components, as shown in Figure 1 for the two faces that are perpendicular to the x-axis. The shear stress parallel to the y-axis (σ_{yx}) acts on a surface perpendicular to the x-axis. When the stress indices are the same (as σ_{xx}) it is normal to the surface while if they are different (as σ_{yx}) it is tangential or a shearing stress. When the body is in static equilibrium (no whole body rotations or translations), the stresses must be balanced, so by taking moments it is easily shown that $\sigma_{yx} = \sigma_{xy}$ and generally $\sigma_{ij} = \sigma_{ji}$. This will reduce the number of independent stress components into only six.

Strain

Strain is a measure of the relative change in dimensions of the body that is subjected to stress. If we consider a rectangle ABCD in x-y plane as in Figure 2, let A'B'C'D' be the new positions of A,B,C,D when it is under some stress. Let the displacement AA' have u,v components along x, y-axis respectively. If the whole rectangle is displaced by the amounts u and v, then there is no change in size nor shape so there does not exist any stress. However, if the displacements of the vertices are not identical, then the rectangle does undergo change in shape and size. So stress does exist.

Let the coordinates of A and an adjacent point B for the unstrained rectangle be given as:

$$A(x,y), B(x+\delta x, y)$$

After the rectangle is strained by u,v, then A,B become

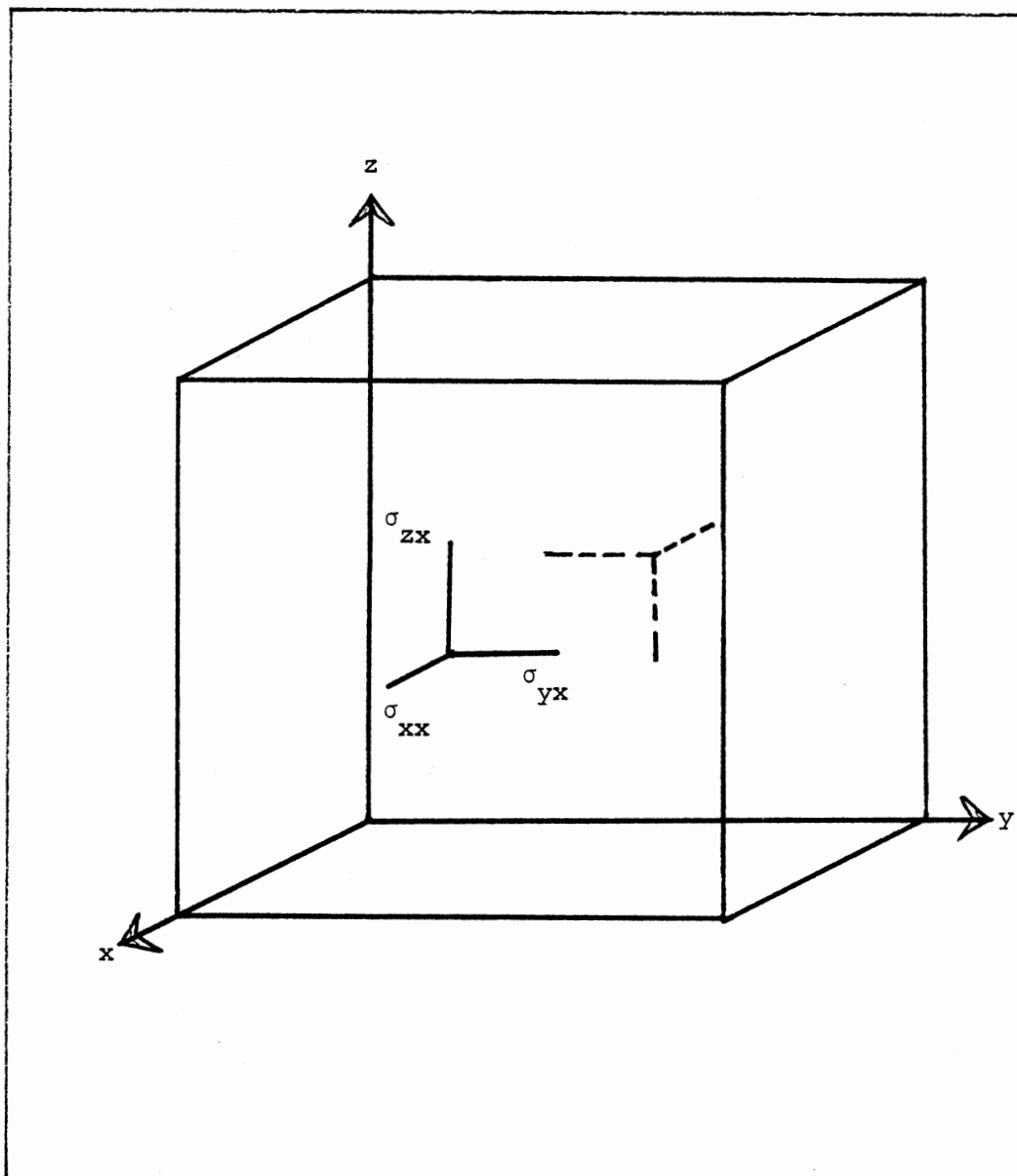


Figure 1. Components of Stress on a Small Rectangular Parallelepiped

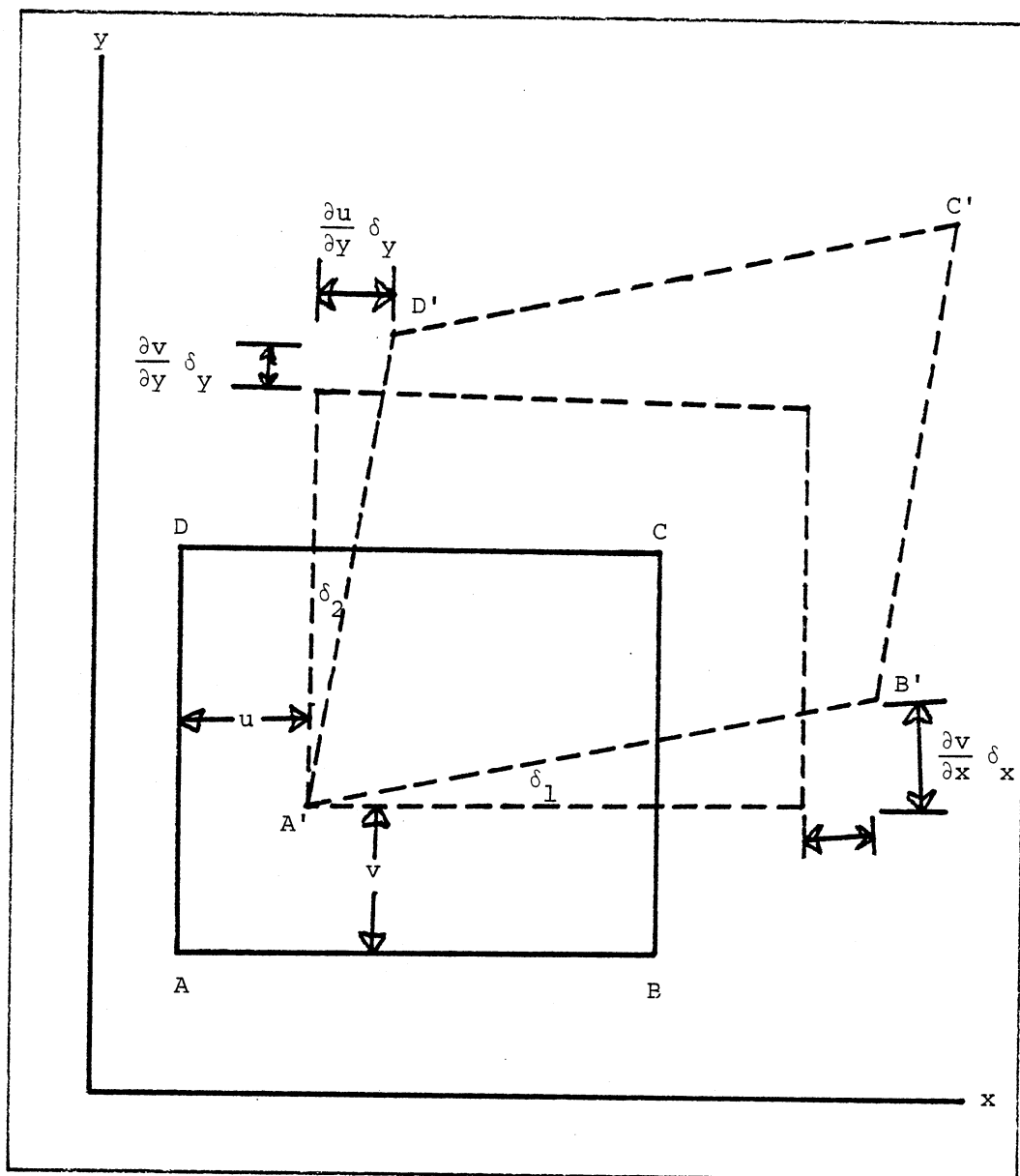


Figure 2. Strain Analysis in Two Dimensions

$$A_{(x+u, y+v)}, B_{(x+\delta x+u+\delta u, y+v+\delta v)}$$

If $u = u(x, y)$ and $v = v(x, y)$, then

$$\delta u = \frac{\partial u}{\partial x} \delta x + \frac{\partial u}{\partial y} \delta y \quad (2.1a)$$

and

$$\delta v = \frac{\partial v}{\partial x} \delta x + \frac{\partial v}{\partial y} \delta y. \quad (2.1b)$$

That is 1st order expansion assuming $\delta x, \delta y$ are very small. We can see from Figure 2 that:

a) The fractional elongation in x and y directions (normal strains) are $\frac{\partial u}{\partial x}$ and $\frac{\partial v}{\partial y}$, respectively.

$$b) \quad \delta_1 \approx \tan \delta_1 = \partial v / \partial x, \quad \delta_2 \approx \tan \delta_2 = \partial u / \partial y.$$

c) The rectangle has rotated about the z -axis counterclockwise through the angle $(\delta_1 - \delta_2) = (\frac{\partial v}{\partial x} - \frac{\partial u}{\partial y}) = \theta_z$. It doesn't involve any change in size or shape and hence it is not a strain.

d) The right angle at A has decreased by an amount $= \delta_1 + \delta_2$
 $\frac{\partial v}{\partial x} + \frac{\partial u}{\partial y}$, so it is a measure of the change in shape of the medium and it is denoted by ϵ_{xy} as shearing strain.

If our analysis is extended to three dimensions in which A has been displaced by u, v, w in the x, y , and z -direction respectively the strains are as follows:

$$\text{Normal strains } \epsilon_{xx} = \frac{\partial u}{\partial x}, \epsilon_{yy} = \frac{\partial v}{\partial y}, \epsilon_{zz} = \frac{\partial w}{\partial z} \quad (2.2a)$$

$$\left. \begin{aligned} \epsilon_{xy} &= \epsilon_{yx} = \frac{\partial v}{\partial x} + \frac{\partial u}{\partial y} \\ \text{Shearing strains } \epsilon_{yz} &= \epsilon_{zy} = \frac{\partial w}{\partial y} + \frac{\partial v}{\partial z} \\ \epsilon_{zx} &= \epsilon_{xz} = \frac{\partial u}{\partial z} + \frac{\partial w}{\partial x} \end{aligned} \right\} \quad (2.2b)$$

Beside that, the body is subjected to rotational deformations about the three axis as follows:

$$\left. \begin{aligned} \theta_x &= \frac{\partial w}{\partial y} - \frac{\partial v}{\partial z} \\ \theta_y &= \frac{\partial u}{\partial z} - \frac{\partial w}{\partial x} \\ \theta_z &= \frac{\partial v}{\partial x} - \frac{\partial u}{\partial y} \end{aligned} \right\} \quad (2.2c)$$

There is a volume change due to the changes in dimensions which are given by the normal strains. This relative change in volume is called dilation and denoted by

$$\Delta = \frac{\delta_x (1 + \epsilon_{xx}) \delta_y (1 + \epsilon_{yy}) (1 + \epsilon_{zz}) \delta_z}{\delta_x \delta_y \delta_z} \quad (2.3)$$

$$\Delta = \epsilon_{xx} + \epsilon_{yy} + \epsilon_{zz}$$

to the 1st order approx. So,

$$\Delta = \frac{\partial u}{\partial x} + \frac{\partial v}{\partial y} + \frac{\partial w}{\partial z}$$

Generally we can decompose strain into dilation and shearing strains

(Love, P. 45, Theory of Elasticity)..

Hooke's Law

When the strains are small (limited stress) they are related to stress according to Hooke's Law which states that strain is linearly related to the applied stress. When several stresses exist, each produces strains independently of the others. This means each strain is a linear function of all of the stresses and vice versa.

So, in general for an anisotropic medium the six components of stress are related to the six components of strain by the following (generalized form of Hooke's Law) matrix equation.

$$\begin{bmatrix} \sigma_{xx} \\ \sigma_{yy} \\ \sigma_{zz} \\ \sigma_{yz} \\ \sigma_{zx} \\ \sigma_{xy} \end{bmatrix} = \begin{bmatrix} C_{11} & C_{12} & C_{13} & C_{14} & C_{15} & C_{16} \\ C_{21} & C_{22} & C_{23} & C_{24} & C_{25} & C_{26} \\ C_{31} & C_{32} & C_{33} & C_{34} & C_{35} & C_{36} \\ C_{41} & C_{42} & C_{43} & C_{44} & C_{45} & C_{46} \\ C_{51} & C_{52} & C_{53} & C_{54} & C_{55} & C_{56} \\ C_{61} & C_{62} & C_{63} & C_{64} & C_{65} & C_{66} \end{bmatrix} \begin{bmatrix} \epsilon_{xx} \\ \epsilon_{yy} \\ \epsilon_{zz} \\ \epsilon_{yz} \\ \epsilon_{zx} \\ \epsilon_{xy} \end{bmatrix} \quad (2.4)$$

where the coefficients are the elastic constants of the material. For the elastic energy to be a univalued function of the strain $c_{rs} = c_{sr}$ (see Love, Fourth Edition, P. 99). This reduces the number of independent coefficients from 36 to 21.

For an isotropic solid, the values of the coefficients are independent of the set of axes chosen. Applying this condition to the above matrix equation reduces the coefficients into just two independent constants denoted by λ and μ , where

$$\left. \begin{aligned} C_{23} &= C_{13} = C_{21} = C_{31} = C_{32} = \lambda \\ C_{44} &= C_{55} = C_{66} = \mu \\ C_{11} &= C_{22} = C_{33} = \lambda + 2\mu, \text{ and the other 24} \end{aligned} \right\} \quad (2.5)$$

coefficients vanish due to the high degree of symmetry so that stress and strain are related by the following simple relations

$$\sigma_{ii} = \lambda \Delta + 2\mu \epsilon_{ii}, \quad i = x, y, z \quad (2.6a)$$

$$\text{and} \quad \sigma_{ij} = \mu \epsilon_{ij}, \quad i, j = x, y, z; \quad i \neq j \quad (2.6b)$$

where

$$\Delta = \epsilon_{xx} + \epsilon_{yy} + \epsilon_{zz}$$

and λ, μ are known as Lamé's constants. This completely defines the elastic properties of an isotropic solid. The reaction to shearing strain is proportional to μ which is often referred to as the modulus of rigidity or shear modulus.

Wave Equation

So far we have been discussing a medium in static equilibrium. Now, we shall concern ourselves with a media experiencing stress gradient. Let us assume that the stresses on the rear face of the parallelepiped are as shown in Figure 1.

$$\sigma_{xx}, \sigma_{yx}, \sigma_{zx},$$

but that the stresses on the front face are respectively

$$\sigma_{xx} + \frac{\partial \sigma_{xx}}{\partial x} \delta_x, \sigma_{yx} + \frac{\partial \sigma_{yx}}{\partial x} \delta_x, \sigma_{zx} + \frac{\partial \sigma_{zx}}{\partial x} \delta_x$$

so the net unbalanced stresses are

$$\frac{\partial \sigma_{xx}}{\partial x} \delta_x, \frac{\partial \sigma_{yx}}{\partial x} \delta_x, \frac{\partial \sigma_{zx}}{\partial x} \delta_x$$

these stresses act on a face having an area of $\delta_y \delta_z$ and affect the volume $(\delta_x \delta_y \delta_z)$. So, the net force per unit volume in the x, y, and z-directions are

$$\frac{\partial \sigma_{xx}}{\partial x}, \frac{\partial \sigma_{yx}}{\partial x}, \frac{\partial \sigma_{zx}}{\partial x},$$

respectively. Similar expressions hold for the other faces. The total force in the x-direction is

$$\left(\frac{\partial \sigma_{xx}}{\partial x} + \frac{\partial \sigma_{xy}}{\partial y} + \frac{\partial \sigma_{xz}}{\partial z} \right)$$

and the equation of motion according to Newton's second law is

$$F_{x \text{ net}} = m a_x \quad (2.7)$$

or $F_{x \text{ net}}$ per unit volume = $\rho \frac{\partial^2 u}{\partial t^2}$, where ρ is the density.

The net acceleration due to the difference in stress on the faces of the rectangular parallelepiped are given by

$$\rho \frac{\partial^2 u}{\partial t^2} = \frac{\partial \sigma_{xx}}{\partial x} + \frac{\partial \sigma_{xy}}{\partial y} + \frac{\partial \sigma_{xz}}{\partial z} \quad (2.8a)$$

and similarly,

$$\rho \frac{\partial^2 \mathbf{v}}{\partial t^2} = \frac{\partial \sigma_{yx}}{\partial x} + \frac{\partial \sigma_{yy}}{\partial y} + \frac{\partial \sigma_{yz}}{\partial z}, \quad (2.8b)$$

$$\rho \frac{\partial^2 \mathbf{w}}{\partial t^2} = \frac{\partial \sigma_{zx}}{\partial x} + \frac{\partial \sigma_{zy}}{\partial y} + \frac{\partial \sigma_{zz}}{\partial z}. \quad (2.8c)$$

These equations of motion will hold, whatever the stress-strain behavior of the medium. In order to solve these equations, we must use the elastic relations. For an isotropic medium these relations are given by Hooke's Law (Equation 2-6) and the definition of strain components (Equation 2.2). From these relations we can rewrite the stress in terms of the strain components yielding the following equations of motion.

$$\begin{aligned} \therefore \rho \frac{\partial^2 u}{\partial t^2} &= \frac{\partial}{\partial x} (\lambda \Delta + 2\mu \epsilon_{xx}) + \frac{\partial}{\partial y} (\mu \epsilon_{xy}) + \frac{\partial}{\partial z} (\mu \epsilon_{xz}) \\ &= \lambda \frac{\partial \Delta}{\partial x} + 2\mu \frac{\partial \epsilon_{xx}}{\partial x} + \mu \frac{\partial \epsilon_{xy}}{\partial y} + \mu \frac{\partial \epsilon_{xz}}{\partial z} \\ &= \lambda \frac{\partial \Delta}{\partial x} + 2\mu \frac{\partial^2 u}{\partial x^2} + \mu \left(\frac{\partial^2 v}{\partial y \partial x} + \frac{\partial^2 u}{\partial y^2} \right) + \mu \left(\frac{\partial^2 w}{\partial z \partial x} + \frac{\partial^2 u}{\partial z^2} \right) \\ &= \lambda \frac{\partial \Delta}{\partial x} + u \nabla^2 \mu + \mu \frac{\partial}{\partial x} \left(\frac{\partial u}{\partial x} + \frac{\partial v}{\partial y} + \frac{\partial w}{\partial z} \right) \\ \left[\rho \frac{\partial^2 u}{\partial t^2} \right] &= (\lambda + \mu) \frac{\partial \Delta}{\partial x} + \mu \nabla^2 u. \end{aligned} \quad (2.9a)$$

where

$$\nabla^2 u = \frac{\partial^2 u}{\partial x^2} + \frac{\partial^2 u}{\partial y^2} + \frac{\partial^2 u}{\partial z^2}.$$

By analogy we can write the following equations:

$$\rho \frac{\partial^2 \mathbf{v}}{\partial t^2} = (\lambda + \mu) \frac{\partial \Delta}{\partial \mathbf{y}} + \mu \nabla^2 \mathbf{v}, \quad (2.9b)$$

$$\rho \frac{\partial^2 \omega}{\partial t^2} = (\lambda + \mu) \frac{\partial \Delta}{\partial z} + \mu \nabla^2 \omega \quad (2.9c)$$

To obtain the wave equation, we differentiate equations (2.9a,b,c) with respect to x , y , and z , respectively and then by adding them we get

$$\rho \frac{\partial^2}{\partial t^2} \left[\frac{\partial u}{\partial x} + \frac{\partial v}{\partial y} + \frac{\partial w}{\partial z} \right] = (\lambda + \mu) \left\{ \frac{\partial^2}{\partial x^2} + \frac{\partial^2}{\partial y^2} + \frac{\partial^2}{\partial z^2} \right\} \Delta + \mu \nabla^2 \left(\frac{\partial u}{\partial x} + \frac{\partial v}{\partial y} + \frac{\partial w}{\partial z} \right)$$

or

$$\rho \frac{\partial^2 \Delta}{\partial t^2} = (\lambda + 2\mu) \nabla^2 \Delta \quad \left[\frac{1}{\alpha^2} \frac{\partial^2 \Delta}{\partial t^2} = \nabla^2 \Delta \right] \quad (2.10a)$$

which is the wave equation for a dilational wave propagating through the medium with a speed α where

$$\alpha^2 = \frac{\lambda + 2\mu}{\rho} \quad (2.10b)$$

By subtracting the derivative of Eq. (2.9b) w.r.t. z from the derivative of Eq. (2.9c) w.r.t. y we get

$$\rho \frac{\partial^2}{\partial t^2} \left(\frac{\partial w}{\partial y} - \frac{\partial v}{\partial z} \right) = \mu \nabla^2 \left(\frac{\partial w}{\partial y} - \frac{\partial v}{\partial z} \right)$$

that gives

$$\rho \frac{\partial^2}{\partial t^2} (\theta_x) = \mu \nabla^2 \theta_x \quad (2.10c)$$

where θ_x is a rotation about x -axis given by Eq. (2.2c), or

$$\frac{1}{\beta^2} \frac{\partial^2 \theta_x}{\partial t^2} = \nabla^2 \theta_x$$

where

$$\beta^2 = \frac{\mu}{\rho} \quad (2.10d)$$

That represents a rotational wave about the x-axis that is propagating through the medium with speed

$$\beta = (\mu/\rho)^{1/2}.$$

Similar equations may be obtained for θ_y and θ_z . So generally we can write

$$\frac{1}{\beta^2} \frac{\partial^2 \psi}{\partial t^2} = \nabla^2 \psi \quad (2.11)$$

For a purely rotational wave (the dilations is zero) Equations (2.9a,b and c) become

$$\rho \frac{\partial^2 u}{\partial t^2} = \mu \nabla^2 u \quad (2.12a)$$

similarly,

$$\rho \frac{\partial^2 v}{\partial t^2} = \mu \nabla^2 v \quad (2.12b)$$

and

$$\rho \frac{\partial^2 w}{\partial t^2} = \mu \nabla^2 w \quad (2.12c)$$

The conditions for a purely dilational wave that is when all the rotations θ_x , θ_y and θ_z vanish is satisfied if u , v and w satisfy the following conditions

$$u = \frac{\partial \phi}{\partial x}, \quad v = \frac{\partial \phi}{\partial y}, \quad w = \frac{\partial \phi}{\partial z}$$

where ϕ is some potential function, thus

$$\begin{aligned} \Delta &= \frac{\partial u}{\partial x} + \frac{\partial u}{\partial y} + \frac{\partial w}{\partial z} \\ &= \nabla^2 \phi \end{aligned}$$

and

$$\frac{\partial \Delta}{\partial x} = \nabla^2 \frac{\partial \phi}{\partial x} = \nabla^2 u \quad (2.13)$$

So by substituting in Eq. (2.9a) we get

$$\rho \frac{\partial^2 u}{\partial t^2} = (\lambda + 2\mu) \nabla^2 u \quad (2.14a)$$

and similarly for v and w in Eqs. (2.9b) and (2.9c) we get

$$\rho \frac{\partial^2 v}{\partial t^2} = (\lambda + 2\mu) \nabla^2 v, \quad (2.14b)$$

$$\rho \frac{\partial^2 w}{\partial t^2} = (\lambda + 2\mu) \nabla^2 w \quad (2.14c)$$

So we see that for an unbounded isotropic elastic solid two and only two waves can exist. Waves involving no rotation travel with a speed $[(\lambda+2\mu)/\rho]^{\frac{1}{2}}$. These are called irrotational waves or dilational, longitudinal, compressional, or pressure (p-) waves. Waves involving no

dilation travel with speed $(\mu/\rho)^{1/2}$. These are called rotational, distortion, transverse, or shear (s-) waves.

Bounded Medium and Boundary Conditions

If the medium to which the equations of motion are applied is bounded, some other kinds of elastic waves may also occur. These waves are called surface waves, since they are confined to the vicinity of one of the surfaces which bound the system. The most important type of surface waves is a Rayleigh wave which was discovered by Lord Rayleigh (1887). This wave travels along the surface of the earth with a velocity that is always less than the shear wave velocity. The amplitude of this wave decreases exponentially with depth. Another type of surface wave is called a Love wave which is observed in earthquake seismology. It involves transverse motion parallel to the surface of the ground and sometimes is called an SH wave. Love waves have velocities intermediate between the s-wave velocity at the surface and that in deeper layers.

There are conditions on the stress and strain that must be satisfied for a bounded medium. These expressions express the behavior of stresses and displacements at the boundaries. For solid elastic media we assume that they are welded together at the surface of contact implying continuity of all stress and strain components across the boundary. At a solid-liquid interface slippage can occur, so continuity of only normal stresses and displacements is required. Since liquids don't resist tangential stress (i.e., rigidity vanishes in the liquid), tangential stresses in the solid must vanish at the interface and for a full surface of a solid or fluid (ideally a surface in vacuum where there can be no refracted waves), all stress components vanish; and the boundary condi-

tions can't be satisfied by assuming that only one wave type is reflected. But rather another type of wave is needed to satisfy the boundary conditions. In the most general case for any incident wave (p-wave or s-wave) four separate waves are generated. A wave of each type is reflected, and a wave of each type is refracted.

General Solution for the Reflection and Refraction of Plane Waves at an Interface

For an incident plane wave on a plane interface of two semi-infinite isotropic media (assumed to be two elastic solids in the general case) it produces compressional and distortional waves in both media. Four boundary conditions must be satisfied, requiring continuity of normal and tangential components of displacements and stresses across the interface.

We start with an incident p-wave in the x-z plane, so all waves have no dependent on y, z is positive into the first medium. This incident p-wave will generate two reflected and two refracted waves at the boundary interface as shown in Figure 3.

Let the displacement vector \vec{s} ; $\vec{s} = u\hat{i} + v\hat{j} + w\hat{k}$ be expressed in terms of a scalar potential ϕ , and a vector potential $\vec{\Omega}$.

$$\vec{s} = \vec{\nabla}\phi + \vec{\nabla}\times\vec{\Omega} \quad (2.15)$$

The scalar and vector potentials represent two independent wave types propagating in an unbounded medium. For a pure dilational wave that involves no rotation, $\vec{\Omega}$ vanishes and the displacement vector is given by

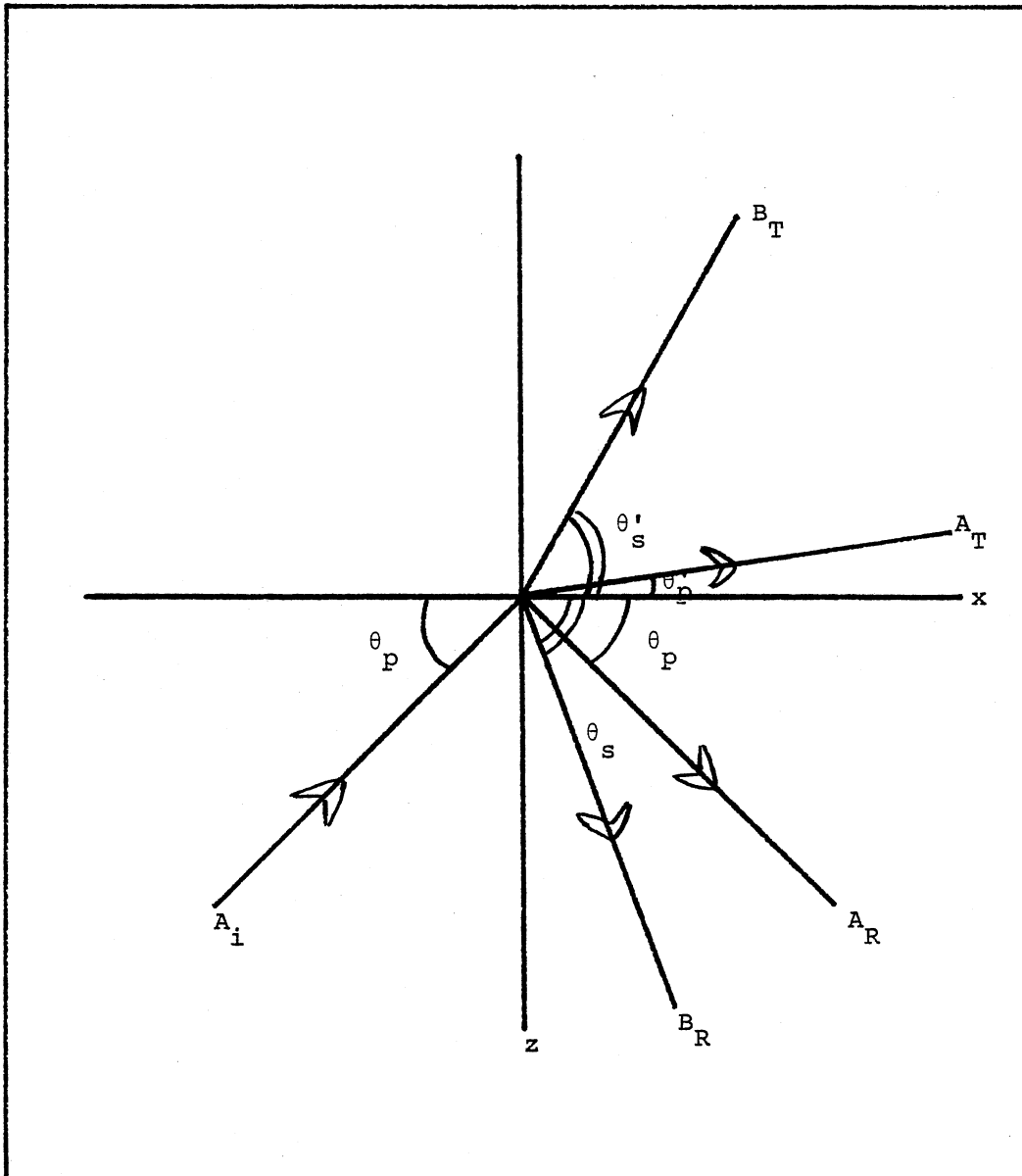


Figure 3. Reflection and Refraction of Incident P-Wave at an Interface of Two Elastic Solids

$$\vec{s} = \frac{\partial \phi}{\partial x} \hat{i} + \frac{\partial \phi}{\partial y} \hat{j} + \frac{\partial \phi}{\partial z} \hat{k}$$

and the wave equation is

$$\nabla^2 \phi = \frac{1}{\alpha^2} \frac{\partial^2 \phi}{\partial t^2} \quad (2.16a)$$

which is a dilational wave propagating with a phase velocity α , where

$$\alpha^2 = \frac{\lambda + 2\mu}{\rho}.$$

For a rotational wave that involves no dilation ϕ vanishes,

$\vec{\Omega} = (\psi_1, \psi_2, \psi_3)$ in general, and the displacement vector is

$$\vec{s} = \left(\frac{\partial \psi_3}{\partial y} - \frac{\partial \psi_2}{\partial z} \right) \hat{i} + \left(\frac{\partial \psi_1}{\partial z} - \frac{\partial \psi_3}{\partial x} \right) \hat{j} + \left(\frac{\partial \psi_2}{\partial x} - \frac{\partial \psi_1}{\partial y} \right) \hat{k}$$

and the wave equation is

$$\nabla^2 \psi_i = \frac{1}{\beta^2} \frac{\partial^2 \psi_i}{\partial t^2}, \quad i = 1, 2, 3 \quad (2.16b)$$

which is a rotational wave propagating with a phase velocity β , where

$$\beta^2 = \frac{\mu}{\rho}$$

Equations (2.16a) and (2.16b) show that ϕ is associated with the dilation produced by the disturbance while ψ_i is associated with the rotation, and the introduction of the scalar and the vector potentials has thus enabled us to separate the effects of dilation and rotation in the medium.

For the case when the motion is in the x-z plane, let us assume that ϕ is a function of x and z only, and $\vec{\Omega} = (0, \psi, 0)$ where ψ is a function of x and z.

The displacement corresponding to both the waves is given by

$$\begin{aligned}\vec{s} &= \nabla\phi + \vec{\nabla}_x \vec{\Omega} \\ &= \left(\frac{\partial\phi}{\partial x} - \frac{\partial\psi}{\partial z}\right)\hat{i} + \frac{\partial\phi}{\partial y}\hat{j} + \left(\frac{\partial\phi}{\partial z} + \frac{\partial\psi}{\partial x}\right)\hat{k}\end{aligned}\quad (2.17)$$

$$\therefore u = \frac{\partial\phi}{\partial x} - \frac{\partial\psi}{\partial z} \quad (2.18a)$$

$$v = \frac{\partial\phi}{\partial y} = 0 \quad (\phi \neq \phi(y)) \quad (2.18b)$$

$$\text{and} \quad w = \frac{\partial\phi}{\partial z} + \frac{\partial\psi}{\partial x} \quad (2.18c)$$

where ϕ and ψ satisfy the wave equations

$$\nabla^2 \phi = \frac{1}{\alpha^2} \frac{\partial^2 \phi}{\partial t^2} \quad (2.19a)$$

$$\text{and} \quad \nabla^2 \psi = \frac{1}{\beta^2} \frac{\partial^2 \psi}{\partial t^2} \quad (2.19b)$$

The form of a pressure wave ϕ propagating with a phase velocity α , and having a phase velocity c along the x-direction is

$$\phi = f(z) e^{-i(k_{px}x - \omega t)} \quad (2.20a)$$

$$\text{where} \quad k_{px} = \frac{\omega}{c} \quad \text{and} \quad k_p = \frac{\omega}{\alpha}$$

The form of a shear wave ψ propagating with a phase velocity β , and having a phase velocity c' along the x direction is

$$\psi = g(z)e^{-i(k_{sx}x - \omega t)} \quad (2.20b)$$

where $k_{sx} = \frac{\omega}{c'}$ and $k_s = \frac{\omega}{\beta}$

It will be shown later that both waves have the same phase velocity along the x -direction ($c=c'$), and hence both waves have the same phase factor. To solve for $f(z)$ and $g(z)$ we substitute the expressions of $f(z)$ and $g(z)$ from Equations (2.20a,b) into Equations (2.19a,b).

$$\nabla^2 \phi = \frac{1}{\alpha^2} \frac{\partial^2 \phi}{\partial t^2}$$

$$-k_{px}^2 f(z) + f''(z) = -\frac{\omega^2}{\alpha^2} f(z)$$

$$\frac{d^2 f(z)}{dz^2} + k_{pz}^2 f(z) = 0$$

$$\therefore f(z) = A_i e^{ik_{pz}z} + A_r e^{-ik_{pz}z} \quad \text{if } k_{pz} \neq 0 \ (\theta_p \neq 0) \quad (2.21a)$$

$$f(z) = C_1 + C_2 z \quad \text{if } k_{pz} = 0 \ (\theta_p = 0) \quad (2.21b)$$

In a physical solution $C_2=0$, but if $C_2 \neq 0$; $f(z) \rightarrow \infty$ as $z \rightarrow \infty$ which has no physical meaning. Similarly,

$$g(z) = B_i e^{ik_{sz}z} + B_r e^{-ik_{sz}z} \quad (2.22)$$

$$\therefore \phi = A_i e^{-i(k_{px}x - k_{pz}z - \omega t)} + A_r e^{-i(k_{px}x + k_{pz}z - \omega t)}, \quad (2.23a)$$

$$\psi = B_i e^{-i(k_{sx}x - k_{sz}z - \omega t)} + B_r e^{-i(k_{sx}x - k_{sz}z - \omega t)} \quad (2.23b)$$

and similar expressions for the transmitted waves except that there are no reflected waves in the second medium. So, the transmitted p-wave ϕ' has the form

$$\phi' = A_t e^{-i(k'_{px}x - k'_{pz}z - \omega t)} \quad (2.23c)$$

where

$$k'_{px} = \frac{\omega}{c}, \quad k'_{pz} = \frac{\omega}{\alpha'}$$

and α' is the phase velocity for the transmitted p-wave.

The transmitted s-wave ψ' has the form

$$\psi' = B_t e^{-i(k'_{sx}x - k'_{sz}z - \omega t)} \quad (2.23d)$$

where

$$k'_{sx} = \frac{\omega}{c}, \quad k'_{sz} = \frac{\omega}{\beta'}$$

and β' is the phase velocity for the transmitted s-wave.

The reflected and transmitted waves of either kind must satisfy some boundary conditions (B.C.) on the stress and strain.

Before we solve for the boundary conditions we are going to develop a generalized form for Snell's Law that relates different angles of emergence to the different wave velocities.

Assuming a steady state solution, then B.C. are independent of time

$t \rightarrow$ frequency $\omega = \text{constant}$ and B.C. are independent of position $x \rightarrow$ the x -component of the wave vector $k = \text{const.}$

$$k = k_{px} = k'_{px} = k_{sx} = k'_{sx} = \text{const.} \quad (2.24a)$$

or
$$k_p \cos \theta_p = k'_p \cos \theta'_p = k_s \cos \theta_s = k'_s \cos \theta'_s$$

$$(\theta_{pr} = \theta_{pi} = \theta_p)$$

or
$$\frac{\omega}{\alpha} \cos \theta_p = \frac{\omega}{\alpha'} \cos \theta'_p = \frac{\omega}{\beta} \cos \theta_s = \frac{\omega}{\beta'} \cos \theta'_s = \frac{\omega}{c}$$

where
$$c = \frac{\alpha}{\cos \theta_p} = \frac{\alpha'}{\cos \theta'_p} = \frac{\beta}{\cos \theta_s} = \frac{\beta'}{\cos \theta'_s} \quad (2.24b)$$

and c is the phase velocity along the interface.

This generalized Snell's Law can be derived also as a result of requiring that the projections of the wave fronts on the x -axis travel with the same phase velocity c along the interface.

Consider a special example of liquid/liquid interface. An incident p -wave of wave length λ , which is the distance between successive wave fronts, meets the x -axis which represents a discontinuity in the medium. Part of the wave is reflected, and the other part transmitted such that wave fronts have the same projections along the interface. Let t be the time interval between successive wave fronts which are shown in Figure 4.

For the reflected p -wave consider the two triangles QPO and STO .

$$QO = SO = ct$$

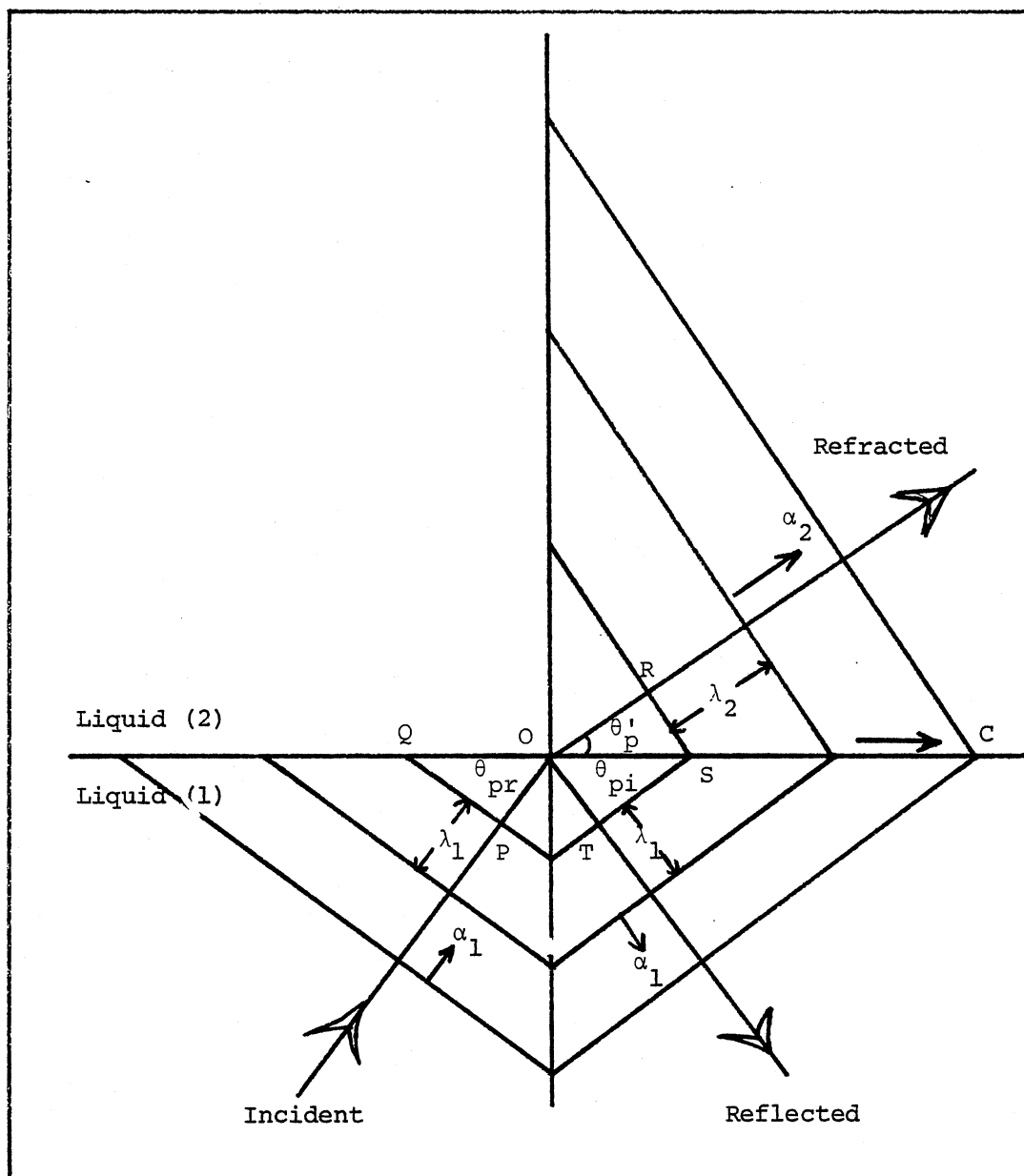


Figure 4. Phase Velocity Along the Interface of Mode Converted Waves

and

$$PO = TO = \alpha t$$

$$\therefore \theta_{pr} = \theta_{pi} = \theta_p$$

$$\begin{aligned} \tan \theta_p &= \frac{PQ}{PO} = \frac{\sqrt{c^2 t^2 - \alpha^2 t^2}}{\alpha t} \\ &= \sqrt{\left(\frac{c}{\alpha}\right)^2 - 1} \end{aligned} \quad (2.25a)$$

and

$$\cos(\theta_p) = \frac{\alpha t}{ct} = \frac{\alpha}{c}$$

or

$$\alpha = \frac{c}{\cos(\theta_p)}$$

For the transmitted p-wave consider the triangle ORS

$$OS = ct$$

and

$$OR = \alpha' t$$

$$\begin{aligned} \tan \theta'_p &= \frac{RS}{RO} = \frac{\sqrt{c^2 t^2 - \alpha'^2 t^2}}{\alpha' t} \\ &= \sqrt{\left(\frac{c}{\alpha'}\right)^2 - 1} \end{aligned} \quad (2.25b)$$

and

$$\cos \theta'_p = \frac{\alpha' t}{ct} = \frac{\alpha'}{c}$$

or

$$c = \frac{\alpha'}{\cos \theta'_p}$$

Similar expressions will be found for the reflected and transmitted s-wave for the general case of solid/solid interface. So,

$$\tan \theta_s = \sqrt{\left(\frac{c}{\beta}\right)^2 - 1} \quad (2.25c)$$

or,
$$c = \frac{\beta}{\cos \theta_s}$$

and
$$\tan \theta'_s = \sqrt{\left(\frac{c}{\beta'}\right)^2 - 1} \quad (2.25d)$$

or,
$$c = \frac{\beta'}{\cos \theta'_s}$$

So, by using simple geometry we were able to derive the generalized Snell's Law

$$c = \frac{\alpha}{\cos \theta_p} = \frac{\alpha'}{\cos \theta'_p} = \frac{\beta}{\cos \theta_s} = \frac{\beta'}{\cos \theta'_s}$$

Boundary Conditions

The reflected and transmitted waves of both kinds (pressure-wave and shear-wave) have to satisfy the following B.C. on stress and strain along the interface of both media, i.e., the x-axis ($z=0$) in Figure 3.

Continuity of Tangential Displacement u

$$u|_{z=0} = u'|_{z=0} \quad (2.26a)$$

where

$$u = \frac{\partial \phi}{\partial x} - \frac{\partial \psi}{\partial z}$$

$$-ik(A_i + A_r) - ik b(B_i - B_r) = (A' + b'B')(-ik)$$

$$\text{or} \quad A_i + A_r + b(B_i - B_r) = A' + b'B' \quad (2.26b)$$

Continuity of Vertical Displacement ω

$$\omega|_{z=0} = \omega'|_{z=0} \quad (2.27a)$$

$$\text{where} \quad \omega = \frac{\partial \phi}{\partial z} + \frac{\partial \psi}{\partial x}$$

$$ik a(A_i - A_r) - ik(B_i + B_r) = ika'A' - ikB'$$

$$\text{or} \quad a(A_i - A_r) - (B_i + B_r) = a'A' - B' \quad (2.27b)$$

Continuity of Tangential Stress

$$\sigma_{zx} = \sigma'_{zx} \quad (2.28a)$$

$$\text{where} \quad \sigma_{zx} = \mu \epsilon_{zx}$$

$$= \mu \left(\frac{\partial \omega}{\partial x} + \frac{\partial \mu}{\partial z} \right)$$

$$= \mu \left\{ \frac{\partial}{\partial x} \left(\frac{\partial \psi}{\partial z} + \frac{\partial \psi}{\partial x} \right) + \frac{\partial}{\partial z} \left(\frac{\partial \psi}{\partial x} - \frac{\partial \psi}{\partial z} \right) \right\}$$

$$= \mu \left\{ 2 \frac{\partial^2 \psi}{\partial x \partial z} + \frac{\partial^2 \psi}{\partial x^2} - \frac{\partial^2 \psi}{\partial z^2} \right\}$$

$$\therefore \mu \left(2 \frac{\partial^2 \psi}{\partial x \partial z} + \frac{\partial^2 \psi}{\partial x^2} - \frac{\partial^2 \psi}{\partial z^2} \right) = \mu' \left(2 \frac{\partial^2 \psi'}{\partial x \partial z} + \frac{\partial^2 \psi'}{\partial x^2} - \frac{\partial^2 \psi'}{\partial z^2} \right)$$

$$\mu \{ 2(ik)^2 (-a) (A_i - A_r) + (-ik)^2 (B_i + B_r) - (ik)^2 b^2 (B_i + B_r) \}$$

$$= \mu' \{ 2(ik)^2 (-a') A' + (-ik)^2 B' - (ik)^2 b'^2 B' \}$$

$$\therefore \rho \beta^2 [2a(A_i - A_r) + (b^2 - 1)(B_i + B_r)] = \rho' \beta'^2 [2a' A' + (b'^2 - 1) B'] \quad (2.28b)$$

Continuity of Normal Stress at z

$$\sigma_{zz} = \sigma'_{zz}; \quad (2.29a)$$

where

$$\sigma_{zz} = \lambda \Delta + 2\mu \epsilon_{zz}$$

$$= \lambda \Delta^2 \phi + 2\mu \left(\frac{\partial \omega}{\partial z} \right)$$

$$= \lambda \nabla^2 \phi + 2\mu \left(\frac{\partial^2 \phi}{\partial z^2} + \frac{\partial^2 \psi}{\partial z \partial x} \right)$$

$$\lambda \nabla^2 \phi + 2\mu \left(\frac{\partial^2 \phi}{\partial z^2} + \frac{\partial^2 \psi}{\partial z \partial x} \right) = \lambda' \nabla'^2 \psi' + 2\mu' \left(\frac{\partial^2 \phi'}{\partial z^2} + \frac{\partial^2 \psi'}{\partial z \partial x} \right)$$

$$\lambda \{ (-k^2) (1+a^2) (A_i + A_r) \} + 2\mu \{ (-k^2) a^2 (A_i + A_r) + (-k^2) (-b) (B_i - B_r) \}$$

$$= \lambda' \{ (-k'^2) (1+a'^2) A' \} + 2\mu' \{ (-k'^2) a'^2 A' + (-k'^2) (-b') B' \}$$

$$\therefore \rho \left(\frac{\lambda+2\mu}{\rho} \right) a^2 (A_i + A_r) + \frac{\mu}{\rho} \frac{\lambda}{\mu} \rho (A_i + A_r) - 2 \frac{\mu b}{\rho} \rho (B_i - B_r)$$

$$= \left(\frac{\lambda'+2\mu'}{\rho'} \right) \rho' a'^2 A' + \frac{\mu' \lambda'}{\rho' \mu'} \rho' A' - 2 \frac{\mu' b'}{\rho'} \rho' B'$$

or

$$\rho [\alpha^2 a^2 (A_i + A_r) + \frac{\lambda}{\mu} \beta^2 (A_i + A_r) - 2b\beta^2 (B_i - B_r)]$$

$$= \rho' [\alpha'^2 a'^2 A' + \frac{\lambda'}{\mu'} \beta'^2 A' - 2b'\beta'^2 B']$$

but

$$\frac{\lambda}{\mu} = \frac{\lambda+2\mu}{\mu} - 2 = \frac{\alpha^2}{\beta^2} - 2,$$

$$\begin{aligned} \text{So, } & \rho[\alpha^2 a^2 (A_i + A_r) + (\frac{\alpha^2}{\beta^2} - 2) B^2 (A_i + A_r) - 2b\beta^2 (B_i - B_r)] \\ &= \rho'[\alpha'^2 a'^2 A' + (\frac{\alpha'^2}{\beta'^2} - 2) \beta'^2 A' - 2b'\beta'^2 B'] \end{aligned}$$

$$\begin{aligned} \therefore & \rho[(A_i + A_r) \{\alpha^2 a^2 + \alpha^2 - 2\beta^2\} - 2b\beta^2 (B_i - B_r)] \\ &= \rho'[A' \{\alpha'^2 a'^2 + \alpha'^2 - 2\beta'^2\} - 2b'\beta'^2 B'] \\ & \rho[(A_i + A_r) \{\alpha^2 (a^2 + 1) - 2\beta^2\} - 2b\beta^2 (B_i - B_r)] \\ &= \rho'[A' \{\alpha'^2 (a'^2 + 1) - 2\beta'^2\} - 2b'\beta'^2 B'] \end{aligned}$$

but

$$\begin{aligned} a^2 + 1 &= \tan^2 \theta_p + 1 = \sec^2 \theta_p, \\ \alpha^2 (a^2 + 1) &= \alpha^2 \sec^2 \theta_p = c^2 \end{aligned}$$

Similarly,

$$\alpha'^2 (a'^2 + 1) = \alpha'^2 \sec^2 \theta'_p = c^2$$

$$\begin{aligned}
\therefore \rho[(A_i + A_r) \{1 - 2 \frac{\beta^2}{c^2}\} - 2b \frac{\beta^2}{c^2} (B_i - B_r)] \\
= \rho'[A' \{1 - 2 \frac{\beta'^2}{c^2}\} - 2b' \frac{\beta'^2}{c^2} B']
\end{aligned}$$

but

$$\frac{c^2}{\beta^2} - 2 = b^2 - 1$$

and

$$\frac{c^2}{\beta'^2} - 2 = b'^2 - 1$$

$$\therefore \rho\beta^2[(A_i + A_r)(b^2 - 1) - 2b(B_i - B_r)] = \rho'\beta'^2[A'(b'^2 - 1) - 2b'B'] \quad (2.29b)$$

It seems that we have six unknowns and four equations, but

1. We have one type of incident wave, so for an incident p-wave $B_i = 0$, and for an incident s-wave $A_i = 0$.
2. We can normalize the amplitudes to the incident wave amplitude so we have ratios w.r.t. A_i or B_i .

So for an incident p-wave ($B_i = 0$) we have the following equations:

$$A_i + A_r - bB_r = A' + b'B' \quad (2.30a)$$

$$a(A_i - A_r) - B_r = a'A' - B' \quad (2.30b)$$

$$\rho\beta^2[2a(A_i - A_r) + (b^2 - 1)B_r] = \rho'\beta'^2[2a'A' + (b'^2 - 1)B'] \quad (2.30c)$$

$$\rho[(A_i + A_r) \{1 - \frac{2\beta^2}{c^2}\} + 2b \frac{\beta^2}{c^2} B_r] = \rho'[A'(1 - \frac{2\beta'^2}{c^2}) B'] \quad (2.30d)$$

and for an incident s-wave ($A_i = 0$) so we have the following equations.

$$A_r + b(B_i - B_r) = A' + b'B' \quad (2.31a)$$

$$aA_r - (B_i + B_r) = a'A' - B' \quad (2.31b)$$

$$\rho\beta^2[-2aA_r + (b^2 - 1)(B_i + B_r)] = \rho'\beta'^2[2a'A' + (b'^2 - 1)B'] \quad (2.31c)$$

$$\rho[A_r\{1 - 2\frac{\beta^2}{c^2}\} - 2b\frac{\beta^2}{c^2}(B_i - B_r)] = \rho'[A'\{1 - 2\frac{\beta'^2}{c^2}\} - 2b'\frac{\beta'^2}{c^2}B'] \quad (2.31d)$$

Partitioning of Energy

The disturbance caused by the traveling waves induces the particles of the medium to possess both types of energy (kinetic and potential). Because the displacement is harmonic, the total energy can be found using maximum potential energy (i.e. when the displacement is maximum in magnitude) or the maximum kinetic energy. The total energy then is

$$E_T = (E_k)_{\max} = \frac{1}{2} \rho (\mu_{\max}^2 + \omega_{\max}^2) \quad (2.32)$$

where this is the kinetic energy per unit volume for the dilation mode.

$$\text{Incident p-wave } \psi_{\text{in}} = A_i e^{ik(ct - x + az)}$$

$$u_i^{(p)} = \frac{\partial \psi_i}{\partial x} = -ik \psi_i$$

$$\dot{u}_i^{(p)} = \frac{\partial u}{\partial t} = \frac{\partial^2 \phi_i}{\partial t \partial x} = -C(ik)^2 \phi_i = ck^2 \phi_i \quad (2.33a)$$

$$\omega^{(d)} = \frac{\partial \phi_i}{\partial z} = a(ik) \phi_i$$

$$\dot{\omega}_i^{(d)} = \frac{\partial \omega_i^{(d)}}{\partial t} = \frac{\partial^2 \phi_i}{\partial t \partial z} = ac(ik)^2 \phi_i = -cak^2 \phi_i \quad (2.33b)$$

$$\begin{aligned} \therefore E_i^{(d)} &= (E_{k_i}^{(d)})_{\max} = \frac{1}{2} \rho [(ck^2)^2 + (-cak^2)^2] A_i^2 \\ &= \frac{1}{2} \rho c^2 k^4 (1+a^2) A_i^2 \\ &= \frac{1}{2} \frac{\rho c^2 k^2}{\omega^2} \frac{\omega^2}{\alpha^2} \cos^2 \theta_p \sec^2 \theta_p A_i^2 \\ &= \frac{1}{2} \rho \frac{\omega^4}{\alpha^2} A_i^2 \end{aligned} \quad (2.33c)$$

Power incident per unit area = $U_{\text{normal}} \cdot E_{\text{in}}$

$$\begin{aligned} &= (\alpha \sin \theta_p) \frac{1}{2} \rho \frac{\omega^4}{\alpha^2} A_i^2 \\ &= \frac{1}{2} \rho \frac{\omega^4}{\alpha} A_i^2 \end{aligned} \quad (2.33d)$$

For the reflected p-wave:

$$\psi_r = A_r e^{ik(ct-x-az)}$$

so similarly,

$$E_r^{(p)} = \frac{1}{2} \rho \frac{\omega^4}{\alpha} A_r^2 \quad (2.34a)$$

and

$$P_r^{(p)} = \frac{1}{2} \rho \frac{\omega^4}{\alpha} \sin^2 \theta_p A_r^2 . \quad (2.34b)$$

For the transmitted p-wave:

$$\phi_t = A_c e^{ik(ct-x+a'z)}$$

$$E_t^{(p)} = \frac{1}{2} \rho' \frac{\omega^4}{\alpha'^2} A_t^2 \quad (2.34c)$$

and

$$P_t^{(p)} = \frac{1}{2} \rho' \frac{\omega^4}{\alpha'} \sin^2 \theta'_p A_t^2 . \quad (2.34d)$$

For the reflected s-wave:

$$\psi_r = B_r e^{ik(ct-x-bz)}$$

$$E_r^{(s)} = \frac{1}{2} \rho \frac{\omega^4}{\beta^2} B_r^2 , \quad (2.35a)$$

$$P_r^{(s)} = \frac{1}{2} \rho \frac{\omega^4}{\beta} \sin^2 \theta_s B_r^2 \quad (2.35b)$$

For the transmitted s-wave:

$$\psi_t = B' e^{ik(ct-x+b'z)}$$

$$E_t^{(s)} = \frac{1}{2} \rho' \frac{\omega^4}{\beta'^2} B'^2 \quad (2.35c)$$

$$P_t^{(s)} = \frac{1}{2} \rho' \frac{\omega^4}{\beta'} \sin\theta'_s B'^2 \quad (2.35d)$$

Due to conservation of energy the power per unit area in the z-direction is conserved.

$$P_i^{(p)} = P_r^{(p)} + P_r^{(s)} + P_t^{(p)} + P_t^{(s)} \quad (2.36)$$

or

$$\begin{aligned} \frac{1}{2} \rho \frac{\omega^4}{\alpha} \sin\theta_p A_i^2 &= \frac{1}{2} \rho \frac{\omega^4}{\alpha} \sin\theta_p A_r^2 + \frac{1}{2} \rho' \frac{\omega^4}{\alpha'} \sin\theta'_p A_t^2 \\ &+ \frac{1}{2} \rho \frac{\omega^4}{\beta} \sin\theta_s B_r^2 + \frac{1}{2} \rho' \frac{\omega^4}{\beta'} \sin\theta'_s B'^2 \end{aligned}$$

or by normalizing the energies w.r.t. the incident energy

$$\begin{aligned} 1 &= \left(\frac{A_r}{A_i}\right)^2 + \frac{\rho'}{\rho} \frac{\alpha}{\alpha'} \frac{\sin\theta'_p}{\sin\theta_p} \left(\frac{A_t}{A_i}\right)^2 + \frac{\alpha}{\beta} \frac{\sin\theta_s}{\sin\theta_p} \left(\frac{B_r}{A_i}\right)^2 + \frac{\rho'}{\rho} \frac{\alpha}{\beta'} \frac{\sin\theta'_s}{\sin\theta_p} \left(\frac{B'}{A_i}\right)^2 \\ &= \xi_r^2 + \xi_t^2 + \eta_r^2 + \eta_t^2 \end{aligned} \quad (2.37)$$

where:

$$\begin{aligned} \xi_r &= \frac{A_r}{A_i}, \quad \xi_t = \sqrt{\frac{\rho'}{\rho} \frac{\alpha}{\alpha'} \frac{\sin\theta'_p}{\sin\theta_p}} \frac{A_r}{A_i} \\ \eta_r &= \sqrt{\frac{\alpha}{\beta} \frac{\sin\theta_s}{\sin\theta_p}} \frac{B_r}{A_i}, \quad \eta_t = \sqrt{\frac{\rho'}{\rho} \frac{\alpha}{\beta'} \frac{\sin\theta'_s}{\sin\theta_p}} \frac{B'}{A_i}. \end{aligned} \quad (2.38)$$

where ξ_r , ξ_t , η_r , and η_t are the square root of energy for the reflected

p-wave, transmitted p-wave, reflected s-wave and transmitted s-wave respectively for an incident p-wave of unit energy. But since

$$C = \frac{\alpha}{\cos\theta_p} = \frac{\alpha'}{\cos\theta'_p} = \frac{\beta}{\cos\theta_s} = \frac{\beta'}{\cos\theta'_s}$$

$$\therefore \frac{\alpha}{\beta} = \frac{\cos\theta_p}{\cos\theta_s}, \frac{\alpha}{\alpha'} = \frac{\cos\theta_p}{\cos\theta'_p}, \frac{\alpha}{\beta'} = \frac{\cos\theta_p}{\cos\theta'_s}$$

so we can write the relative square root energies as follows:

$$\xi_r = \frac{A_r}{A_i} \quad (2.39a)$$

$$\xi_t = \sqrt{\frac{\rho'a'}{\rho a}} \frac{A_t}{A_i} \quad (2.39b)$$

$$\eta_r = \sqrt{\frac{b}{a}} \frac{B_r}{A_i} \quad (2.39c)$$

and

$$\eta_t = \sqrt{\frac{\rho'b'}{\rho a}} \frac{B_t}{A_i} \quad (2.39d)$$

After solving for the square root of energies of the reflected and transmitted plane waves as a function of the corresponding angles, i.e.

$$\xi_r(\theta_p), \xi_t(\theta'_p), \eta_r(\theta_s), \text{ and } \eta_t(\theta'_s)$$

we will present them in polar plots to show their directivity patterns in a concise way.

Then some linear plot is presented of the geophone response of the reflected waves as a function of offset, as discussed later for different interfaces.

CHAPTER III

MODE CONVERSION DUE TO AN INCIDENT 'P-WAVE'

AT A PLANE INTERFACE

When a plane wave of either type (pressure-wave or shear-wave) meets a discontinuity in the medium in which it is propagating part of it is reflected and part of it is transmitted, besides that a wave of the other type (shear wave for an incident pressure wave and a pressure wave for an incident shear wave) is reflected and transmitted as well. This mode converted wave is necessary to satisfy the boundary conditions at the interface.

I will be discussing all possible cases of interfaces, starting with the simple case of solid/vacuum interface where all waves are reflected and no waves are transmitted, then to liquid/liquid interface where only p-wave exists then to liquid/solid interface where no s-wave is reflected, next to solid-liquid interface where no s-wave is transmitted and finally to the most general case of solid/solid interface where an incident 'p-wave' will produce four waves; reflected and transmitted waves of both types of waves.

In this chapter all cases are taken where the incident wave has a phase velocity that is higher than all other wave-velocities, so we avoided the possibility of any critical angle, but the following chapter, Chapter IV, is devoted for critical angles and the associated total reflections.

Solid/Vacuum Interface

Boundary conditions that must be satisfied are:

1. Vanishing of tangential stresses, and
2. Vanishing of normal stresses.

In other words, no disturbance can transfer across the boundary so there are no transmitted waves as shown in Figure 5. Using solutions that were found for the general case:

1. $\sigma_{zx} = \sigma'_{zx}; \sigma'_{zx} = 0$ in the liquid.

$$\rho\beta^2[2a(A_i - A_r) + (b^2 - 1)(B_i + B_r)] = 0$$

$B_i = 0$ for an incident p-wave.

$$\therefore 2a(A_i - A_r) + (b^2 - 1)B_r = 0 \quad (3.1a)$$

2. $\sigma_{zz} = \sigma'_{zz}; \sigma'_{zz} = 0$ in the liquid.

$$\therefore \rho\beta^2[(A_i + A_r)(b^2 - 1) + 2b B_r] = 0$$

or $(A_i + A_r)(b^2 - 1) + 2b B_r = 0 \quad (3.1b)$

we can solve for $\frac{A_r}{A_i}$ and $\frac{B_r}{A_i}$ from these equations (3.1a,b).

$$\frac{A_r}{A_i} = \frac{4ab - (b^2 - 1)^2}{4ab + (b^2 - 1)^2}, \quad (3.2a)$$

$$\frac{B_r}{A_i} = \frac{4a(b^2 - 1)}{4ab + (b^2 - 1)^2} \quad (3.2b)$$

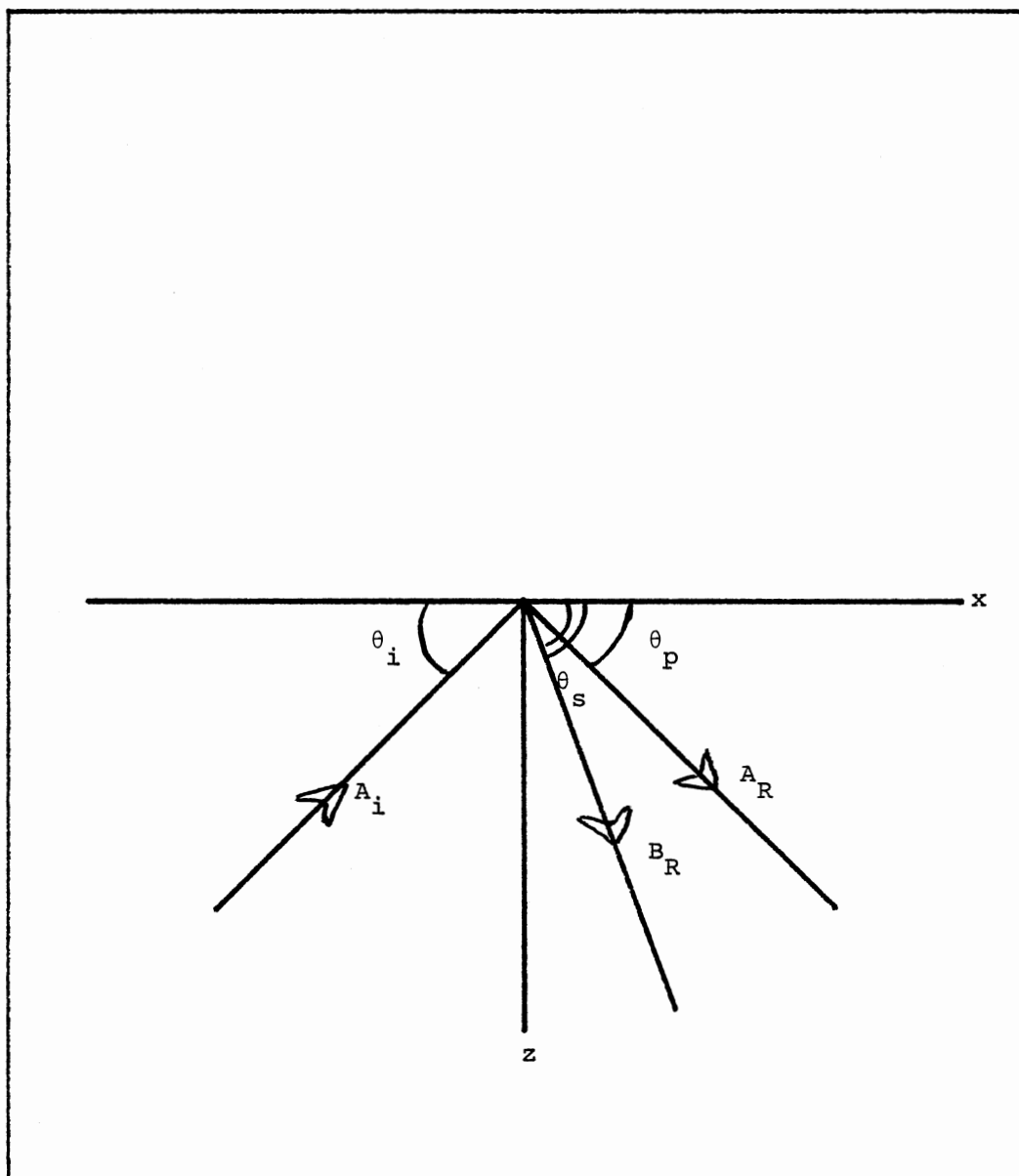


Figure 5. Reflection of Incident P-Wave at Free Surface of Elastic Solid

Using Equation (2.12) (relations for square roots of energies),

$$\xi_r = \frac{A_r}{A_i} = \frac{4ab - (b^2 - 1)^2}{4ab + (b^2 - 1)^2}, \quad (3.3a)$$

$$\eta_r = \sqrt{\frac{b}{a}} \frac{B_r}{A_i} = - \sqrt{\frac{b}{a}} \frac{4a(b^2 - 1)}{4ab + (b^2 - 1)^2} \quad (3.3b)$$

Noting that $\xi_r^2 + \eta_r^2$ should be equal to 1. Use Equation (3.3a and 3.3b) to show this.

$$\begin{aligned} \xi_r^2 + \eta_r^2 &= \left\{ \frac{4ab - (b^2 - 1)^2}{4ab + (b^2 - 1)^2} \right\}^2 + \left(- \sqrt{\frac{b}{a}} \right)^2 \left\{ \frac{4a(b^2 - 1)}{4ab + (b^2 - 1)^2} \right\}^2 \\ &= \frac{(4ab)^2 - 8ab(b^2 - 1)^2 + (b^2 - 1)^4 + 16ab(b^2 - 1)^2}{\{4ab + (b^2 - 1)^2\}^2} \\ &= 1 \text{ (conservation of normal energy flux)} \end{aligned} \quad (3.3c)$$

The above equations were derived for any general elastic solid, but in some literature they took the special case where $\lambda = \mu$, or

$$\text{Poisson's ratio } \sigma = 0.25 \quad \left(\sigma = \frac{\lambda}{2(\lambda + \mu)} \right)$$

as the case for most solids.

If $\lambda = \mu$, then

$$\frac{\alpha^2}{\beta^2} = \frac{\lambda + 2\mu}{\mu} = 3 \quad (3.4a)$$

but since

$$c = \alpha \sec \theta_p = \beta \sec \theta_s \quad (\text{Generalized Snell's Law})$$

$$\therefore \sec^2 \theta_s = \frac{\alpha^2}{\beta^2} \sec^2 \theta_p$$

$$= 3 \sec^2 \theta_p$$

$$\text{or} \quad (1+b^2) = 3(1+a^2)$$

$$\therefore b^2 - 1 = 1 = 3a^2 \quad (3.4b)$$

$$\text{so,} \quad \frac{A_r}{A_i} = \frac{4ab - (1 + 3a^2)^2}{4ab + (1 + 3a^2)^2} \quad (3.5a)$$

$$\text{and} \quad \frac{B_r}{A_i} = - \frac{4a(1 + 3a^2)}{4ab + (1 + 3a^2)^2} \quad (3.5b)$$

For normal incidence ($\theta_p = 90^\circ$)

$$\cos \theta_s = (\beta/\alpha) \cos \theta_p = 0 \rightarrow \theta_s = 90^\circ$$

$$(a^2 + 1)\alpha^2 = (b^2 + 1)\beta^2 \quad (3.6a)$$

$$a^2 \alpha^2 \approx b^2 \beta^2$$

$$\text{or} \quad b \approx \frac{\alpha}{\beta} a \quad (3.6b)$$

$$\lim_{\theta_p \rightarrow 90^\circ} \frac{A_r}{A_i} = \lim_{a, b \rightarrow \infty} \frac{4ab - (b^2 - 1)^2}{4ab + (b^2 - 1)^2}$$

$$\begin{aligned}
&= \lim_{a \rightarrow \infty} \frac{4a(\alpha/\beta)a - \{(\alpha^2/\beta^2)a^2\}^2}{4a(\alpha/\beta)a + (\alpha^2/\beta^2)a^2} \\
&= -1
\end{aligned} \tag{3.7a}$$

$$\begin{aligned}
\lim_{\theta_p \rightarrow 90^\circ} \frac{B_r}{A_i} &= \lim_{a, b \rightarrow \infty} \frac{-4a(b^2-1)}{4ab + (b^2-1)^2} \\
&= \lim_{a \rightarrow \infty} \frac{-4a(\alpha^2/\beta^2)a^2}{4a(\alpha/\beta)a + (\alpha^2/\beta^2)a^2} \\
&= \lim_{a \rightarrow \infty} \frac{a^3(-\alpha^2/\beta^2)}{a^2(4\alpha/\beta) + a^4(\alpha^4/\beta^4)} = 0
\end{aligned} \tag{3.7b}$$

For grazing incidence:

$$\theta_p = 0 \rightarrow a = \tan \theta_p = 0,$$

$$\cos \theta_s = (\beta/\alpha) \cos \theta_p = \beta/\alpha \text{ or } \sec \theta_s = \alpha/\beta$$

$$b^2 = \tan^2 \theta_s = \sec^2 \theta_s - 1 = \alpha^2/\beta^2 - 1 \rightarrow b^2 - 1 = \frac{\alpha^2}{\beta^2} - 2 = \frac{\lambda}{\mu} > 0$$

$$\text{so } b = \sqrt{\alpha^2/\beta^2 - 1} > 0 \tag{3.7c}$$

$$\begin{aligned}
\lim_{\theta_p \rightarrow 0} \frac{A_r}{A_i} &= \lim_{\theta_p \rightarrow 0} \frac{4ab - (b^2-1)^2}{4ab + (b^2-1)^2} \\
&= -1
\end{aligned} \tag{3.8a}$$

$$\lim_{\theta_p \rightarrow 0} \frac{B_r}{A_i} = \lim_{a \rightarrow 0} \frac{-4a(b^2-1)}{4ab + (b^2-1)^2}$$

$$= 0 \quad (3.8b)$$

So we have total reflection for grazing and normal incidence, and the mode converted "S-wave" vanishes in these two cases.

Reflected "P-Wave" Vanishes

If
$$4ab = (b^2 - 1)^2$$

for the special case when $\lambda = \mu$ ($b^2 - 1 = 3a^2 + 1$) it reduces to $16a^2(3a^2 + 2) = (3a^2 + 1)^4$ which has two positive roots

$$a_1 = 0.2272 \rightarrow \theta_{p_1} = 12^\circ 48' ,$$

$$a_2 = 0.5773 \rightarrow \theta_{p_2} = 30^\circ$$

Liquid/Liquid Interface

Liquids don't resist any shear stress ($\mu = \mu' = 0$) so S-wave can't propagate in liquids ($\beta = \beta' = 0$). Hence all S-wave coefficients vanishes $B_i = B_r = B' = 0$ but $b \rightarrow \infty$ as $\beta \rightarrow 0$ such that $b^2 \beta^2 \rightarrow \alpha^2 \sin^2 \theta_p = c^2$ since $c^2 = \alpha^2 \sin^2 \theta_p = \beta^2 \sin^2 \theta_s = \beta^2 (1 + b^2) = \beta'^2 (1 + b'^2)$ while $b\beta^2 \rightarrow 0$, $b'\beta'^2 \rightarrow 0$.

Boundary Conditions

1. Continuity of normal displacement, and
2. Continuity of normal stress.

So, from the equations that we have derived for the general case (2.27b)

$$a(A_i - A_r) - (B_i^0 + B_r^0) = a'A' - B^0, \text{ or}$$

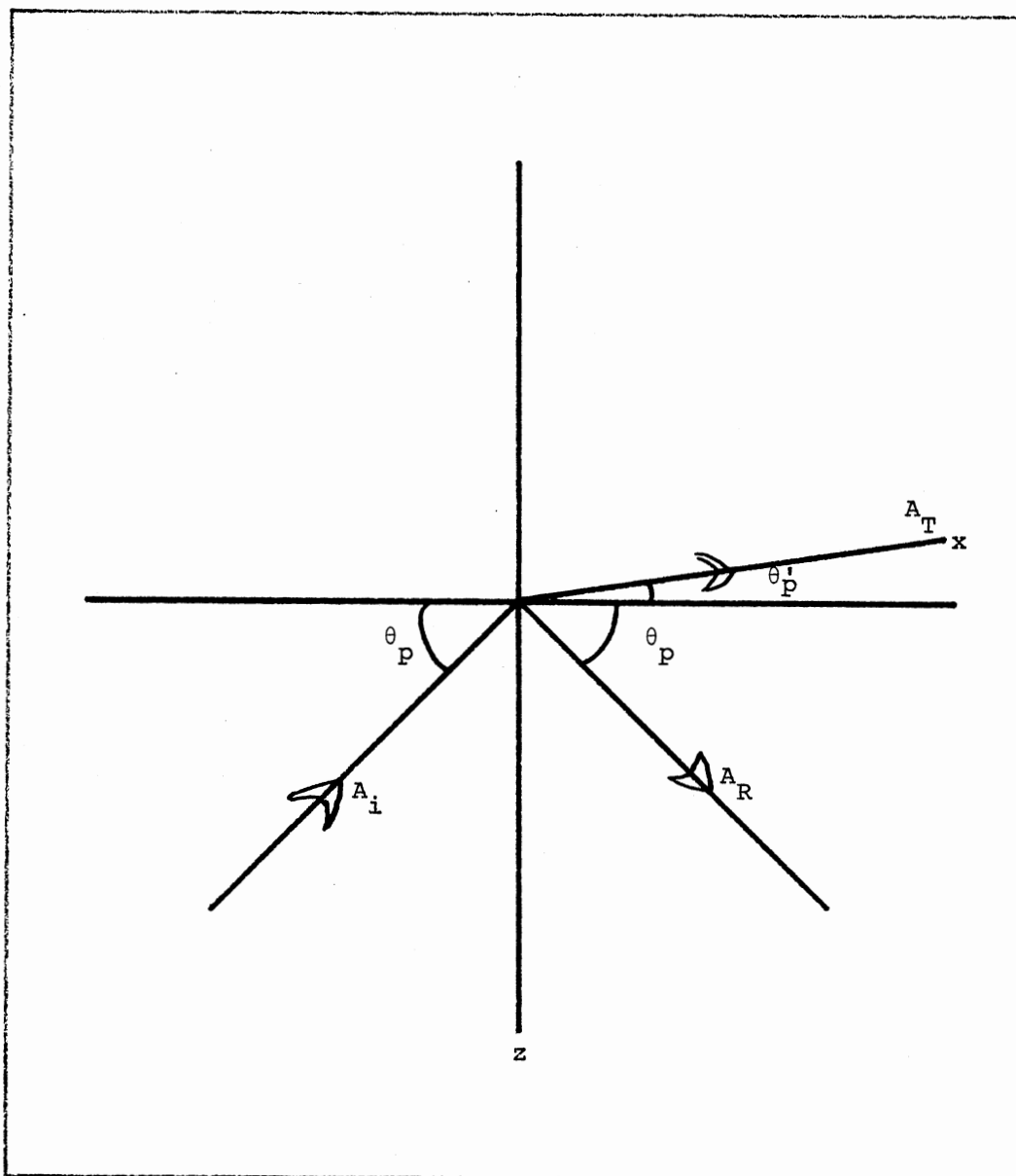


Figure 6. Reflection and Refraction of Incident P-Wave at Liquid/
Liquid Interface

$$a(A_i - A_r) = a'A' , \quad (3.9a)$$

Eq. (2.29b)

$$\begin{aligned} & \rho\beta^2[(A_i + A_r)(b^2 - 1) - 2b(\beta_i^0 - \beta_r^0)] \\ &= \rho'\beta'^2[A'(b'^2 - 1) - 2b'B'^0] \end{aligned}$$

or
$$\rho\beta^2(b^2 - 1)(A_i + A_r) = \rho'\beta'^2(b'^2 - 1)A'$$

since as $b \rightarrow \infty$, $b' \rightarrow \infty$ $c^2 = \beta^2 b^2 = \beta'^2 b'^2$

$$\therefore \rho(A_i + A_r) = \rho'A' \quad (3.9b)$$

Solving 3.9a and 3.9b we have

$$\begin{aligned} \frac{A_r}{A_i} &= \frac{\rho'a - \rho a'}{\rho'a + \rho a'} \\ &= \frac{\rho'/\rho - a'/a}{\rho'/\rho + a'/a} \end{aligned} \quad (3.10a)$$

and

$$\begin{aligned} \frac{A'}{A_i} &= \frac{2a\rho}{\rho a' + \rho'a} \\ &= \frac{2}{\rho'/\rho + a'/a} \end{aligned} \quad (3.10b)$$

Partitioning of the energy for the reflected P-wave:

$$\xi_r = \frac{A_r}{A_i} = \frac{\rho'/\rho - a'/a}{\rho'/\rho + a'/a} \quad (3.11a)$$

For the transmitted "P-wave",

$$\begin{aligned} \xi_t &= \sqrt{\frac{\rho' a'}{\rho a}} \frac{A_t}{A_i} \\ &= \sqrt{\frac{\rho' a'}{\rho a}} \frac{2}{\rho'/\rho + a'/a} ; \end{aligned} \quad (3.11b)$$

To insure the conservation of normal energy flux,

$$\begin{aligned} \xi_r^2 + \xi_t^2 &= \frac{(\rho'/\rho - a'/a)^2}{(\rho'/\rho + a'/a)^2} + \frac{\rho' a'}{\rho a} \frac{4}{(\rho'/\rho + a'/a)^2} \\ &= \frac{(\rho'/\rho)^2 + (a'/a)^2 - 2(\rho'/\rho)(a'/a) + 4(\rho'/\rho)(a'/a)}{(\rho'/\rho + a'/a)^2} \\ &= 1 \end{aligned} \quad (3.12)$$

(That verifies the conservation of normal energy flux).

For normal incidence:

$$\theta_p = 90^\circ \rightarrow \cos \theta'_p = \frac{\alpha'}{\alpha} \cos \theta_p = 0$$

$$\therefore \theta'_p = 90^\circ$$

$$\text{so as } \theta_p \rightarrow 90^\circ \quad \theta'_p \rightarrow 90^\circ \quad \text{and } a, a' \rightarrow \infty$$

so since

$$\alpha^2 \sec^2 \theta_p = \alpha'^2 \sec^2 \theta'_p$$

$$\alpha^2 (1+a^2) = \alpha'^2 (1+a'^2) \quad (3.13a)$$

$$\therefore \alpha^2 a^2 = \alpha'^2 a'^2$$

or

$$\frac{a'}{a} = \frac{\alpha}{\alpha'} \quad (3.13b)$$

so

$$\lim_{\theta_p \rightarrow 90^\circ} \frac{A_r}{A_i} = \lim_{a, a' \rightarrow \infty} \frac{\rho'/\rho - a'/a}{\rho'/\rho + a'/a}$$

$$= \frac{\rho'/\rho - \alpha/\alpha'}{\rho'/\rho + \alpha/\alpha'}$$

or

$$\frac{A_r}{A_i} = \frac{\rho'\alpha' - \rho\alpha}{\rho'\alpha' + \rho\alpha} \quad (3.14a)$$

$$= \frac{Z' - Z}{Z' + Z} ; Z = \rho\alpha \text{ is the impedance of the medium}$$

$$\lim_{\theta'_p \rightarrow 90^\circ} \frac{A_t}{A_i} = \lim_{a, a' \rightarrow \infty} \frac{2}{\rho'/\rho + a'/a}$$

$$= \frac{2}{\rho'/\rho + \alpha/\alpha'}$$

$$= \frac{2 \rho\alpha'}{\rho'\alpha' + \rho\alpha} \quad (3.14b)$$

For grazing incidence:

$$\theta_p = 0 \rightarrow \cos \theta'_p = \frac{\alpha'}{\alpha} \cos \theta_p = \frac{\alpha'}{\alpha}$$

$$a = \tan \theta_p = 0, \quad a'^2 = \tan^2 \theta'_p = \left(\frac{\alpha}{\alpha'}\right)^2 - 1$$

We are considering the case for $\alpha > \alpha'$. The other case is delayed to the discussion of total reflection in the next chapter.

$$\begin{aligned} \lim_{\theta_p \rightarrow 0} \frac{A_r}{A_i} &= \lim_{\substack{a \rightarrow 0 \\ (a' \text{ is finite}) \\ \neq 0}} \frac{\rho' a - \rho a'}{\rho' a + \rho a'} \\ &= -1 \end{aligned} \quad (3.15a)$$

(so we have a total reflection for grazing incidence and $\alpha > \alpha'$ with a phase shift of π);

$$\begin{aligned} \lim_{\theta_p \rightarrow 0} \frac{A_t}{A_i} &= \lim_{\substack{a \rightarrow 0 \\ (a' \text{ is finite}) \\ \neq 0}} \frac{2a\rho}{a'\rho + a\rho'} = 0 \end{aligned} \quad (3.15b)$$

Liquid/Solid Interface

For the case of liquid solid interface slippage can occur, so tangential displacement is not continuous and tangential stresses has to vanish at the boundary.

From the equations that we derived for the general case:

1. Continuity of normal displacement.

$$\begin{aligned} a(A_i - A_r) - (B_i \rightarrow 0 + B_r \rightarrow 0) &= a'A' - B' \\ \therefore a(A_i - A_r) &= a'A' - B' \end{aligned} \quad (3.16a)$$

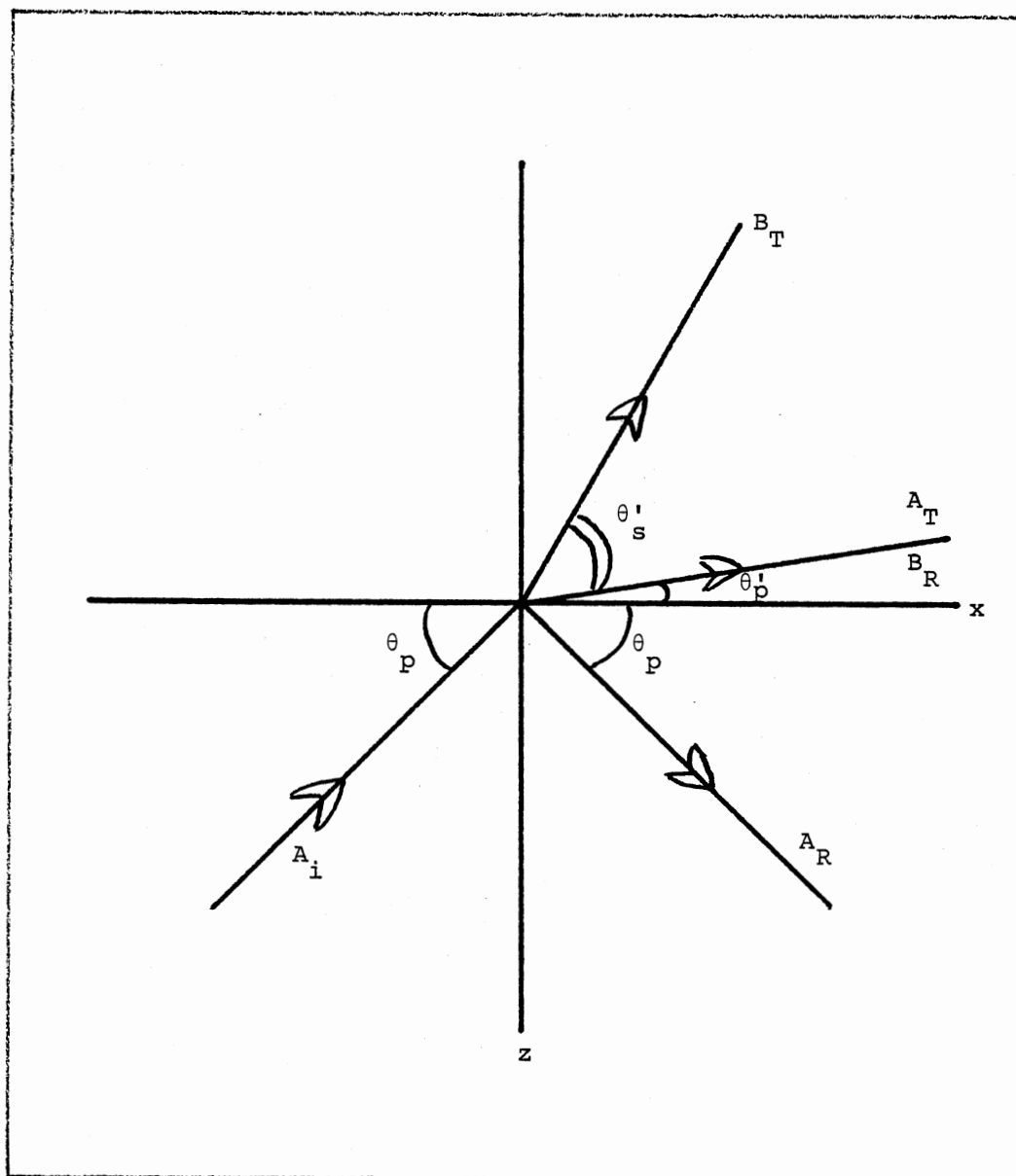


Figure 7. Reflection and Refraction of Incident P-Wave at Liquid/Solid Interface

2. Continuity of tangential stress

$$\sigma_{zx} = \sigma'_{zx} = 0 \text{ at } z = 0$$

$$\therefore 0 = \rho' \beta'^2 [2a'A' + (b'^2 - 1)B']$$

$$\text{or} \quad 2a'A' + (b'^2 - 1) B' = 0 \dots \quad (3.16b)$$

3. Continuity of normal stress

$$\therefore \rho \beta^2 [(A_i + A_r)(b^2 - 1) - 2b(B_i \rightarrow 0 - B_r \rightarrow 0)]$$

$$= \rho' \beta'^2 [A'(b'^2 - 1) - 2b'B']$$

$$\beta \rightarrow 0 \text{ but } b \rightarrow \infty \text{ such that } \beta b \rightarrow c$$

$$\therefore \rho c^2 (A_i + A_r) = \rho' \beta'^2 [A'(b'^2 - 1) - 2b'B']$$

$$\text{or} \quad A_i + A_r = \frac{\rho'}{\rho} \frac{\beta'^2}{c^2} [A'(b'^2 - 1) - 2b'B'] \quad (3.16c)$$

These equations can be written as follows:

$$\frac{A_r}{A_i} + \frac{a'}{a} \frac{A'}{A_i} - \frac{1}{a} \frac{B'}{A_i} = 1 \quad (3.17a)$$

$$0 \frac{A_r}{A_i} + 2a' \frac{A'}{A_i} + (b'^2 - 1) \frac{B'}{A_i} = 0 \quad (3.17b)$$

$$\frac{A_r}{A_i} = \frac{\rho' \beta'^2}{\rho c^2} (b'^2 - 1) \frac{A'}{A_i} + \frac{2b' \rho'}{\rho} \frac{\beta'^2}{c^2} \frac{B'}{A_i} = 1 \quad (3.17c)$$

or is the matrix form $\underline{A} \underline{X} = \underline{B}$

$$\begin{bmatrix} a_{11} & a_{12} & a_{13} \\ a_{21} & a_{22} & a_{23} \\ a_{31} & a_{32} & a_{33} \end{bmatrix} \begin{bmatrix} A_r/A_i \\ A_t/A_i \\ B'/A_i \end{bmatrix} = \begin{bmatrix} 1 \\ 0 \\ -1 \end{bmatrix} \quad (3.18)$$

where:

$$\begin{aligned} a_{11} &= 1, & a_{12} &= a'/a, & a_{13} &= -1/a \\ a_{21} &= 0, & a_{22} &= 2a', & a_{23} &= (b'^2 - 1) \\ a_{31} &= 1, & a_{32} &= \frac{-\rho'}{\rho} \frac{\beta'^2}{c^2} (b'^2 - 1), & a_{33} &= 2b' \frac{\rho'}{\rho} \frac{\beta'^2}{c^2} \end{aligned} \quad (3.19)$$

Noting the following that we are dealing here with just three cases that is:

1. For normal incidence,
2. For grazing incidence,
3. For oblique incidence; but we are considering the case when all the coefficients (a' , b') are real.

The first two cases [(a) and (b)] are solved algebraically avoiding any singularity that may happen for $\theta = \pi/2$ or $\theta = 0^\circ$.

The other two cases where a' is imaginary but not b' or both a' and b' are imaginary are treated in the next chapter of total reflections

and critical angles.

As an illustration we solve for A_r , A' and B' to obtain

$$A_i - A_r = \frac{a'}{a} A' - \frac{1}{a} B' \quad (3.20a)$$

$$B' = \frac{-2a'}{(b'^2-1)} A' \quad (3.20b)$$

$$A_i + A_r = \frac{\rho' \beta'^2}{\rho C^2} (b'^2-1) A' - 2b' \frac{\rho'}{\rho} \frac{\beta'^2}{C^2} B' \quad (3.20c)$$

By adding Equations (3.20a) and (3.20c) and substituting for B' from (3.20b)

$$2A_i = A' \left[\frac{\rho' \beta'^2}{\rho C^2} (b'^2-1) + \frac{a'}{a} - (2b' \frac{\rho'}{\rho} \frac{\beta'^2}{C^2} + \frac{1}{a}) \left(\frac{-2a'}{b'^2-1} \right) \right],$$

or

$$A_i \{ 2a\rho C^2 (b'^2-1) \} = A' [\rho' \beta'^2 (b'^2-1)^2 a + a' \rho C^2 (b'^2-1) + 4aa'b' \rho' \beta'^2 + 2a' \rho C^2]$$

or

$$\frac{A'}{A_i} = \frac{2a\rho C^2 (b'^2-1)}{\rho' \beta'^2 a [(b'^2-1)^2 + 4a'b'] + a' \rho C^2 (b'^2+1)} \quad (3.21a)$$

$$= \frac{2a\rho C^2 (b'^2-1)}{a' \rho C^2 (b'^2+1) + a\rho' \beta'^2 \{ (b'^2-1)^2 + 4a'b' \}}$$

$$\therefore \frac{B'}{A_i} = \frac{4aa'\rho C^2}{a' \rho C^2 (b'^2+1) + a\rho' \beta'^2 \{ (b'^2-1)^2 + 4a'b' \}} \quad (3.21b)$$

$$\begin{aligned}
\frac{A_r}{A_i} &= 1 - \frac{a'}{a} \frac{A'}{A_i} + \frac{1}{a} \frac{B'}{A_i} \\
&= \frac{-\rho a' C^2 (b'^2 + 1) + a \rho' \beta'^2 \{ (b'^2 - 1)^2 + 4a'b' \}}{a' \rho C^2 (b'^2 + 1) + a \rho' \beta'^2 \{ (b'^2 - 1)^2 + 4a'b' \}} \quad (3.21c)
\end{aligned}$$

For normal incidence:

$$\theta_p = \frac{\pi}{2} \rightarrow \theta'_p \text{ and } \theta'_s = \frac{\pi}{2}$$

as $\theta_p \rightarrow \frac{\pi}{2}$ $a \rightarrow \infty$, $a' \rightarrow \infty$ and $b' \rightarrow \infty$.

So the identity $C^2 = \alpha^2 \sec^2 \theta_p = \alpha'^2 \sec^2 \theta'_p = \beta'^2 \sec^2 \theta'_s$ as $\theta_p \rightarrow \frac{\pi}{2}$

$$C^2 \approx \alpha^2 a^2 \approx \alpha'^2 a'^2 \approx \beta'^2 b'^2. \quad (3.22)$$

$$\therefore \lim_{\theta_p \rightarrow \frac{\pi}{2}} \frac{A'}{A_i} = \lim_{a, a', b' \rightarrow \infty} \frac{2a \rho C^2 (b'^2 - 1)}{a' \rho C^2 (b'^2 + 1) + a \rho' \beta'^2 [(b'^2 - 1)^2 + 4a'b']}$$

$$= \lim_{a \rightarrow \infty} \frac{2\rho a (\alpha^2 a^2) \left(\frac{\alpha^2}{\beta'^2} a^2 \right)}{(\alpha/\alpha' a) \rho (\alpha^2 a^2) \left(\alpha^2 \frac{a^2}{\beta'^2} \right) + a \rho' \beta'^2 \left[\left(\frac{\alpha^2}{\beta'^2} a^2 \right) + 4 \left(\frac{\alpha}{\alpha'} a \right) \left(\frac{\alpha}{\beta'} a \right) \right]}$$

$$= \lim_{a \rightarrow \infty} \frac{2\rho \frac{\alpha^4}{\beta'^2} a^5}{\rho' \beta'^2 \left[\frac{\alpha^4}{\beta'^2} a^5 + \frac{4\alpha^2}{\alpha' \beta'} a^3 \right] + \rho \frac{\alpha^5}{\alpha' \beta'^2} a^5}$$

$$= \lim_{a \rightarrow \infty} \frac{2\rho \alpha^4 / \beta^2}{\rho' \beta'^2 [\alpha^4 / \beta'^2 + \frac{4\alpha^2}{\alpha' \beta'}] + \rho \frac{\alpha^5}{\alpha' \beta'^2}}$$

$$\therefore \frac{A'}{A_i} = \frac{2}{\rho'/\rho + \alpha/\alpha'} \quad (3.23a)$$

$$\lim_{\theta \rightarrow 90^\circ} \frac{B'}{A_i} = \lim_{a, a', b' \rightarrow \infty} = \frac{4a a' \rho C^2}{a' \rho C^2 (b'^2 + 1) + a \rho' b'^2 [(b'^2 - 1)^2 + 4a' b']}$$

$$= \lim_{a \rightarrow \infty} \frac{-4a (\frac{\alpha}{\alpha'} a) \rho (\alpha^2 a^2)}{\rho (\alpha/\alpha' a) (\alpha^2 a^2) (\frac{\alpha^2}{\beta'^2} a^2) + \rho' b'^2 a [(\frac{\alpha^2 a^2}{\beta'^2})^2 + 4 (\frac{\alpha}{\alpha'} a) \frac{\alpha a}{b'}]}$$

$$= \lim_{a \rightarrow \infty} \frac{-4\rho \alpha^3 / \alpha' a^4}{\frac{\rho \alpha^5}{\alpha' \beta'^2} a^5 + \rho' \alpha^4 a^5 + 4\alpha^2 \frac{b'}{\alpha'} \rho' a^3}$$

$$= \lim_{a \rightarrow \infty} \frac{-4\rho \alpha^3 / \alpha'}{\frac{\rho \alpha^5}{\alpha' \beta'} + \rho' \alpha^4 a + 4\alpha^2 b' \frac{\rho'}{\alpha a'}}$$

$$= 0 \quad (3.23b)$$

So, there is no transmitted S-wave at normal incidence.

$$\lim_{\theta \rightarrow 90^\circ} \frac{A_r}{A_i} = \lim_{a, a' \rightarrow \infty} 1 - \frac{a'}{a} \frac{A'}{A_i} + \frac{1}{a} \frac{B'}{A_i}$$

$$= 1 - \frac{\alpha}{\alpha'} \left(\frac{2}{\rho'/\rho + \alpha/\alpha'} \right)$$

$$\begin{aligned}
&= 1 - \frac{2\alpha\rho}{\alpha'\rho' + \alpha\rho} \\
&= \frac{\alpha'\rho' - \alpha\rho}{\alpha'\rho' + \alpha\rho} \\
&= \frac{Z' - Z}{Z' + Z} \quad (3.23c)
\end{aligned}$$

Partioning of energy at normal incidence is as follows:

$$\xi_r = \frac{A_r}{A_i} = \frac{\rho'\alpha' + \rho\alpha}{\rho'\alpha' + \rho\alpha}, \quad (3.24a)$$

$$\begin{aligned}
\xi_t &= \sqrt{\frac{\rho'}{\rho} \frac{a'}{a}} \frac{A_t}{A_i} \\
&= \sqrt{\frac{\rho'}{\rho} \frac{\alpha}{\alpha'}} \frac{2}{\rho'/\rho + \alpha/\alpha'}, \quad (3.24b)
\end{aligned}$$

$$\eta_t = 0 \quad (3.24c)$$

The total normal energy flux is given by

$$\begin{aligned}
\xi_r^2 + \xi_t^2 + \eta_t^2 &= \left(\frac{\rho'\alpha' - \rho\alpha}{\rho'\alpha' + \rho\alpha} \right)^2 + \frac{\rho'\alpha}{\rho\alpha'} \frac{4}{(\rho'/\rho + \alpha/\alpha')^2} \\
&= \frac{(\rho'\alpha')^2 - (\rho\alpha)^2 - 2(\rho'\alpha')(\rho\alpha) + 4 \frac{\rho'\alpha}{\rho\alpha'} (\rho'^2\alpha'^2)}{(\rho'\alpha' + \rho\alpha)^2} \\
&= \frac{(\rho'\alpha')^2 + (\rho\alpha)^2 + 2(\rho'\alpha')(\rho\alpha)}{(\rho'\alpha' + \rho\alpha)^2} \\
&= 1 \quad (3.25)
\end{aligned}$$

This assures the conservation of normal energy flux.

For grazing incidence:

$$\text{For } \alpha > \alpha' \text{ if } \theta_p = 0 \quad \theta'_p = \cos^{-1}(\alpha'/\alpha), \quad \theta'_s = \cos^{-1}(\beta'/\alpha)$$

$\rightarrow \alpha > \beta'$ so $a = 0$ but $a', b' \neq 0$.

$$\begin{aligned} \text{So } \lim_{\theta_p \rightarrow 0} \frac{A'}{A_i} &= \lim_{a \rightarrow 0} \frac{2a^0 \rho C^2 (b'^2 - 1)}{\underbrace{a' \rho C^2 (b'^2 + 1)}_{\neq 0} + a^0 \rho' \beta'^2 \{(b'^2 - 1)^2 + 4a'b'\}} \\ &= 0, \end{aligned} \quad (3.26a)$$

$$\begin{aligned} \lim_{\theta_p \rightarrow 0} \frac{B'}{A_i} &= \lim_{a \rightarrow 0} - \frac{4a^0 a' \rho C^2}{a' \rho C^2 (b'^2 + 1) + a^0 \rho' \beta'^2 \{(b'^2 - 1)^2 + 4a'b'\}} \\ &= 0. \end{aligned} \quad (3.26b)$$

$$\begin{aligned} \text{So } \lim_{\theta_p \rightarrow 0} \frac{A_r}{A_i} &= \lim_{a \rightarrow 0} \left[1 - \frac{a'}{a} \frac{A'}{A_i} + \frac{1}{2} \frac{B'}{A_i} \right] \\ &= 1 - \lim_{a \rightarrow 0} \frac{a'}{a} \frac{A'}{A_i} + \lim_{a \rightarrow 0} \frac{1}{a} \frac{B'}{A_i} \end{aligned} \quad (3.26c)$$

Although $\frac{A'}{A_i} \rightarrow 0$ as $a \rightarrow 0$, but $\frac{a'}{a} \frac{A'}{A_i} \rightarrow \text{finite} \neq 0$ as $a \rightarrow 0$

Similarly, $\frac{B'}{A_i} \rightarrow 0$ as $a \rightarrow 0$, but $\frac{1}{a} \frac{B'}{A_i} \rightarrow \text{finite} \neq 0$

$$\lim_{a \rightarrow 0} \frac{a'}{a} \frac{A'}{A_i} = \lim_{a \rightarrow 0} \frac{2a' \neq 0 \rho C^2 (b'^2 - 1)}{\underbrace{a' \rho C^2 (b'^2 + 1)}_{\neq 0} + a^0 \rho' \beta'^2 \{(b'^2 - 1)^2 + 4a'b'\}}$$

$$\begin{aligned}
&= \frac{2(b'^2 - 1)}{(b'^2 + 1)} \\
&= \frac{2(\alpha^2/\beta'^2 - 2)}{(\alpha^2/\beta'^2)}, \quad (3.27a)
\end{aligned}$$

$$\begin{aligned}
\lim_{a \rightarrow 0} \frac{1}{a} \frac{B'}{A_i} &= - \frac{4a'\rho'C^2}{\rho a'C^2(b'^2 + 1) + a_o\rho'\beta'^2\{(b'^2 - 1)^2 + 4a'b'\}} \\
&= - \frac{4}{(b'^2 + 1)} \\
&= - \frac{4}{(\alpha^2/\beta'^2)} \quad (3.27b)
\end{aligned}$$

$$\begin{aligned}
\therefore \lim_{a \rightarrow 0} \frac{A_r}{A_i} &= 1 - \frac{2(\alpha^2/\beta'^2 - 2)}{(\alpha^2/\beta'^2)} + \frac{(-4)}{(\alpha^2/\beta'^2)} \\
&= 1 - 2 + \frac{4}{(\alpha^2/\beta'^2)} - \frac{4}{(\alpha^2/\beta'^2)} \\
&= 1 \quad (3.27c)
\end{aligned}$$

We have a total reflection with phase shift of π . The partitioning of energy at grazing incidence is

$$\xi_r^2 = \left(\frac{A_i}{A_r}\right)^2 = (-1)^2 = 1 \quad (3.28a)$$

$$\xi_t^2 = \frac{\rho'a'}{\rho a} \frac{A_t^2}{A_i^2} = \frac{\rho'}{\rho} \frac{a_o}{a'} \underbrace{\left(\frac{a'}{a} \frac{A_t}{A_i}\right)^2}_{\text{Finite}} = 0 \quad (2.28b)$$

$$\eta_t^2 = \frac{\rho'}{\rho} \frac{b'}{a} \frac{B_t^2}{A_i^2} = \frac{\rho'}{\rho} b' a' \underbrace{\left(\frac{1}{a} \frac{B_t}{A_i} \right)^2}_{\text{Finite}} = 0 \quad (3.28c)$$

where $\xi_r^2 + \xi_r^2 + \eta_t^2 = 1$ indicating conservation of normal energy flux.

Solid/Liquid Interface

Slippage occurs at the solid/liquid boundary, so the tangential stress vanishes at the boundary (no shear wave is transmitted to the liquid medium), and the tangential displacement is not continuous.

The boundary conditions are:

1. Continuity of normal displacement.
2. Continuity of tangential stress.
3. Continuity of normal stress.

For an incident p-wave, $\beta_i = 0$, $\beta' = 0$ (no s-wave is transmitted), using the corresponding equations for the boundary conditions from the general solution we have continuity of normal displacement;

$$a(A_i - A_r) - (B_i + B_r) = a'A' - B'$$

or $a(A_i - A_r) - B_r = a'A' \quad (3.29a)$

Continuity of tangential stress ($\sigma_{zx} = \sigma'_{zx} = 0$);

$$\rho\beta^2[2a(A_i - A_r) + (b^2 - 1)B_r] = 0$$

or $2a(A_i - A_r) + (b^2 - 1)B_r = 0; \quad (3.29b)$

continuity of normal stress

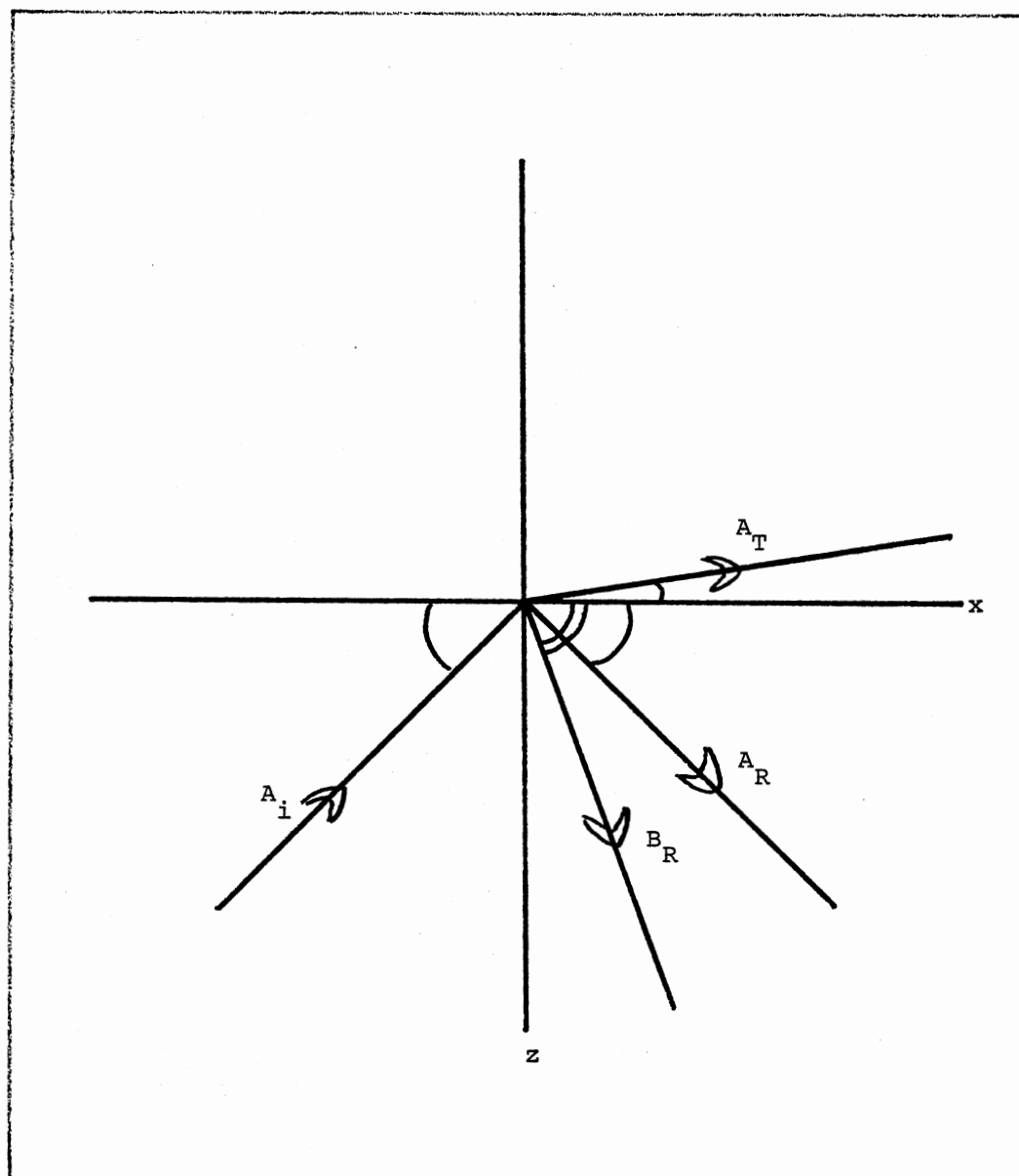


Figure 8. Reflection and Refraction of Incident P-Wave at Solid/Liquid Interface

$$\rho\beta^2[(A_i+A_r)(b^2-1) - 2b(B_i-B_r)] = \rho'\beta'^2[A'(b'^2-1)^2 - 2b'B'_o]$$

$$\beta' \rightarrow 0 \text{ but } b'\beta' \rightarrow C, b'\beta'^2 \rightarrow 0$$

$$\text{or} \quad \rho\beta^2[(A_i+A_r)(b^2-1) + 2b B_r] = \rho'C^2 A' \quad (3.29c)$$

Solving for the reflected, transmitted, and mode converted amplitudes (A_r, A_t, B_r) we find the following:

$$\frac{B_r}{A_i} = \frac{-4aa'(b^2-1)\rho\beta^2}{\rho'C^2a(b^2+1) + \rho\beta^2a'(b^2-1)^2 + 4aa'b\rho\beta^2}, \quad (3.30a)$$

$$\frac{A_t}{A_i} = \frac{2a\rho\beta^2(b^4-1)}{\rho'C^2a(b^2+1) + \rho\beta^2a'(b^2-1)^2 + 4aa'b\rho\beta^2} \quad (3.30b)$$

$$\text{and} \quad \frac{A_r}{A_i} = \frac{\rho'C^2a(b^2+1) - a'\rho\beta^2(b^2-1)^2 + 4aa'b\rho\beta^2}{\rho'C^2a(b^2+1) + a'\rho\beta^2(b^2-1)^2 + 4aa'b\rho\beta^2} \quad (3.30c)$$

For normal incidence:

$$\theta_p \rightarrow 90^\circ \rightarrow \theta'_p, \theta'_s \rightarrow \frac{\pi}{2} \rightarrow a, a', b \rightarrow \infty, \text{ since } C^2 = \alpha^2 \sin^2 \theta_p = \alpha'^2 \sin^2 \theta'_p =$$

$$\beta^2 \sin^2 \theta_s \text{ as } \theta_p \rightarrow \frac{\pi}{2} \rightarrow C^2 \approx \alpha^2 a^2 \approx \alpha'^2 \alpha'^2 \approx \beta^2 b^2. \quad (3.31)$$

$$\begin{aligned} \lim_{\theta_p \rightarrow \frac{\pi}{2}} \frac{B_r}{A_i} &= \lim_{a, a', b \rightarrow \infty} \frac{-4aa'(b^2-1)\rho\beta^2}{\rho'C^2a(b^2+1) + \rho\beta^2a'(b^2-1)^2 + 4aa'b\rho\beta^2} \\ &= 0, \end{aligned}$$

$$\begin{aligned}
\lim_{\theta \rightarrow \frac{\pi}{2}} \frac{A'}{A_i} &= \lim_{a, a', b \rightarrow \infty} \frac{2a\rho\beta^2(b^2-1)}{\rho'C^2a(b^2+1) + \rho\beta^2a'(b^2-1)^2 + 4aa'b\rho\beta^2} \\
&= \frac{2}{\rho'/\rho + \alpha/\alpha'} \quad (3.32a)
\end{aligned}$$

$$\begin{aligned}
\lim_{\theta \rightarrow \frac{\pi}{2}} \frac{A_r}{A_i} &= \lim_{a, a', b \rightarrow \infty} \frac{\rho'C^2a(b^2+1) - a'\rho\beta^2(b^2-1)^2 + 4aa'\rho\beta^2b}{\rho'C^2a(b^2+1) + a'\rho\beta^2(b^2-1)^2 + 4aa'\rho\beta^2b} \\
&= \frac{\rho'\alpha' - \rho\alpha}{\rho'\alpha' + \rho\alpha} \\
&= \frac{Z' - Z}{Z' + Z} \quad (3.32b)
\end{aligned}$$

Solid/Solid Interface

This interface is subject to the most complex set of boundary conditions which leads to both transmitted and reflected mode converted shear waves consisting of the reflected and transmitted p-wave, and the reflected and transmitted s-wave.

All of the boundary conditions that were found for the general case are satisfied, namely the continuity of the normal and tangential stresses as well as continuity of the normal and tangential displacements. Using the equations that were derived for the general case for an incident p-wave ($B_i = 0$).

$$A_i + A_r - bB_r = A' + b'B' \quad (3.33a)$$

$$a(A_i - A_r) - B_r = a'A' - B' \quad (3.33b)$$

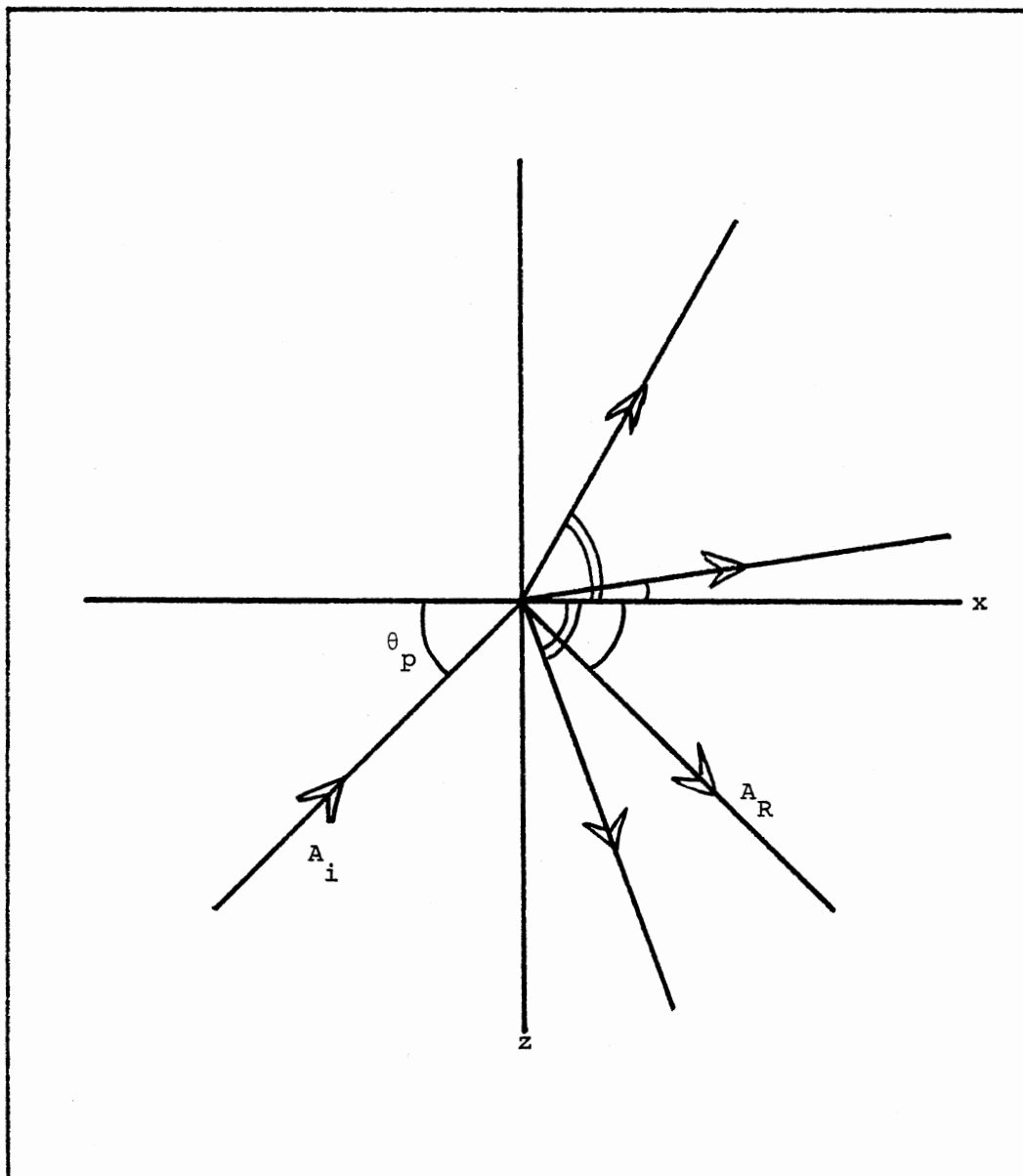


Figure 9. Reflected, Transmitted, and Mode Converted Waves Due to an Incident P-Wave at Solid/Solid Interface

$$\rho\beta^2[2a(A_i - A_r) + (b^2 - 1)B_r] = \rho'\beta'^2[2a'A' + (b'^2 - 1)B'] \quad (3.33c)$$

$$\rho\beta^2[(A_i + A_r)(b^2 - 1) + 2bB_r] = \rho'\beta'^2[A'(b'^2 - 1) - 2b'B'] \quad (3.33d)$$

We can rewrite these equations as

$$\frac{A_r}{A_i} - \frac{A'}{A_i} - b \frac{B_r}{A_i} - b' \frac{B'}{A_i} = -1 \quad (3.34a)$$

$$\frac{A_r}{A_i} + \frac{a'}{a} \frac{A'}{A_i} + \frac{1}{a} \frac{B_r}{A_i} - \frac{1}{a} \frac{B'}{A_i} = 1 \quad (3.34b)$$

$$\frac{A_r}{A_i} + \frac{\rho'\beta'^2}{\rho\beta^2} \frac{a'}{a} \frac{A'}{A_i} - \frac{(b^2 - 1)}{2a} \frac{B_r}{A_i} + \frac{\rho'\beta'^2}{\rho\beta^2} \frac{(b'^2 - 1)}{2a} B' = 1 \quad (3.34c)$$

$$\frac{A_r}{A_i} - \frac{\rho'\beta'^2}{\rho\beta^2} \frac{(b'^2 - 1)}{(b^2 - 1)} \frac{A'}{A_i} + \frac{2b}{(b^2 - 1)} \frac{B_r}{A_i} + \frac{\rho'\beta'^2}{\rho\beta^2} \frac{2b'}{(b^2 - 1)} \frac{B'}{A_i} = -1 \quad (3.34d)$$

or in the matrix form

$$\underline{A} \underline{X} = \underline{B} \leftrightarrow a_{ij} x_j = b_i \quad (3.35)$$

where:

$$\begin{array}{llll} a_{11} = 1 & a_{12} = -1 & a_{13} = -b & a_{14} = -b' \\ a_{21} = 1 & a_{22} = \frac{a'}{a} & a_{23} = \frac{1}{a} & a_{24} = -\frac{1}{a} \end{array} \quad (3.36)$$

$$a_{31} = 1 \quad a_{32} = \frac{\rho' \beta'^2}{\rho \beta^2} \frac{a'}{a} \quad a_{33} = \frac{-(b'^2 - 1)}{2a} \quad a_{34} = \frac{\rho' \beta'^2}{\rho \beta^2} \frac{(b'^2 - 1)}{2a}$$

$$a_{41} = 1 \quad a_{42} = -\frac{\rho' \beta'^2 (b'^2 - 1)}{\rho \beta^2 (b^2 - 1)} \quad a_{43} = \frac{2b}{(b^2 - 1)} \quad a_{44} = \frac{\rho' \beta'^2}{\rho \beta^2} \frac{2b'}{(b^2 - 1)}$$

$$b_1 = -1 \quad b_2 = 1 \quad b_3 = 1 \quad \text{and} \quad b_4 = -1 \quad (3.37)$$

For normal incidence:

$\theta_p \rightarrow \frac{\pi}{2} \rightarrow \theta'_p$, $\theta_s \rightarrow \frac{\pi}{2} \rightarrow \theta'_s$ and $a, a', b, b' \rightarrow \infty$. We can rewrite the above equations as follows:

$$A_i + A_r - \left(\frac{\alpha}{\beta}\right) a B_r = A' + (\alpha/\beta') a B'$$

by dividing by a (terms with $\frac{1}{a} \rightarrow 0$).

$$\therefore -\frac{\alpha}{\beta} B_r = \frac{\alpha}{\beta'} B' \text{ or } B_r = -\frac{B}{B'} B'_0;$$

$$\rho \beta^2 [2a(A_i - A_r) + (\alpha^2/\beta^2) a^2 B_r] = \rho' \beta'^2 \left[\frac{2\alpha}{\alpha'} a A' + (\alpha/\beta') a^2 B' \right]$$

dividing by a^2 (terms that have $\frac{1}{a}$ vanish).

$$\therefore \rho \beta^2 (\alpha^2/\beta^2) B_r = \rho' \beta'^2 (\alpha^2/\beta'^2) B'$$

$$\text{or} \quad B_r = \frac{\rho'}{\rho} B'$$

from 3.e(5) and 3.e(6)

$$B_r = B' = 0$$

($\rho, \rho', \beta, \beta'$ are arbitrary numbers), from 3-3(2)

$$a(A_i - A_r) - B_r = (\alpha/\alpha') A' - B'$$

dividing by a

$$\therefore A_i - A_r = \frac{\alpha}{\alpha'} A',$$

3.e(4).

$$\rho\beta^2[(A_i + A_r)(\alpha/\beta a)^2 + 2(\alpha/\beta a)B_r] = \rho'\beta'^2[(\alpha/\beta' a)^2 A' - 2b'B']$$

or dividing by a^2 we have

$$\rho\beta^2(\alpha^2/\beta^2)(A_i + A_r) = \rho'\beta'^2(\alpha^2/R'^2)A'$$

or

$$A_i + A_r = \rho'/\rho A'$$

and

$$A_i - A_r = \frac{\alpha}{\alpha'} A'$$

$$\frac{A'}{A_i} = \frac{2}{\alpha/\alpha' + \rho'/\rho},$$

$$\frac{A_r}{A_i} = 1 - \frac{\alpha}{\alpha'} \frac{A'}{A_i}$$

$$= 1 - \frac{2}{1 + \rho'\alpha'/\rho\alpha}$$

$$= \frac{\rho'\alpha' - \rho\alpha}{\rho'\alpha' + \rho\alpha}$$

$$= \frac{Z' - Z}{Z' + Z}$$

Noting that in all of the solutions we have derived we used the coefficients a, a', b, b' which are defined earlier as

$$a = \tan \theta_p = \sqrt{c^2/\alpha^2 - 1}, \quad (3.38a)$$

$$a' = \tan \theta'_p = \sqrt{c^2/\alpha'^2 - 1} \quad (3.38b)$$

$$b = \tan \theta_s = \sqrt{c^2/\beta^2 - 1}, \quad (3.38c)$$

$$b' = \tan \theta'_s = \sqrt{c^2/\beta'^2 - 1} \quad (3.38d)$$

So far we have considered cases where all the coefficients are real quantities. The possibility that some of these coefficients being imaginary is delayed to the following chapter on total reflection.

CHAPTER IV

TOTAL REFLECTION

In the previous chapter we have limited our discussion to the case where the incoming wave velocity is greater than all other velocities, so all the coefficients were real quantities for all angles of incidence. However, when the velocity of propagation for the transmitted wave is higher than that of the incident wave, there will be some angle θ_p^c at which the transmitted wave is propagating parallel to the interface. This angle θ_p^c is called the critical angle, and for any incident angle less than this critical angle it is impossible to satisfy Snell's Law with real angles (since $\sin\theta_2$ cannot exceed unity), so we will have imaginary coefficients that will lead to an exponential decay of the amplitude of the wave which is propagating parallel to the interface. This wave carries no energy across the barrier and moves with a velocity that is determined by the properties of the first medium the angle of incidence and the type of the incident wave.

For the case of an incident p-wave the phase velocity of the transmitted p-wave decreases from

$$c = \alpha' = \frac{\omega}{k'p} \text{ at } \theta = \theta_p^c$$

to

$$c = \alpha = \frac{\omega}{k^p} \text{ at } \theta = 0^\circ$$

as shown in Figure 10.

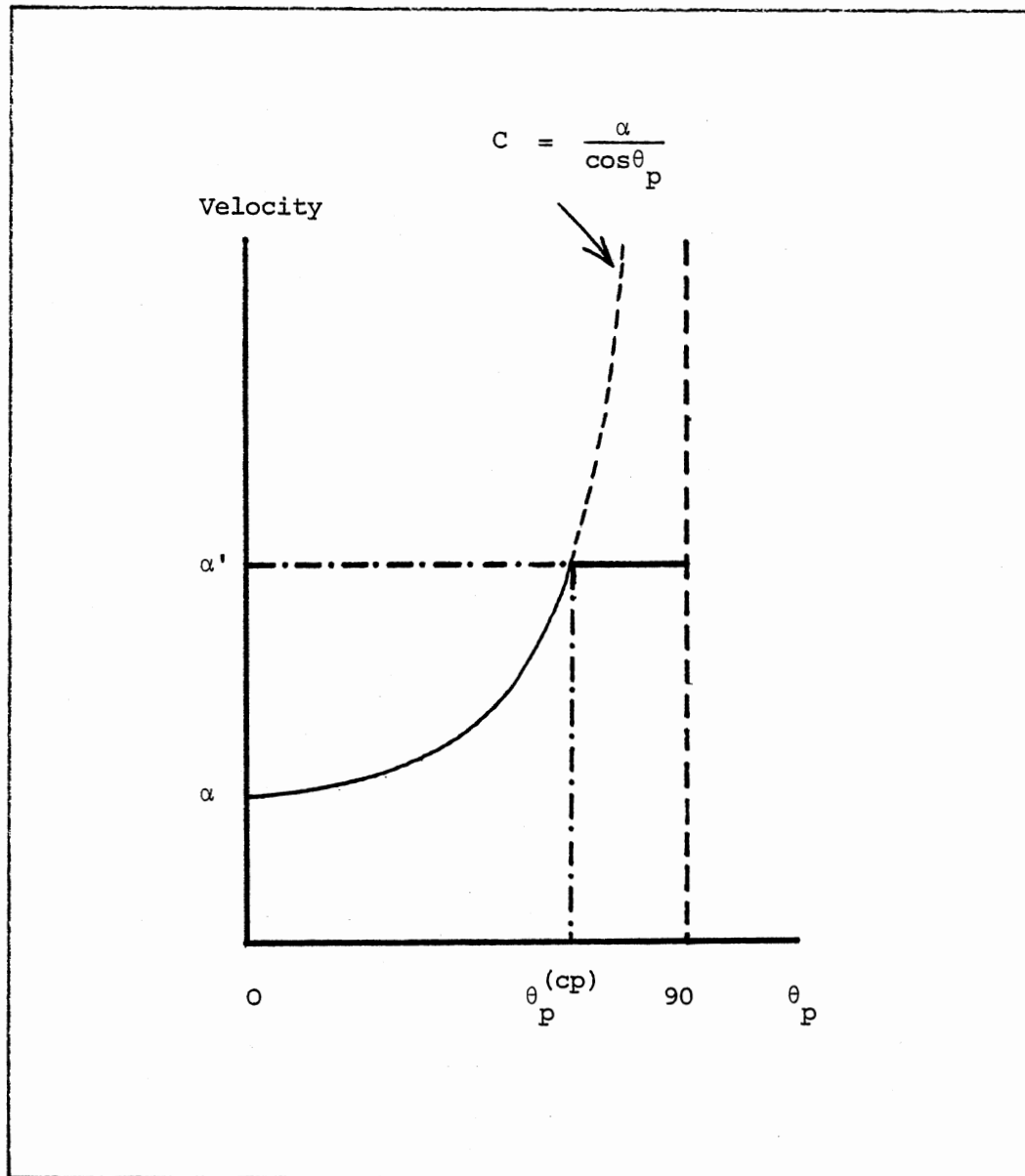


Figure 10. Phase Velocity of the Transmitted P-Wave for Incident P-Wave With a Lower Velocity ($\alpha < \alpha'$)

In the most general case (for no solids) we have two possible critical angles for an incident "P-wave" and three possible critical angles for an incident "S-wave". For an incident "P-wave":

Case 1: If $\alpha > \alpha'$ (hence $\alpha > \beta'$ since $\alpha' > \beta'$ always), there is no possible critical angle.

$$C = \frac{\alpha}{\cos \theta_p} = \frac{\alpha'}{\cos \theta'_p} = \frac{\beta'}{\cos \theta'_B} = \frac{\beta}{\cos \theta_s} \quad (3.39)$$

$$\cos \theta_s = \frac{\beta}{\alpha} \frac{1}{\cos \theta_p} < 1 \text{ always}$$

$$\cos \theta'_p = \frac{\alpha'}{\alpha} \frac{1}{\cos \theta_p} < 1$$

and $\cos \theta'_s = \frac{\beta'}{\alpha} \frac{1}{\cos \theta_p} < 1$

So, for all angles of incidence θ_r , θ'_p and θ'_s are real angles.

Case 2: If $\beta' < \alpha < \alpha'$, we have one critical angle for the transmitted "P-wave", that is when $\theta'_p = 0$ as in Figure 11a.

$$\therefore \frac{\alpha}{\cos \theta_{cp'}} = \frac{\alpha'}{\cos \theta'_p} = \alpha' \quad (3.40a)$$

or $\cos^{-1} \theta_{cp'} = \frac{\alpha}{\alpha'} \quad (3.40b)$

Case 3: If $\alpha < \beta' < \alpha'$

We have two critical angles, one for the transmitted "P-Wave"

$$\theta_p^{(cp')} = \cos^{-1} \left(\frac{\alpha}{\alpha'} \right) \text{ and the other for the transmitted "S-Wave"}$$

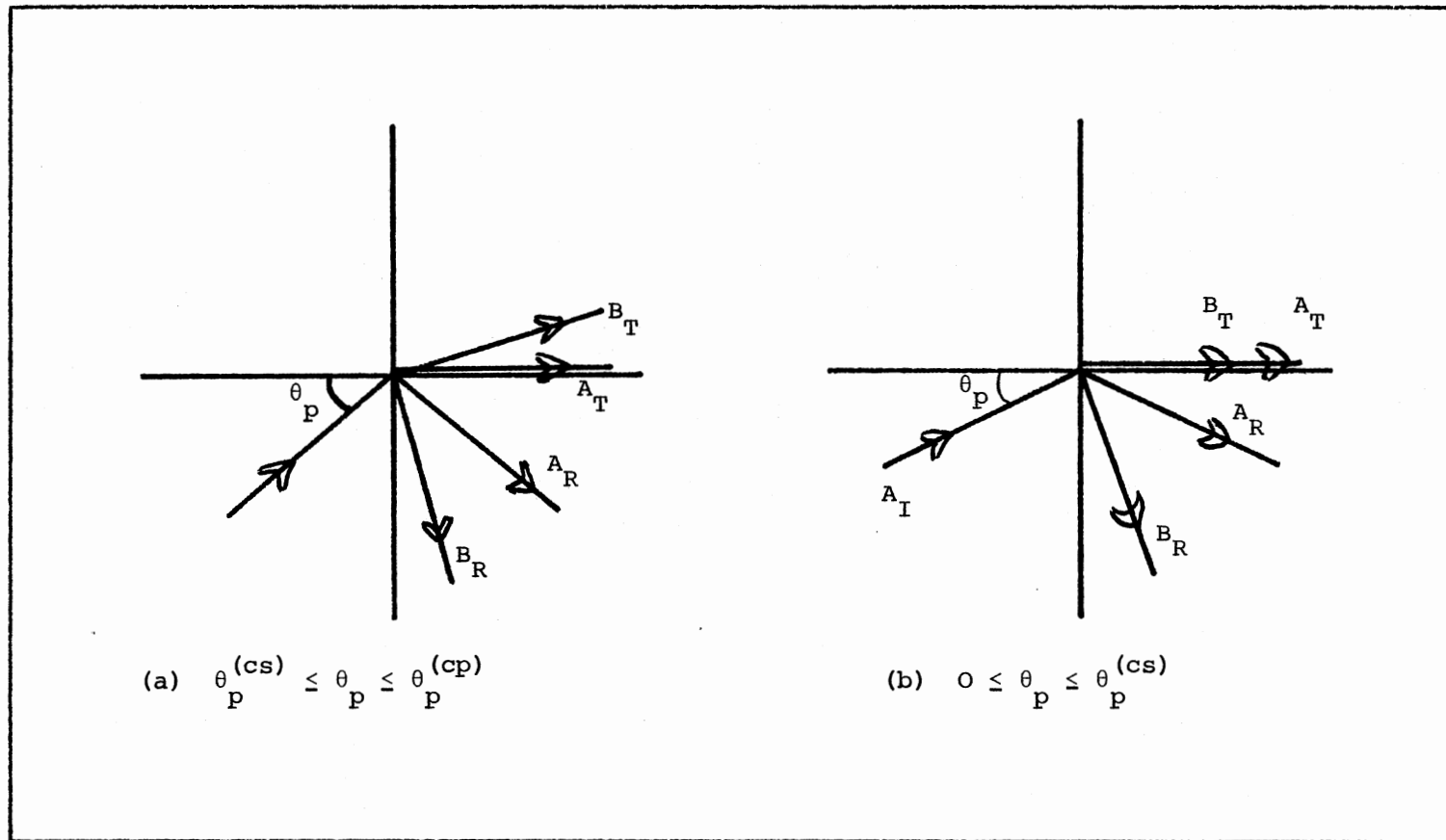


Figure 11. Critical Reflections for an Incident P-Wave at Solid/Solid Interface

$\theta_p^{(cs')} = \cos^{-1}\left(\frac{\alpha}{\beta'}\right)$. Noting that $\theta_p^{(cs')} < \theta_p^{(cp')}$ (since $\alpha' > \beta'$) as in Figure 11.

For an Incident "S-Wave".

Case 1: If $\beta > \alpha'$ (and hence $\beta > \beta'$ since $\alpha' > \beta'$) but $\beta < \alpha$ always, so we have one critical angle for the reflected P-wave, $\theta_s^{(cp)}$ as shown in Figure 12a.

$$\text{Where:} \quad \theta_s^{(cp)} = \cos^{-1}\left(\frac{\beta}{\alpha}\right) \quad (3.41a)$$

Case 2: If $\beta' < \beta < \alpha'$, then we have two critical angles, one for the reflected p-wave $\theta_s^{(cp)}$ and one for the transmitted p-wave $\theta_s^{(cp')}$ as shown in Figure 12b.

$$\text{Where:} \quad \theta_s^{(cp')} = \cos^{-1}(\beta/\alpha') \quad (3.41b)$$

Case 3: If $\beta < \beta'$ (and hence $\beta < \alpha'$ since $\beta' < \alpha'$), then we have three critical angles, the first one for the reflected p-wave $\theta_s^{(cp)}$ and the second one for the transmitted "P-Wave" $\theta_s^{(cp')}$ and the third one for the transmitted S-Wave $\theta_s^{(cs')}$, as shown in Figure 12c.

$$\text{Where:} \quad \theta_s^{(cs')} = \cos^{-1}(\beta/\beta') \quad (3.41c)$$

Noting that $\theta_s^{(cs')} < \theta_s^{(cp')}$ (since $\beta' < \alpha'$).

The coefficients a, b, a' and b' are defined for all cases as follows:

For an Incident P-Wave:

$$c = \frac{\alpha}{\cos \theta_p} \quad c \geq \alpha \quad a = \sqrt{\frac{c^2}{\alpha^2} - 1}$$

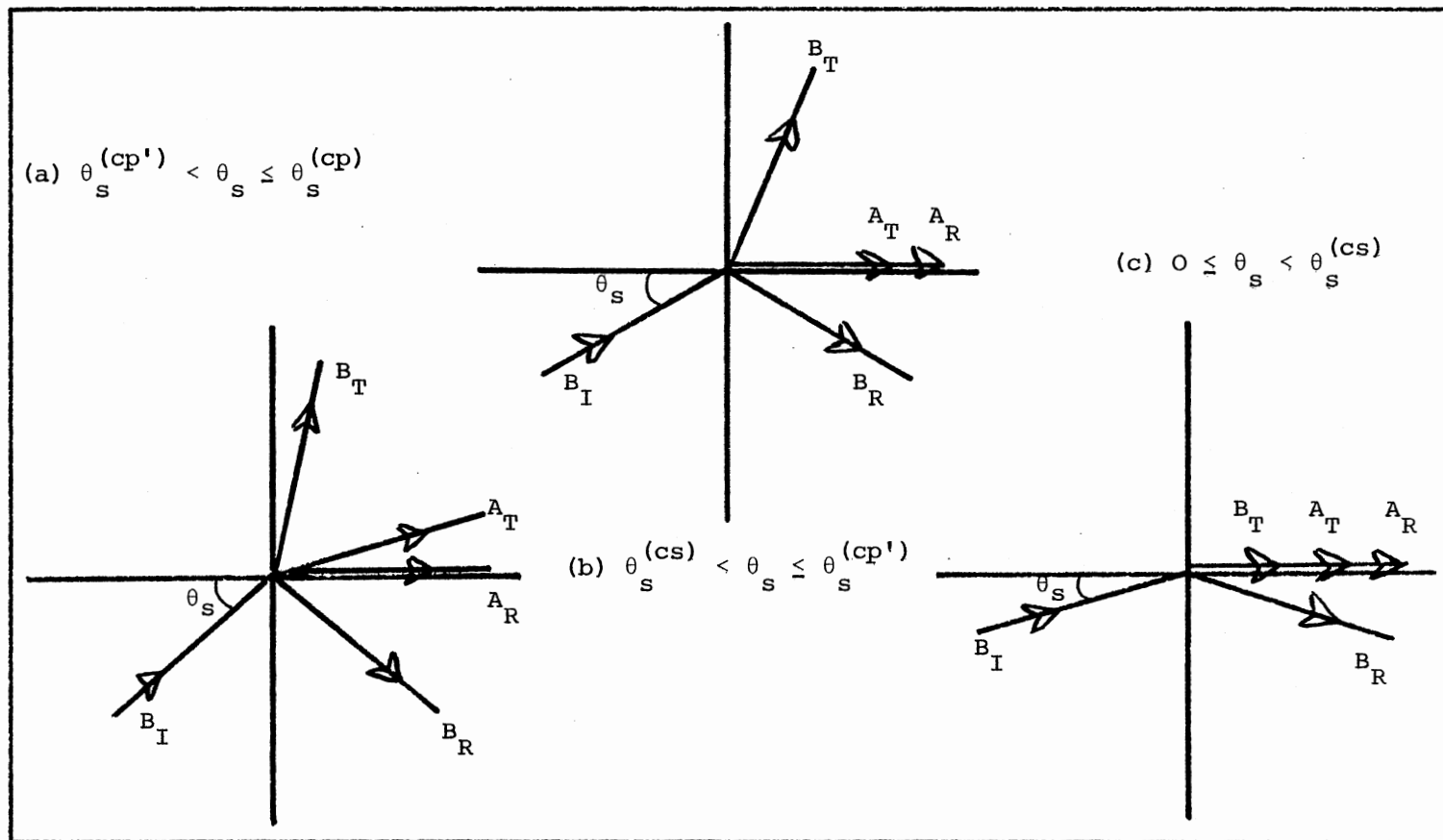


Figure 12. Critical Reflections for an Incident S-Wave at Solid/Solid Interface

$$\begin{aligned}
&\text{and (hence } C > \beta) \quad b = \sqrt{\frac{C^2}{\beta^2} - 1} \\
&\text{for } C \geq \alpha' \quad a' = \sqrt{\frac{C^2}{\alpha'^2} - 1} \text{ and for } C > \beta' \quad b' = \sqrt{\frac{C^2}{\beta'^2} - 1} \\
&\text{for } C < \alpha' \quad a' = -i \sqrt{1 - \frac{C^2}{\alpha'^2}} \\
&\text{for } C < \beta' \quad b' = -i \sqrt{1 - \frac{C^2}{\beta'^2}} \tag{3.42}
\end{aligned}$$

For an Incident S-wave:

$$\begin{aligned}
C &= \frac{\beta}{\cos \theta_s} \text{ so } C > \beta \text{ and } b = \sqrt{\frac{C^2}{\beta^2} - 1} \text{ for all angles of incidence} \\
&\text{for } C \geq \alpha \quad a = \sqrt{\frac{C^2}{\alpha^2} - 1}, \text{ for } C < \alpha \quad a = -i \sqrt{1 - \frac{C^2}{\alpha^2}} \\
&\text{for } C \geq \alpha' \quad a' = \sqrt{\frac{C^2}{\alpha'^2} - 1}, \text{ } C < \alpha' \quad a' = -i \sqrt{1 - C^2/\alpha'^2} \\
&\text{for } C \geq \beta' \quad b' = \sqrt{C^2/\beta'^2 - 1}, \text{ } C < \beta' \quad b' = -i \sqrt{1 - C^2/\beta'^2} \tag{3.43}
\end{aligned}$$

For an Incident "S-Wave" on a free boundary the boundary conditions that must be satisfied are the vanishing of normal and tangential stresses.

So, the corresponding equations as we derived them in Equation (2.10) are:

$$1. \quad \sigma_{zx} = 0$$

$$\rho \beta^2 [-2a A_r + (b^2 - 1)(B_i + B_r)] = 0$$

$$\text{or} \quad 2a A_r - (b^2 - 1)(B_i + B_r) = 0 \tag{4.2}$$

$$2. \quad \sigma_{zz} = 0$$

$$\therefore \rho \beta^2 [A_r (b^2 - 1) - 2b(B_i - B_r)] = 0$$

$$\text{or} \quad A_r (b^2 - 1) - 2b(B_i - B_r) = 0 \quad (4.3)$$

from 4.2 and 4.3 we have

$$A_r = B_i \frac{4b(b^2 - 1)}{4ab + (b^2 - 1)^2}$$

$$\text{and} \quad B_r = B_i \frac{4ab - (b^2 - 1)^2}{4ab + (b^2 - 1)^2}$$

1. For the case $C > \alpha > \beta$, $C = \frac{\beta}{\cos^2 \theta_s}$ all the coefficients are real and the discussion is similar to what we did in the last chapter.

2. For the case $\alpha > C > \beta$,

$$b = \sqrt{\frac{C^2}{\beta^2} - 1}, \quad a = -i \sqrt{1 - \frac{C^2}{\alpha^2}} = -i \sqrt{1 - \frac{\beta^2}{\alpha^2} \frac{1}{\cos^2 \theta_s}}$$

so the reflected amplitudes are as follows:

$$A_r = B_i \frac{4b(b^2 - 1)}{-ir|a|b + (b^2 - 1)^2}$$

$$\text{and} \quad = B_i \frac{4b}{\sqrt{1 + \frac{|b|a|^2 b^2}{(b^2 - 1)^2}}} e^{i\delta_r(p)};$$

$$\delta_r^{(p)} = \tan^{-1} \left\{ \frac{4|a|b}{(b^2-1)^2} \right\}$$

So the reflected P-wave experiences a phase shift of $\delta_r^{(p)}$.

$$B_r = B_i \frac{-i4|a|b - (b^2-1)^2}{-i4|a|b + (b^2-1)^2}$$

$$\therefore B_r = B_i e^{i\pi} e^{i2\delta_2}; \delta_2 = \tan^{-1} \left(\frac{4|a|b}{(b^2-1)^2} \right) = \delta_r^{(p)}$$

$$= B_i e^{i\delta_r^{(s)}}; \delta_r^{(s)} = \pi + 2\delta_r^{(p)}.$$

So the reflected S-wave experiences a phase shift of $\pi + 2\delta_r^{(p)}$. Now due to the fact that a is pure imaginary for $0 \leq \theta \leq \theta_s^{(cp)}$, by replacing the new value for a in the wave function, that is $a = -i|a|$, we have

$$\begin{aligned} \phi &= A_r e^{ik(ct-x-az)} \\ &= A_r e^{-k|a||z|} e^{ik(ct-x)} \end{aligned}$$

that is a wave propagating parallel to the interface with a variable velocity depending on the shear wave velocity and its angle of incident, so it decreases from the p-wave velocity at $\theta_s = \theta_s^{(cp)}$ to the s-wave velocity at $\theta_s = 0^\circ$ as shown in Figure 13. Beyond the critical angle, the p-wave carries no energy across the barrier, and hence the shear wave experiences a total reflection with some phase shift and p-wave amplitude decreases exponentially with the distance from the interface with skin depth γ where

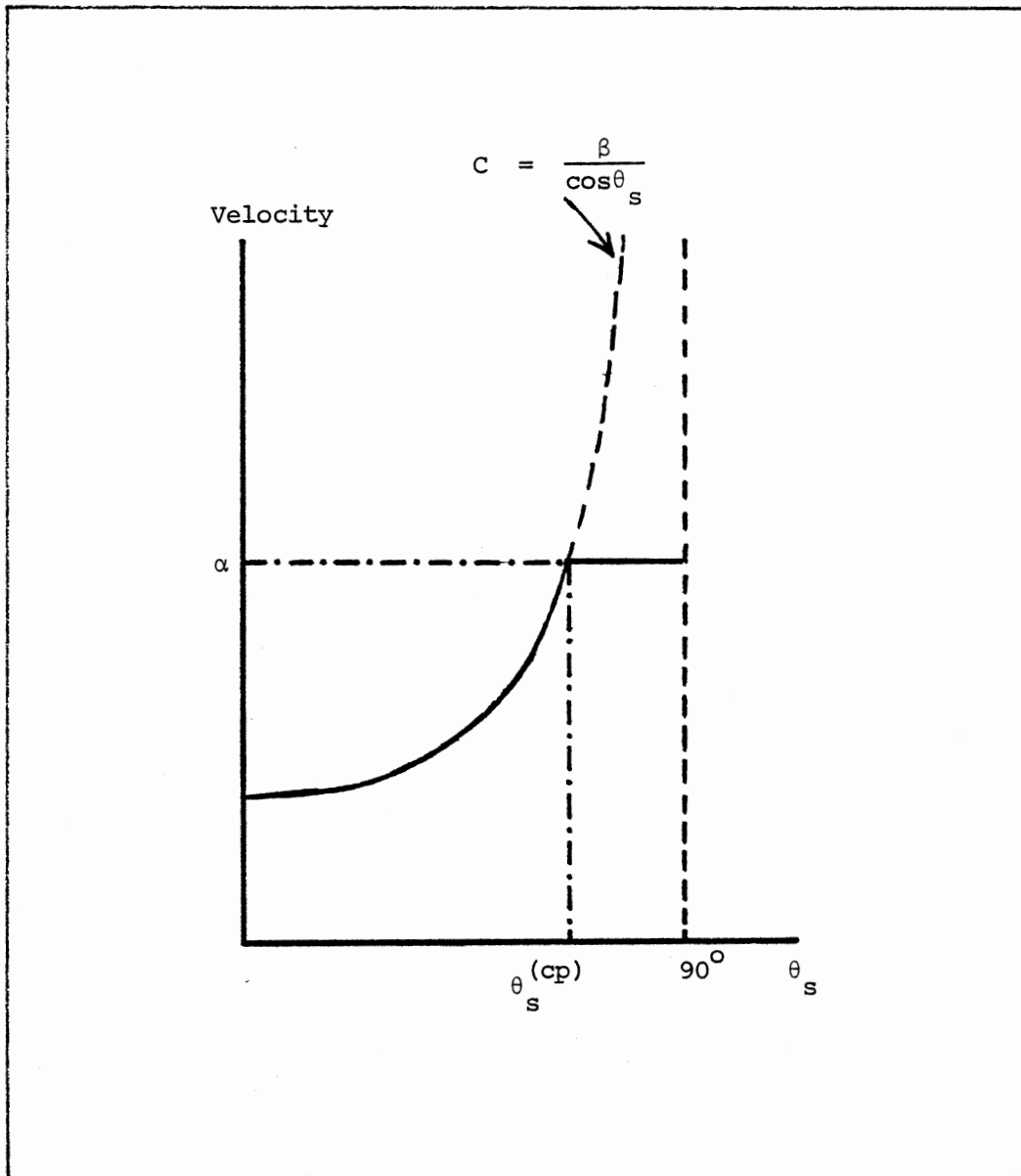


Figure 13. Phase Velocity of the P-Wave for an Incident S-Wave

$$\gamma = \frac{1}{k|a|} = \frac{1}{k\sqrt{1 - \frac{\beta^2}{\alpha^2 \cos^2 \theta_s}}}$$

$$\text{for } 0 \leq \theta_s \leq \theta_s^{(cp)}$$

where:

$$k = \frac{\omega}{\beta} \cos \theta_s$$

$$\therefore \gamma(\theta_s) = \frac{\beta}{\omega} \frac{1}{\sqrt{\cos^2 \theta_s - \frac{\beta^2}{\alpha^2}}} : \cos \theta_s \geq \frac{\beta}{\alpha}$$

$$(0 \leq \theta_s < \theta_s^{(cp)})$$

So for $\theta \geq \theta_s^{(cp)}$ ($\cos \theta_s^{(cp)} = \frac{\beta}{\alpha}$) we have a plane wave moving with a phase velocity $c = \alpha$ without any decaying, then for $\theta_s < \theta_s^{(cp)}$, $\gamma_{(\theta_s)}$ starts decreasing from infinite at $\theta_s = \theta_s^{(cp)}$ to a minimum value γ_o at $\theta_s = 0$, as shown in Figure 14.

where:

$$\gamma_o = \frac{\beta}{\omega} \frac{1}{\sqrt{1 - \frac{\beta^2}{\alpha^2}}} \quad \alpha^2 = \frac{\lambda + 2\mu}{\rho}$$

$$= \frac{\beta}{\omega} \frac{1}{\sqrt{\frac{\lambda + \mu}{\lambda + 2\mu}}} \quad \beta^2 = \frac{\mu}{\rho}$$

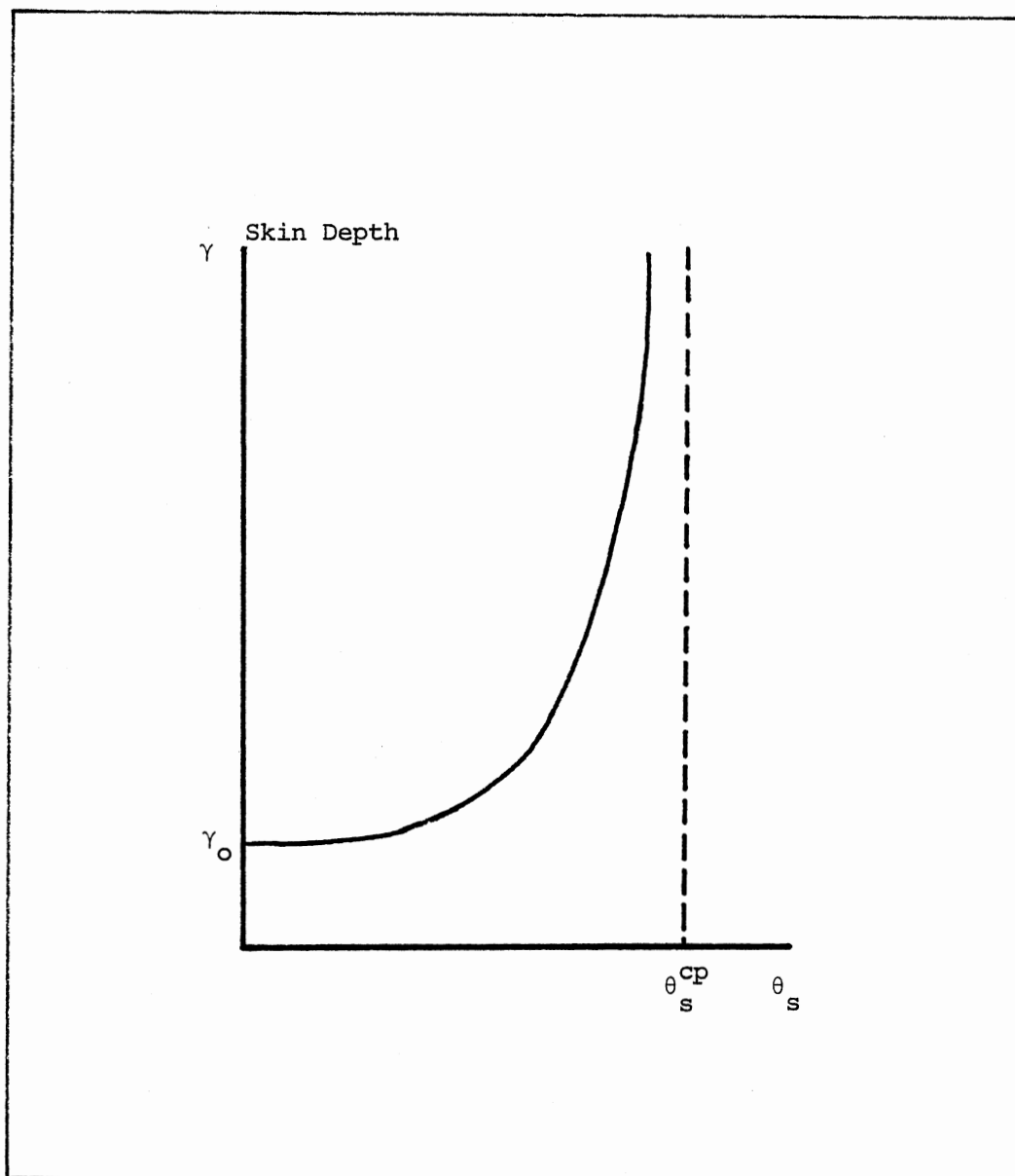


Figure 14. P-Wave Skin Depth Dependence on the Incident Angle of S-Wave at Free Solid Interface

$$= \frac{\beta}{\omega} \sqrt{\frac{\lambda + 2\mu}{\lambda + \mu}} \quad \alpha^2 - \frac{\beta^2}{\alpha^2} = \frac{\lambda + \mu}{\lambda + 2\mu}$$

and the frequency dependence is now obvious, so the wave will attenuate more for higher frequency.

For an incident "P-wave" at a liquid-liquid interface for $\alpha' > \alpha$ and $\theta_p^{(cp)} \leq \theta \leq \frac{\pi}{2} (\cos \theta_p^{(cp)} = \frac{\alpha}{\alpha'})$ all the coefficients are real, and the solution is very similar to what we did earlier for $\alpha' < \alpha$. While for $\alpha' > \alpha$ and $0 \leq \theta_p \leq \theta_p^{(cp)}$, $a' = -i|a'|$ so the reflected "P-wave" has the form

$$\begin{aligned} \frac{A_r}{A_i} &= \frac{\rho'/\rho - i|a'|/a}{\rho'/\rho + i|a'|/a} \\ &= e^{-i2\delta}; \quad \delta = \tan^{-1} \left(\frac{\rho|a'|}{\rho'|a|} \right) \end{aligned} \quad (3.44)$$

So the reflected p-wave experiences a total reflection with a phase shift that varies from 0 at $\theta = \theta_p^{(cp')}$ to π at $\theta_p = 0$. The transmitted P-wave for $0 \leq \theta \leq \theta_p^{(cp)}$ will have the form

$$\begin{aligned} \phi(t) &= A_t e^{ik(ct-x+i|a'| |z|)} \\ &= A_t e^{-k|a'| |z|} e^{+ik(ct-x)} \end{aligned} \quad (3.45)$$

which is a wave propagating parallel to the interface with a variable velocity that depends on the incoming wave velocity α and the incident

angle $C = \frac{\alpha}{\cos \theta_p}$, so it varies from α' the speed in the second medium

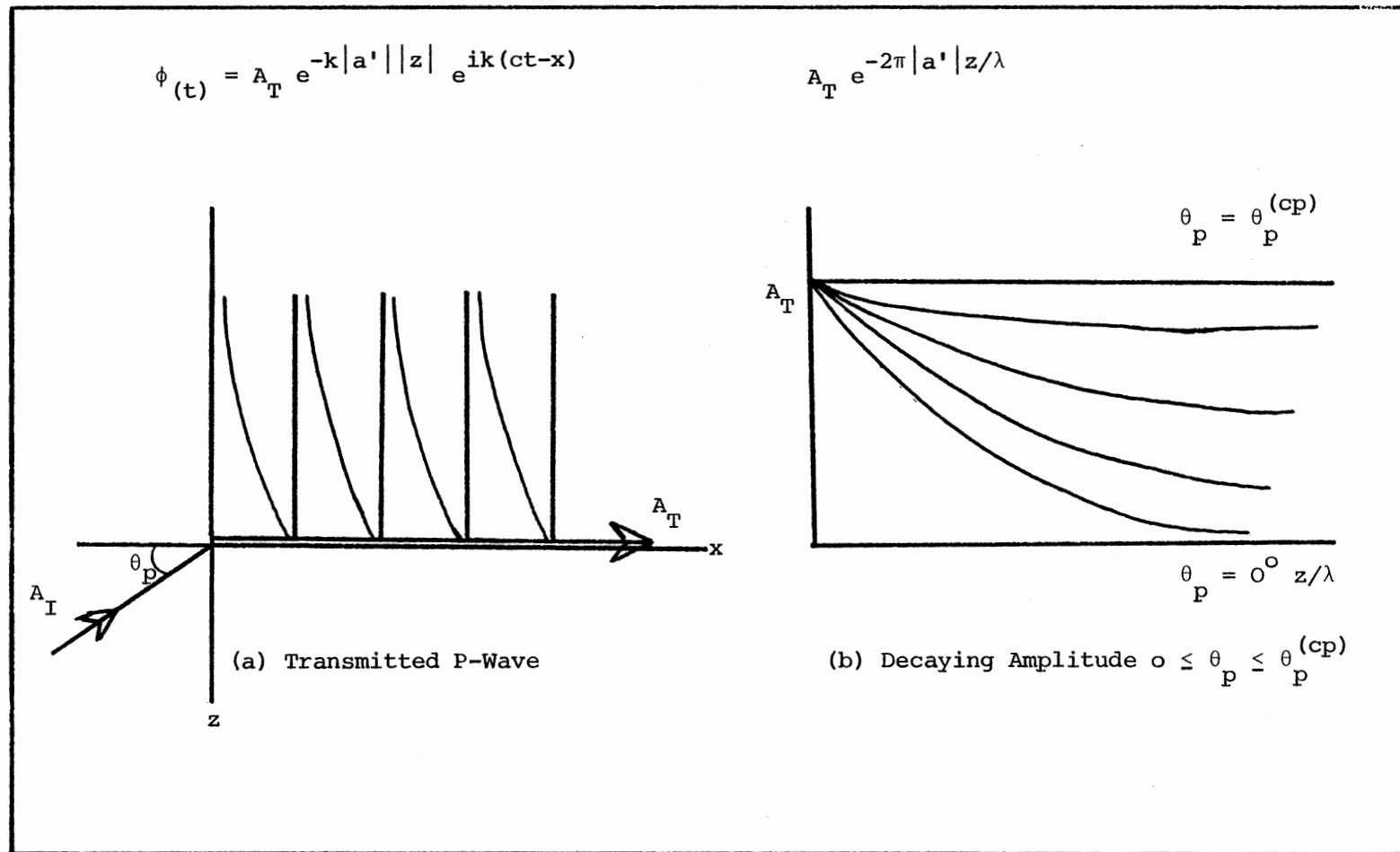


Figure 15. Transmitted P-Wave Due to an Incident P-Wave at Liquid/Liquid Interface Beyond the Critical Angle

when $\theta_p = \theta_p^{(cp)}$ to α the speed of p-wave in the first medium when $\theta_p = 0$, and the amplitude of this wave decreases exponentially with distance from the interface as shown in Figure 15 with a skin depth $\gamma_{(\theta)}$ where

$$\begin{aligned} \gamma_{(\theta)} &= \frac{1}{k|a'|} , \quad k = \frac{\omega}{\alpha} \cos \theta_p , \quad |a'| = \sqrt{1 - \frac{\alpha^2}{\alpha'^2 \cos^2 \theta_p}} \\ &= \frac{\alpha}{\omega} \frac{1}{\sqrt{\cos^2 \theta_p - \frac{\alpha^2}{\alpha'^2}}} \end{aligned} \quad (3.46)$$

where $\gamma_{(\theta)}$ varies from infinity at $\theta_p = \theta_p^{(cp)}$ to γ_0 at $\theta_p = 0$;

$$\gamma_0 = \frac{\alpha}{\omega} \frac{1}{\sqrt{1 - \frac{\alpha^2}{\alpha'^2}}}$$

The frequency dependent of the skin depth is clear and the wave will attenuate more for higher frequency. The transmitted amplitude for this wave is

$$\begin{aligned} \frac{A_t}{A_i} &= \frac{2ap}{i|a'|(\rho + ap')} \\ &= \frac{2}{\sqrt{\frac{\rho'^2}{\rho^2} + \frac{|a'|^2}{a^2}}} : \quad \delta_t = \tan^{-1} \left(\frac{|a'| \rho}{ap'} \right) \end{aligned} \quad (3.47a)$$

$$\text{and} \quad \xi_t = \sqrt{\frac{\rho'}{\rho} \frac{\alpha}{\alpha'}} \frac{\sin \theta_p'}{\sin \theta_p} \frac{A_r}{A_i}$$

$$= o(\sin\theta'_p = 0 \text{ for } 0 \leq \theta \leq \theta_p^{(cp)}) \quad (3.47b)$$

even though the transmitted amplitude doesn't vanish the energy transmitted across the boundary is zero.

So that wave has no contribution as far as energy partitioning is concerned.

For a P-wave incident on liquid/solid interface, we have for $C > \alpha' > \beta'$; the discussion is very similar to what we did in the previous chapter, but for $\alpha' > C > \beta'$ which is the case when $\theta_p^{(cs)} \leq \theta_p < \theta_p^{(cp)}$. The transmitted p-wave propagates along the interface with $C = \alpha'$ at $\theta_p = \theta_p^{(cp)}$ then decreases to $c = \alpha$ at $\theta_p = 0^\circ$ as was shown in Figure 10.

For $C < \beta' < \alpha'$ that is the case for $0 \leq \theta \leq \theta_p^{(cs)}$. The transmitted s-wave travel along the interface with speed $= c = \frac{\alpha}{\cos\theta_p}$, it varies from $C = \beta'$ at $\theta_p = \theta_p^{(cs)}$ to $C = \alpha$ at $\theta_p = 0$ as shown in Figure 16.

For $\theta_p \leq \theta_p^{(cs)}$ we have a total reflection for the p-wave with a phase shift that varies from zero at $\theta_l = \theta_p^{(cs)}$ to π at $\theta_p = 0$.

For an incident p-wave on solid-liquid interface we have just one critical angle $\theta_p^{(cp)}$ where $\theta_p^{(cp)} = \cos^{-1}(\frac{\alpha}{\alpha'})$ and that is only if $\alpha' > \alpha$. So for $\theta_p^{(cp)} < \theta_p < 90^\circ$ (i.e. $C > \alpha'$) we have the same results as was discussed in the previous chapter, but for $\alpha' > C > \alpha$ that is for $0 \leq \theta_p \leq \theta_p^{(cp)}$, and we have both p-wave and s-wave reflected in the solid-medium as shown in Figure 17. The transmitted p-wave propagates along the interface.

For an incident p-wave at a solid-solid interface we have two critical angles $\theta_p^{(cp)}$ and $\theta_p^{(cs)}$, if $\alpha', \beta' > \alpha$ where

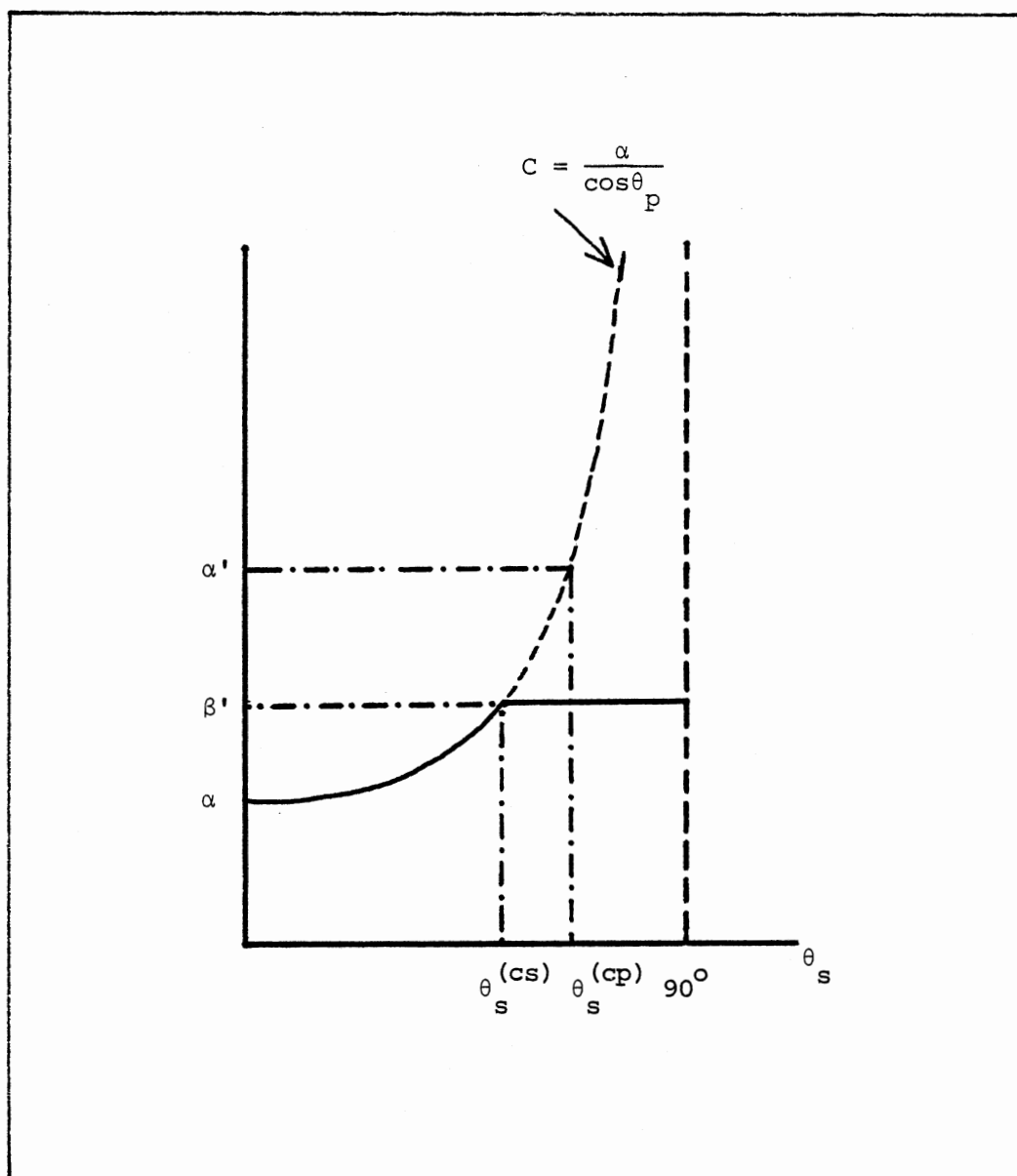


Figure 16. Phase Velocity of the Transmitted S-Wave for an Incident P-Wave With $\alpha < \beta'$

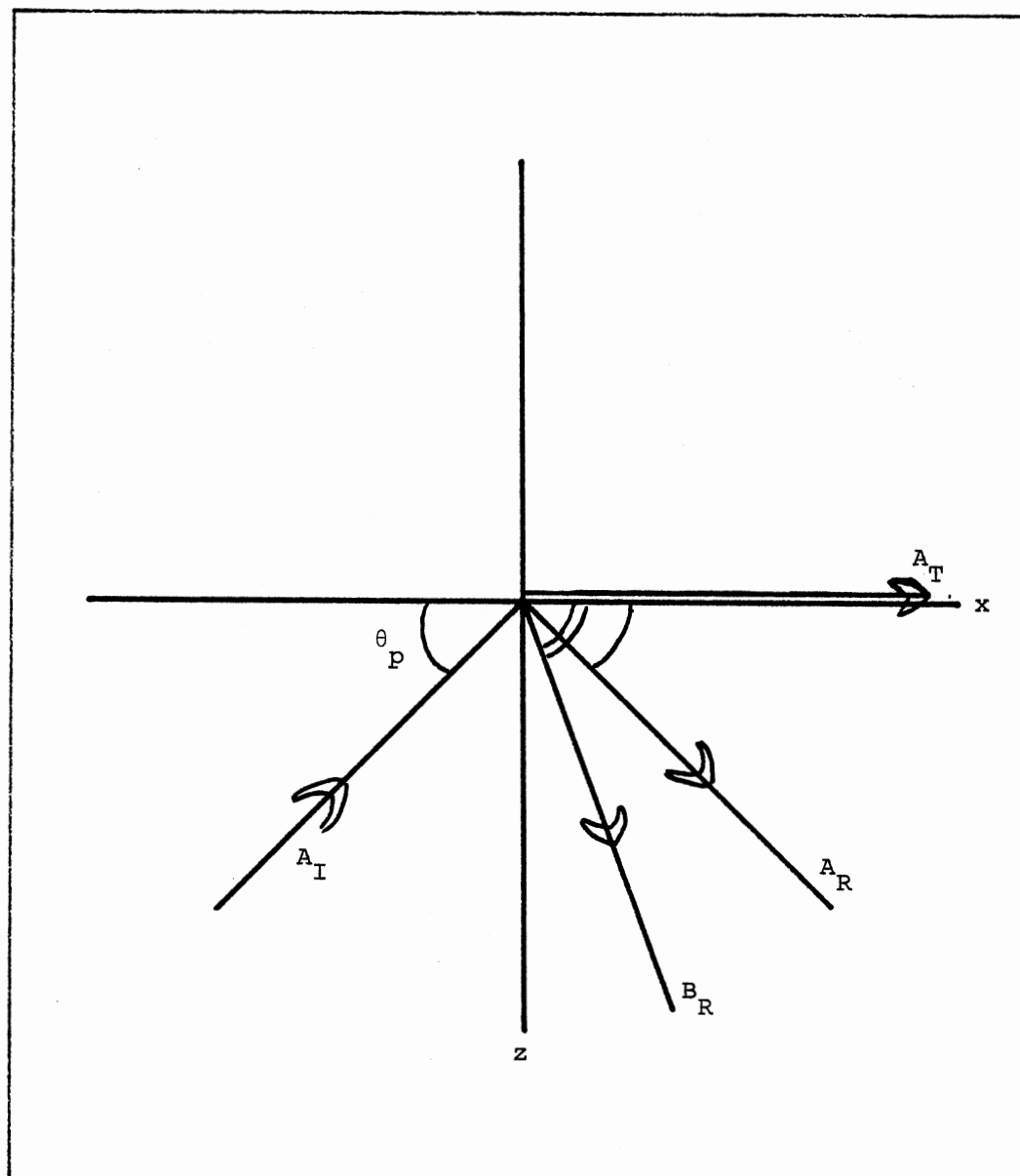


Figure 17. Reflection and Refraction of Incident P-Wave at Solid/
Liquid Interface Beyond the Critical Angle $\theta_p^{(cp)}$

$$\theta_p^{(cp)} = \cos^{-1}(\alpha/\alpha') \quad (3.48a)$$

and

$$\theta_p^{(cs)} = \cos^{-1}(\alpha/\beta') \quad (3.48b)$$

So for $\theta_p^{(cp)} < \theta \leq \frac{\pi}{2}$ the waves are as was shown in Figure 9, and the calculations are as we did in the previous chapter.

For $\theta_p^{(cs)} < \theta < \theta_p^{(cp)}$ the transmitted p-wave propagates along the interface with a decaying amplitude ($a' = -i|a'|$), and the reflected waves are as was shown in Figure Figure 11a.

For $0 \leq \theta \leq \theta_p^{(cs)}$, both transmitted waves, and the reflected waves are as was shown in Figure 11b.

Noting that for this case, the transmitted p-wave, and the mode converted s-wave propagates along the same direction with the same phase velocity C . While the p-wave and s-wave which are reflected in the first medium are reflected with phase shifts $\delta_r^{(p)}$ and $\delta_r^{(s)}$ respectively as shown in Figure 18 and in Figure 19.

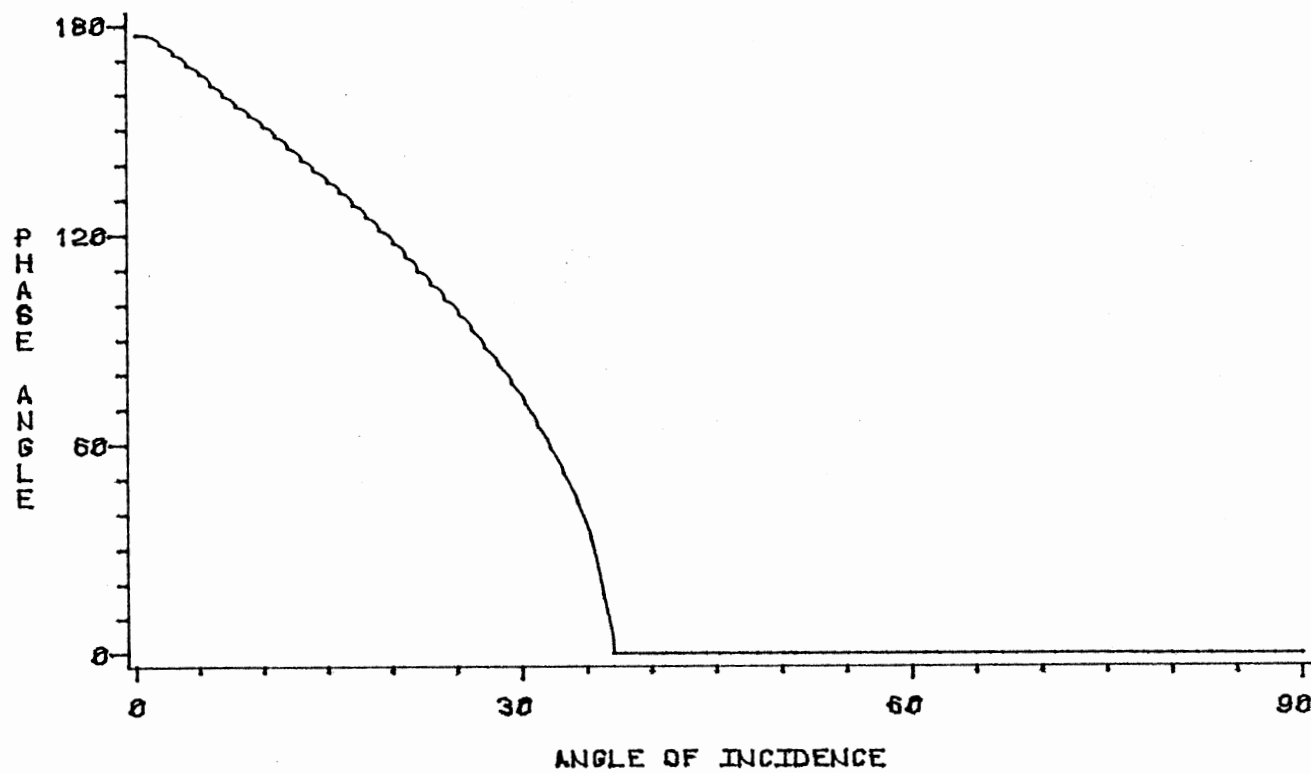


Figure 18. Phase Angle of Reflected P-Wave for an Incident P-Wave on Sandstone/Limestone Interface

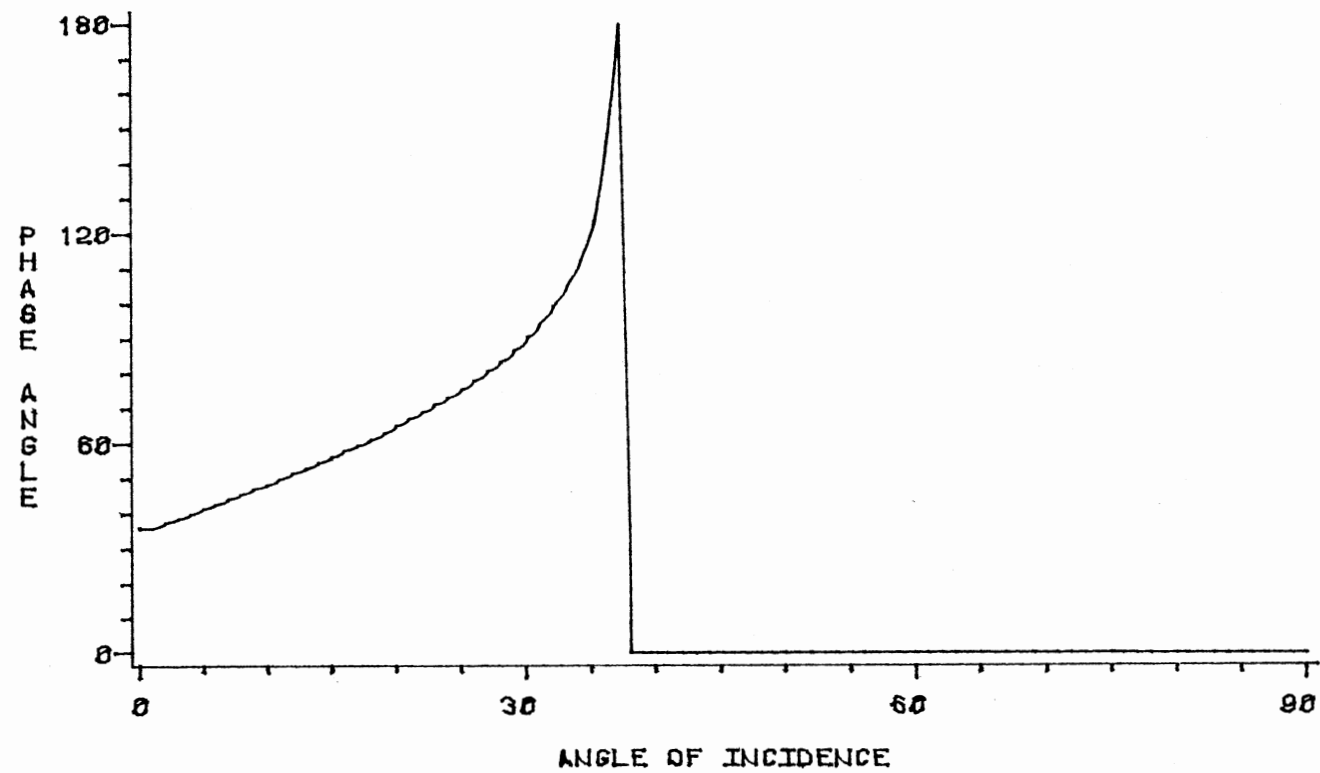


Figure 19. Phase Angle of Reflected S-Wave for an Incident P-Wave on Sandstone/Limestone Interface

CHAPTER V

DIRECTIVITY OF REFLECTED AND TRANSMITTED WAVES

The angular dependence of the reflected, mode converted, and transmitted waves resulting from an incident p-wave of unit amplitude is obtained by solving the boundary value problem for angles of incidence ranging from normal incidence to grazing incidence. A polar representation of the amplitude of each generated wave is obtained by plotting it as a function of the emergent angle. A circular scale is used that represents a unit amplitude p-wave being incident on a plane at different angles. A horizontal line passing through the center of this circle represents the plane interface boundary. The vertical axis that passes the center of the circle represents a normal line to the plane of interface and intersects the common reflection point (CDP). Due to symmetry about the vertical axis the plots are reflected about it. The upper hemisphere is the reflected regime in the upper medium while the lower hemisphere is the transmitted regime in the lower medium. The p-wave and s-wave are plotted separately.

Directivity patterns are presented for realistic examples involving liquid/air, solid/air, liquid/solid, and solid/solid interfaces. In each case several values of velocities and densities are used, this allowing for critical and non-critical situations. Elastic properties of some rocks and fluids that are used are listed in Table I.

In order to have more understanding of these directivity patterns,

TABLE I
ELASTIC PROPERTIES OF ROCKS AND FLUIDS

Type of Fluid or Rock	Density (gr/cm ³)	Pressure Wave Velocity (km/sec)	Shear Wave Velocity (km/sec)
Air	0.00129	0.3444	0.0
Water	1.00	1.50	0.0
Oil	0.8794	1.4554	0.0
Mercury	13.5	1.45	0.0
Dry Sandstone (Porosity = 5.1%)	2.543	4.87	2.85
Wet Sandstone (Porosity = 5.1%)	2.606	4.55	3.10
Limestone (Solenhofer)	2.656	6.05	3.01
Shale	2.38	2.743	1.509
Calcite	2.712	6.53	3.36
Granite	2.634	6.16	3.56
Basalt	2.586	5.66	3.25

a contract is made, for any interface, between two plots. These two plots refer to the two possibilities that the plane wave can be incident at either side of the interface.

By examining these plots we notice the following:

1. In the case of solid/vacuum interface, the reflected p-wave has two total reflections, at normal and grazing incidence. Most of its energy is confined in a region of 30° about the normal. It vanishes at two angles, 13° and 30° from the horizontal at which all the energy is transferred to the mode-converted reflected s-wave. The reflected s-wave has a high directivity about an angle 30° from normal, and in this region, almost all of the energy is carried by the reflected s-wave. The angle beyond which the s-wave vanishes, θ_o , is related to the velocities in the solid as follows:

$$\cos \theta_o = \frac{\beta}{\alpha},$$

which is about 54° for sandstone. There is no wave transmitted into the vacuum as shown in Figure 20a.

2. In the case of liquid/vacuum interface, which is the simplest interface, no wave is transmitted into the vacuum, and no s-wave is generated in the fluid, so the p-wave is totally reflected for all angles of incidence as shown in Figure 20b.

3. In the case of solid/air interface, when the p-wave is incident from the solid side, the situation is very similar to solid vacuum interface for the reflected p-wave as shown in Figure 21b, and for the reflected s-wave as shown in Figure 22b. When the p-wave is incident from the air side, it is totally reflected for all angles of incidence

as shown in Figure 21a, and so s-wave is generated as shown in Figure 22a.

4. For water/air interface the p-wave is almost totally reflected because of the large contrast in impedance of the two media, and the fact that no mode-converted wave is generated as shown in Figure 23. The only difference between the two reflections from either side of the interface is a phase shift of π for the p-wave incident at the surface backed by water. The phase shift is not seen in Figure 23b because we are taking the absolute value of the wave amplitude.

5. For water/oil interface the reflected energy at normal incidence is less than 1% for a p-wave incident at either side of the interface. That is due to fact that both media have nearly the same impedance. Also the p-wave incident from water side is almost completely transmitted for all angles of incidence, except at grazing incidence where it is totally reflected as in Figure 24a. Similarly, the p-wave incident from the oil side is almost completely transmitted until it gets to the critical angle beyond which it is totally reflected as in Figure 24b. The clear distinction between the two cases is that for the case when the p-wave is incident at the surface backed by water (the medium with higher velocity) the total reflection appears in a region, while for the other case the total reflection is just at a point of grazing incidence. The critical angle is related to the p-wave velocities of both media as follows,

$$\theta_p^{cp} = \cos^{-1} \left(\frac{\alpha}{\alpha'} \right),$$

which is about 14° for the case of oil/water boundary.

6. For water/mercury interface, the two media have very different

densities and nearly equal velocities. The large contrast in impedance leads to more than 70% of the energy is reflected for a wide range of angles of incidence. Total reflection appears at grazing incidence for the p-wave incident from the water side as in Figure 25a; and at some critical angle when the p-wave incident from mercury side as in Figure 25b. We notice that the critical angles for mercury/water and oil/water are nearly equal because both media (mercury and oil) have nearly the same p-wave velocity.

7. Water/sandstone interface. The p-wave velocity is less than both waves velocities of sandstone. This leads to two critical reflections for the p-wave incident at the interface backed by sandstone. The first critical reflection is at an angle θ_p^{cp} , which is related to the ratio of p-wave velocities as follows:

$$\theta_p^{(cp)} = \cos^{-1}(\alpha/\alpha')$$

which is about 72° . The second total reflection is at and beyond the other critical angle θ_p^{cs} , which is related to the p-wave velocity of water and the s-wave velocity of sandstone as follows:

$$\theta_p^{(cs)} = \cos^{-1}(\alpha/\beta'),$$

which is about 58° . The transmitted p-wave varies smoothly from 40% at normal incidence to 16% just before the first critical angle. This corresponds to a transmitted angle of 18° as in Figure 26a.

The transmitted s-wave is centered about an angle 60° from normal and it carries less than 50% of the energy. It has a minimum at an angle corresponds to the first critical angle, and it vanishes at and beyond another angle which corresponds to the second critical angle.

There is no s-wave reflected in the water side as shown in Figure 27A. When the p-wave is incident from the solid side the reflected p-wave with 60% of the energy is confined about the normal.

There are two angles at which the reflected p-wave is minimum, and most of the energy is carried by the reflected s-wave. The transmitted p-wave is confined in a very narrow region about the normal and it varies smoothly from 40% at normal incidence to about 17% at grazing incidence corresponding to 18° from normal. I would like to emphasize the point here that the transmitted p-wave does not vanish for any angle of incidence. What is shown in the lower part of Figure 26B is the transmitted p-wave plotted against its real emergent angle which is limited between 72° and 90° according to the relation

$$\cos\theta'_p = \frac{\alpha'}{\alpha} \cos\theta_p$$

So for normal incidence $\theta'_p = 90^\circ$, and for grazing incidence $\theta'_p = 72^\circ$.

The reflected s-wave has a high directivity about an angle 30° from the normal, and it is not as broad as the transmitted s-wave in the solid for the other case. There is no transmitted s-wave in the water as shown in Figure 27B.

8. Water/limestone interface--when the p-wave is incident from the water side, the general behavior of the reflections is similar to that for water/sandstone interface as shown in Figures 28A and 29A. The location of the critical reflections has changed according to the relative velocities of the emergent waves to the incident one. The magnitude of the reflection is also governed by the relative densities of both media. Where the p-wave is incident from the solid side, the

reflection is generally similar to that for water/sandstone interface. The reflected p-wave here has one minimum instead of two, and hence it is missing the miniloop that was there in water/sandstone interface. The transmitted p-wave carries less energy here, and more confined than was before as shown in Figure 28B.

The reflected s-wave, still, has a high directivity; but now about angle closer to the normal than before due to the difference in wave velocities of limestone and sandstone as shown in Figure 29B.

9. Water/shale interface--the p-wave is incident from the water side. The situation is similar to the water/sandstone case but due to the large difference in wave velocities of the two media (sandstone and shale) the critical angles changed considerably; the first angle is about 58° and the other is 6° , so that a very broad s-wave is transmitted as shown in Figure 31A. The transmitted p-wave carries energy that varies smoothly from 60% at normal incidence to 30% at grazing incidence, as shown in Figure 30A. When the p-wave is incident from the solid side, there is no critical angle, and the reflection is generally similar to that of water/sandstone with some changes in the location of extreme values of energy as shown for the reflected and transmitted p-wave in Figure 30B, and for the reflected s-wave in Figure 31B.

10. Sandstone/limestone interface--when the p-wave is incident from the sandstone, it is almost completely transmitted until it gets to the critical angle where it is almost totally reflected as shown in Figure 32A, and no energy is carried by the transmitted p-wave across the boundary. The reflected and transmitted s-waves carries very little energy peaked at an emergent angle which corresponds to the critical angle as shown in Figure 33A. Mode converted waves that are generated

are mainly governed by the relative s-wave velocities and the relative densities. So, when the two media have nearly the same s-wave velocity and density, the mode converted waves almost vanish, as they do in this case. When the p-wave is incident from limestone, there is no critical angle, and it is almost completely transmitted for all angles of incidence except at grazing incidence where it is totally reflected as shown in Figure 32B. The reflected and transmitted s-waves have less energy than the first case, where there was some critical reflection, and thus carry negligible energy as shown in Figure 33B.

11. Sandstone/shale interface--when the p-wave is incident from sandstone, which has a higher velocity than that of shale, the p-wave is almost totally transmitted for all angles of incidence except at grazing incidence where it is totally reflected. The p-wave has a peak about the normal incidence where it carries 8% of the energy as shown in Figure 34A. The reflected and transmitted s-waves have high directivity as shown in Figure 35A, and they have more energy than it was with sandstone/limestone because the two media here have considerably different values in s-wave velocities and densities.

When the p-wave is incident from shale, there are two critical reflections. The first critical angle, at about 55° , corresponds to the p-wave starts propagating parallel to the interface carrying no energy across the boundary, and the second critical angle corresponds to the transmitted s-wave propagating parallel to the interface carrying no energy across the barrier. The p-wave is totally reflected as shown in Figure 34B.

The reflected s-wave has a minimum which corresponds to the first critical angle, and it has more energy than the reflected s-wave in

sandstone in the first case, this occurs because the p-wave drops to zero earlier than before. The transmitted s-wave carries considerable energy between the two critical angles, and it is broader than before (transmitted s-wave in limestone) as shown in Figure 35B.

12. Sandstone/granite interface--when the p-wave is incident from sandstone, the situation is similar to that of sandstone/limestone. Beyond the critical angle the p-wave is not totally reflected, as shown in Figure 36A, and a considerable amount of energy is carried by the reflected and transmitted s-waves as shown in Figure 37A. When the p-wave is incident from granite, the p-wave is almost completely transmitted except at grazing incidence where it is totally reflected as shown in Figure 36B. The reflected and transmitted s-waves are less in amplitude than before, where there was critical reflection, as shown in Figure 37B.

13. Sandstone/basalt, and sandstone/calcite interfaces--since basalt, calcite and granite are igneous rocks with similar acoustic properties, the general reflections for them are similar too. For the case of sandstone/basalt, when the p-wave is incident from sandstone to basalt the reflected and transmitted p-waves are shown in Figure 38A, while the reflected and transmitted s-waves are shown in Figure 39A. The critical angle has shifted away from normal since the p-wave velocity of basalt is less than that of granite. When the p-wave is incident from basalt to sandstone the reflected and transmitted p-waves are shown in Figure 38B, while the reflected and transmitted s-waves are shown in Figure 39B. For the case of sandstone/calcite interface, when the p-wave is incident from sandstone to calcite the reflected and transmitted p-waves are shown in Figure 40A while the reflected and trans-

mitted s-waves are shown in Figure 41A. The critical angle has shifted toward the normal, since the p-wave velocity of calcite is greater than that of granite. When the p-wave is incident from calcite to sandstone the reflected and transmitted p-waves are shown in Figure 40B, while the reflected and transmitted s-waves are shown in Figure 41B.

14. For sandstone (wet)/limestone interface, the general reflection is similar to that of sandstone/limestone. When the p-wave is incident from sandstone (wet) the reflected and transmitted p-waves are shown in Figure 42A, while the reflected and transmitted s-waves are shown in Figure 43A. The critical angle here has shifted away from normal, since the p-wave velocity of sandstone (wet) is less than that of limestone.

When the p-wave is incident from limestone to sandstone (wet) the reflected and transmitted p-waves are shown in Figure 42B, while the reflected and transmitted s-waves are shown in Figure 43B, which shows almost zero energy carried by the mode-converted waves. That is due to the fact that limestone and sandstone (wet) have almost the same density and shear velocity.

15. Sandstone (wet)/shale interface--the general reflection here is similar to that of sandstone/shale interface. The distinction between the two situations is that when the p-wave is incident from sandstone (wet) to shale the reflected p-wave has two minima causing a mini loop as shown in Figure 44A, and the transmitted s-wave carries more energy at its peaked value as shown in Figure 45A.

When the p-wave is incident from shale to limestone the reflected p-wave has less amplitude at the first critical reflection as shown in Figure 44B, and the transmitted s-wave carries more energy than that

was transmitted in sandstone as shown in Figure 45B.

General Comments on the Directivity of Reflected
and Transmitted Waves

1. There is no mode-converted waves at grazing and normal incidence.
2. There is always a total reflection for the p-wave at grazing incidence.
3. Mode-converted waves have high directivity about an angle, away from normal incidence, determined by the relative velocities.
4. If both media have nearly the same density and s-wave velocity, the mode converted waves have very small amounts of energy and they almost vanish when there is no critical reflection.
5. Critical angles exist when the incident wave has less velocity than the generated ones.
6. The first critical angle occurs when the incident p-wave has less velocity than the emergent p-wave, at which the transmitted p-wave drops to zero and hence a sharp increase is noticed for the other waves.
7. The second critical angle occurs when the incident p-wave has less velocity than the transmitted s-wave, beyond which no energy is transmitted and all the energy is carried by the reflected p-wave and s-wave (if it exists).
8. At normal incidence the reflected energy is equal for the p-wave incident from either way of the interface.
9. At normal incidence, the larger the difference in impedance between the media, the more the p-wave is reflected.

10. The relative velocities govern the critical angles, and the relative density affects the general behavior of the reflection.

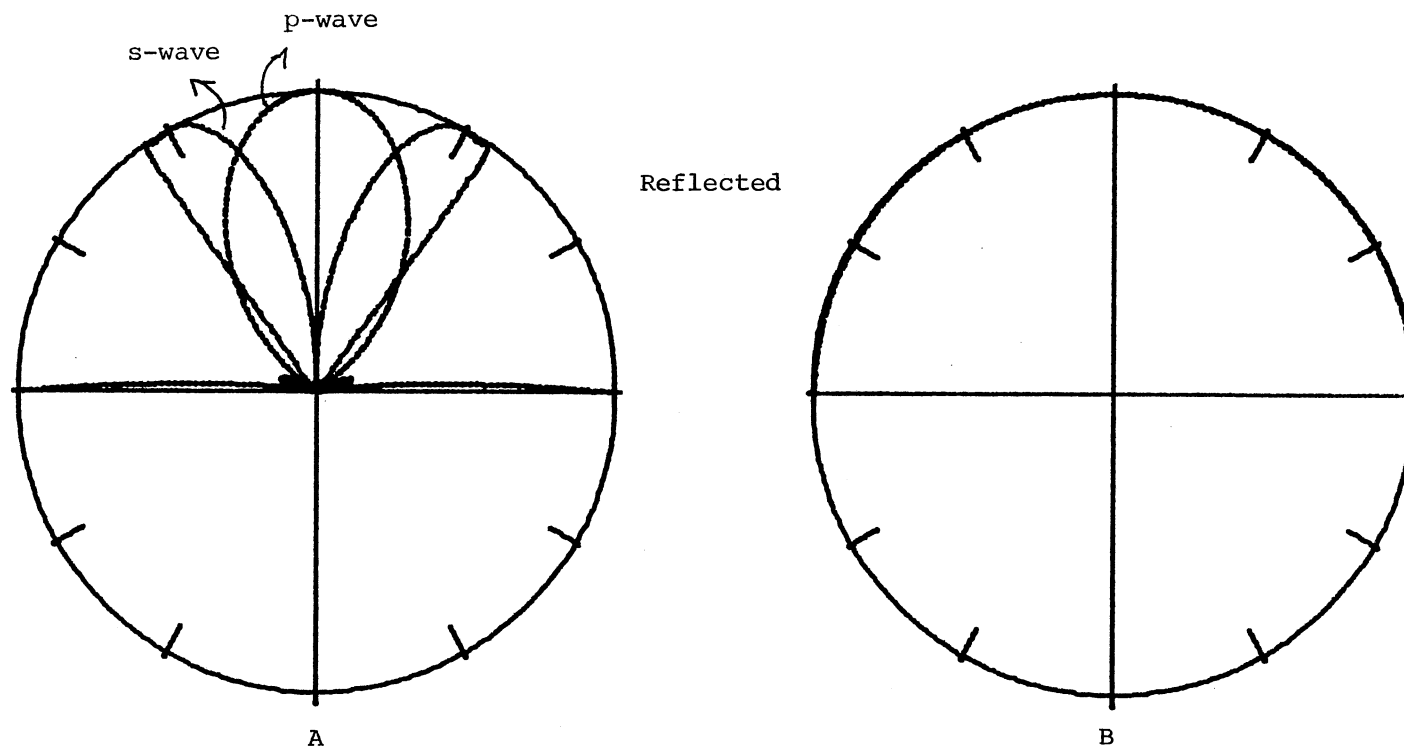


Figure 20. Polar Directivity of Reflected P- and S-Waves for an Incident P-Wave on
 (A) Sandstone/Vacuum Interface and (B) Liquid/Vacuum Interface

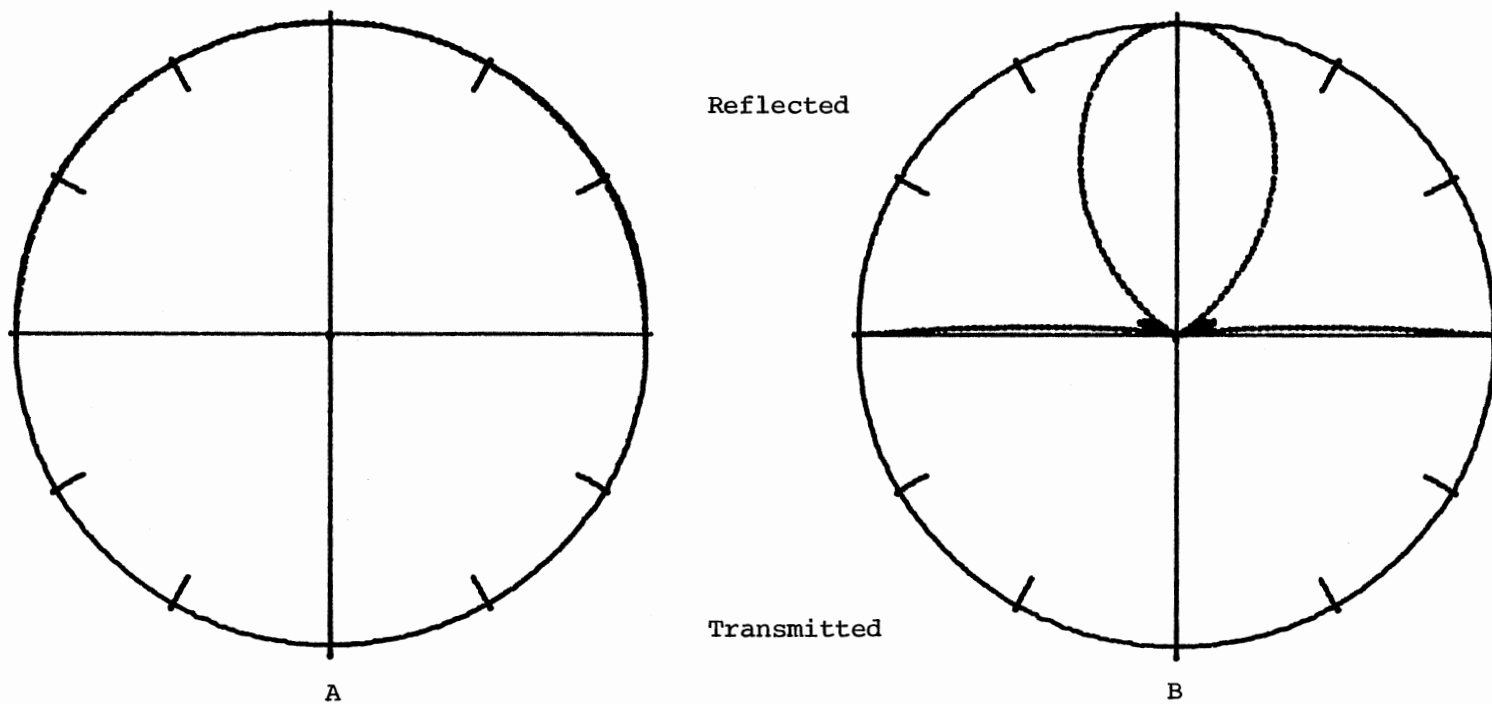


Figure 21. Polar Directivity of Reflected and Transmitted P-Wave for an Incident P-Wave on
 (A) Air/Sandstone Interface and (B) Sandstone/Air Interface

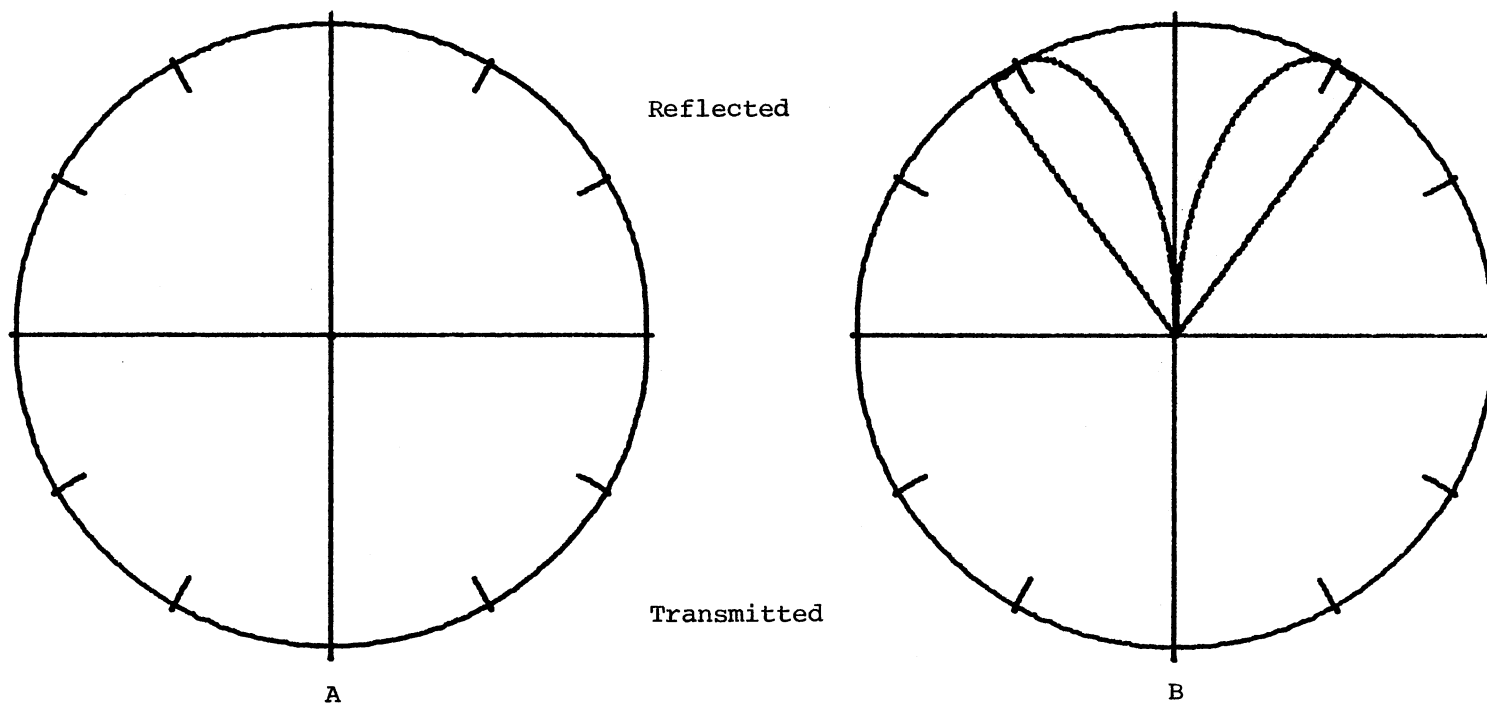


Figure 22. Polar Directivity of Reflected and Transmitted S-Wave for an Incident P-Wave on
 (A) Air/Sandstone Interface and (B) Sandstone/Air Interface

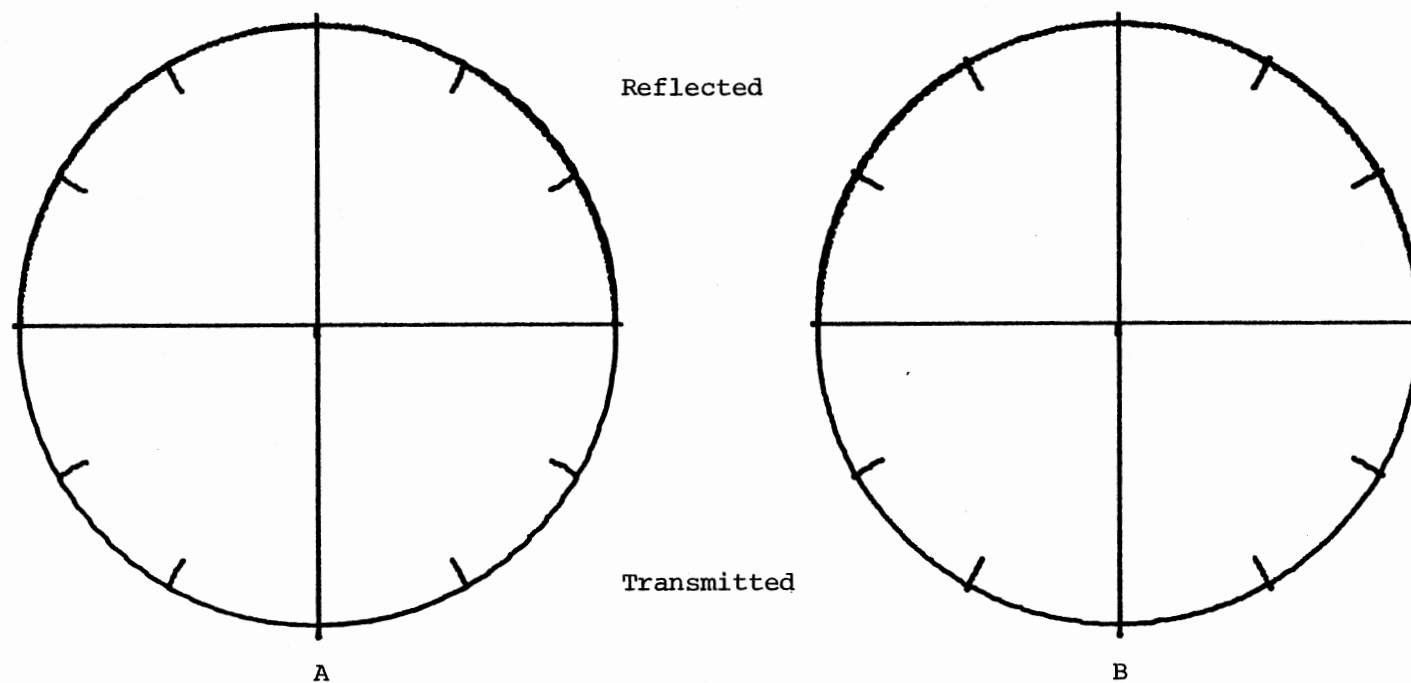


Figure 23. Polar Directivity of Reflected and Transmitted P-Wave for an Incident P-Wave on (A) Water/Air Interface and (B) Air-Water Interface

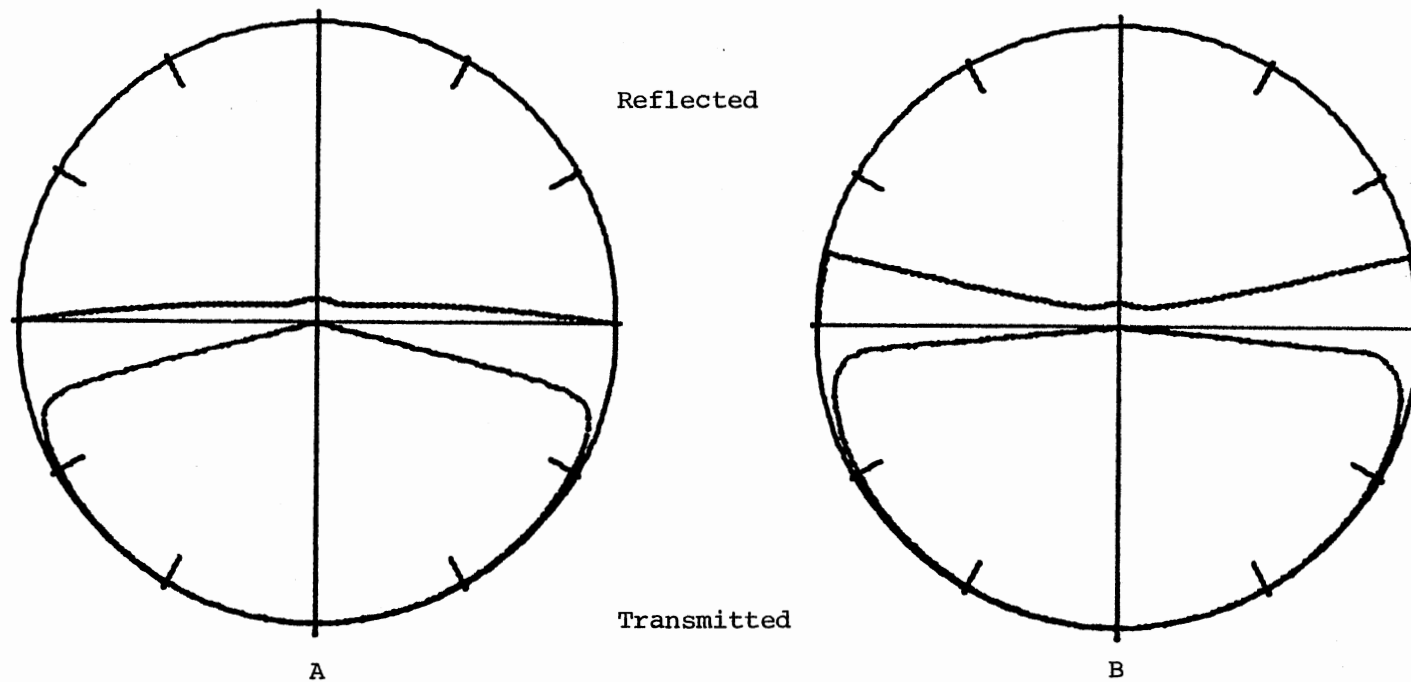


Figure 24. Polar Directivity of Reflected and Transmitted P-Wave for an Incident P-Wave on (A) Water/Oil Interface and (B) Oil-Water Interface

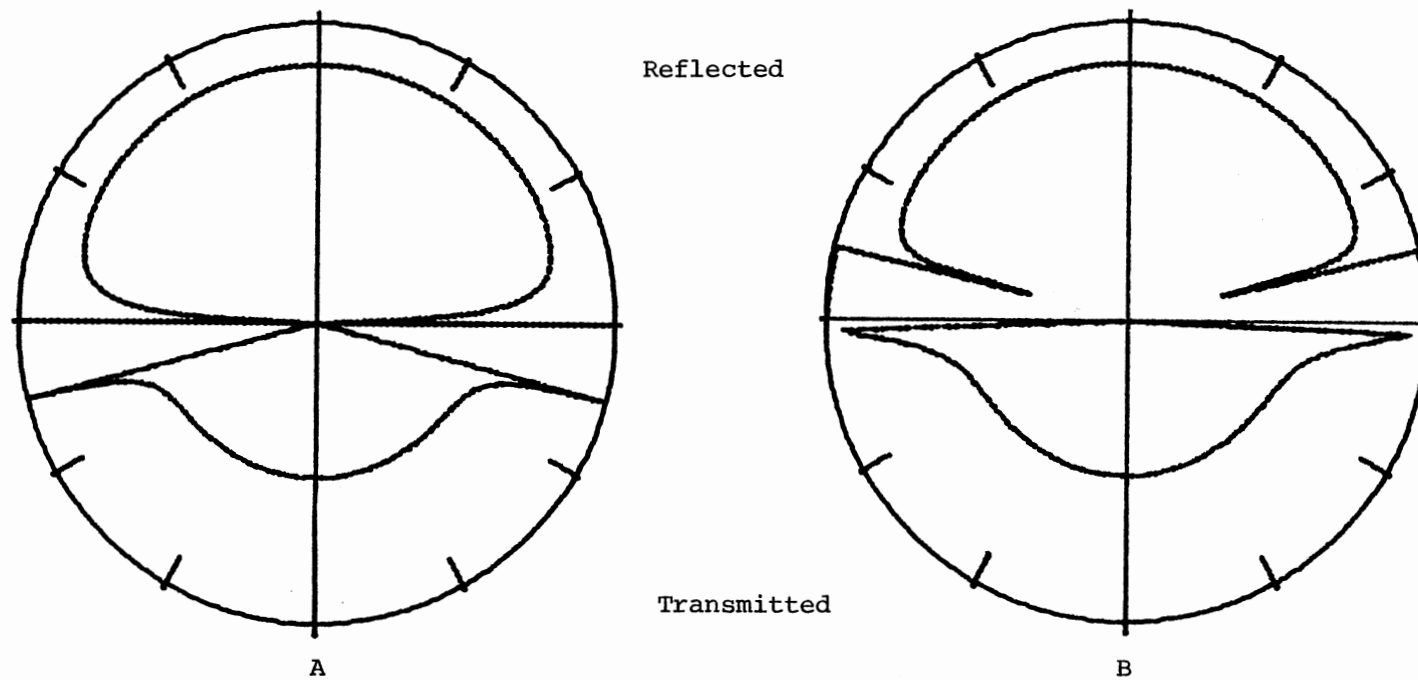


Figure 25. Polar Directivity of Reflected and Transmitted P-Wave for an Incident P-Wave on (A) Water/Mercury Interface and (B) Mercury/Water Interface

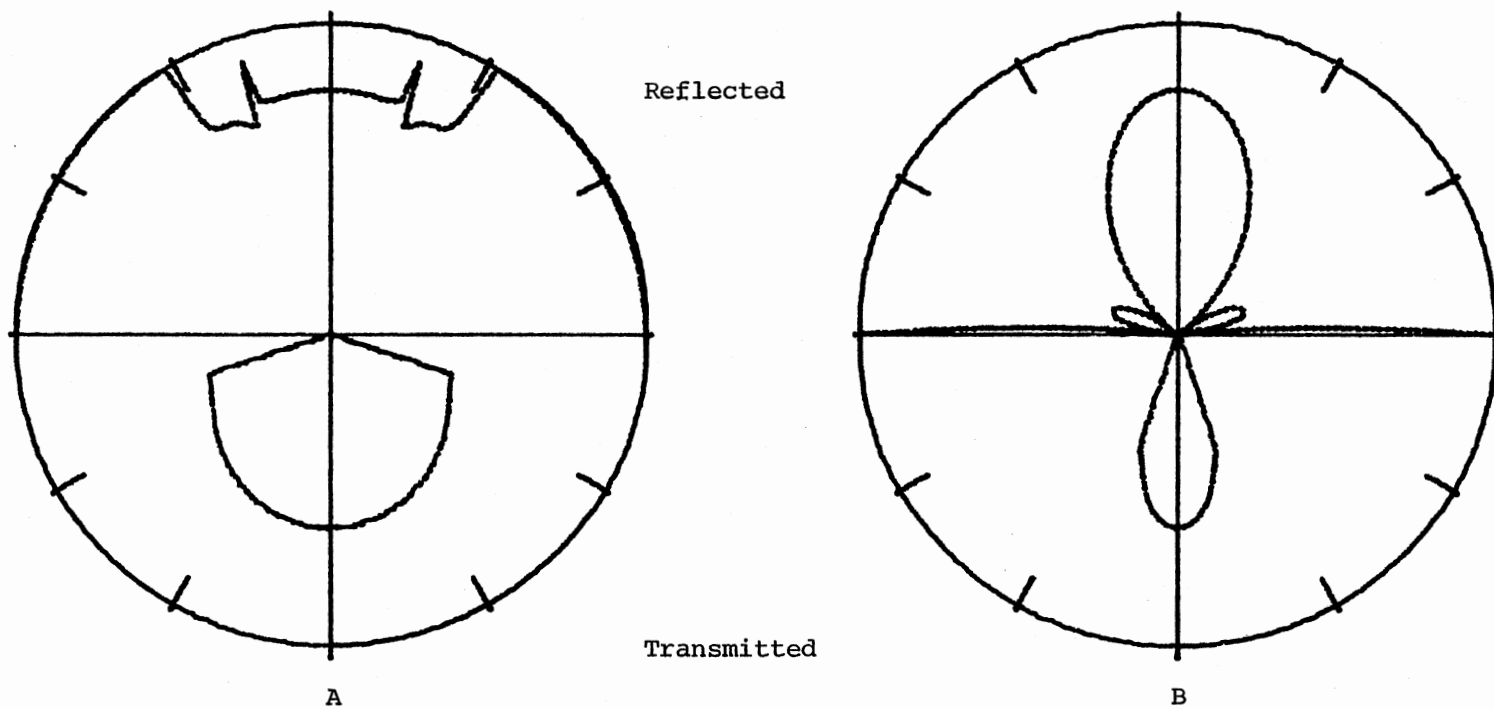


Figure 26. Polar Directivity of Reflected and Transmitted P-Wave for an Incident P-Wave on
 (A) Water/Sandstone Interface and (B) Sandstone/Water Interface

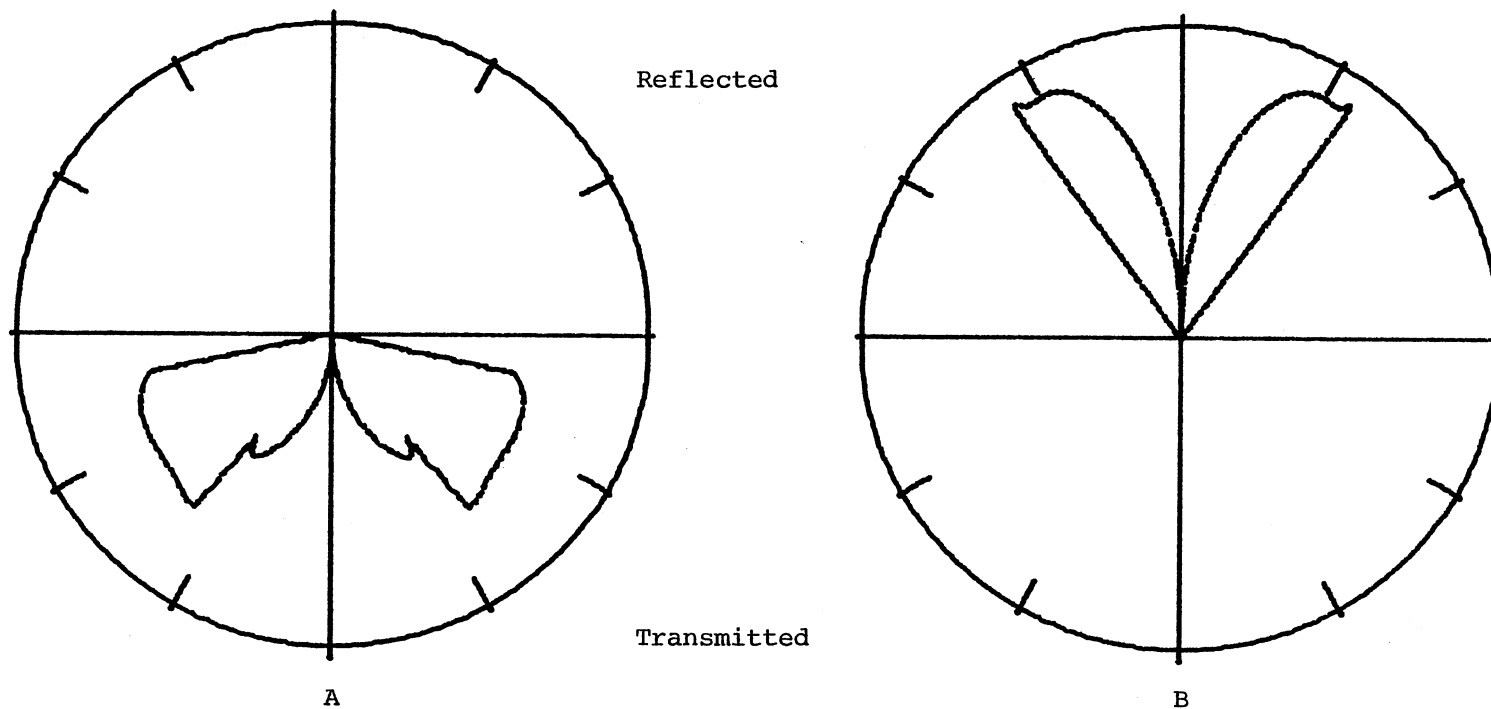


Figure 27. Polar Directivity of Reflected and Transmitted S-Wave for an Incident P-Wave on
 (A) Water/Sandstone Interface and (B) Sandstone/Water Interface

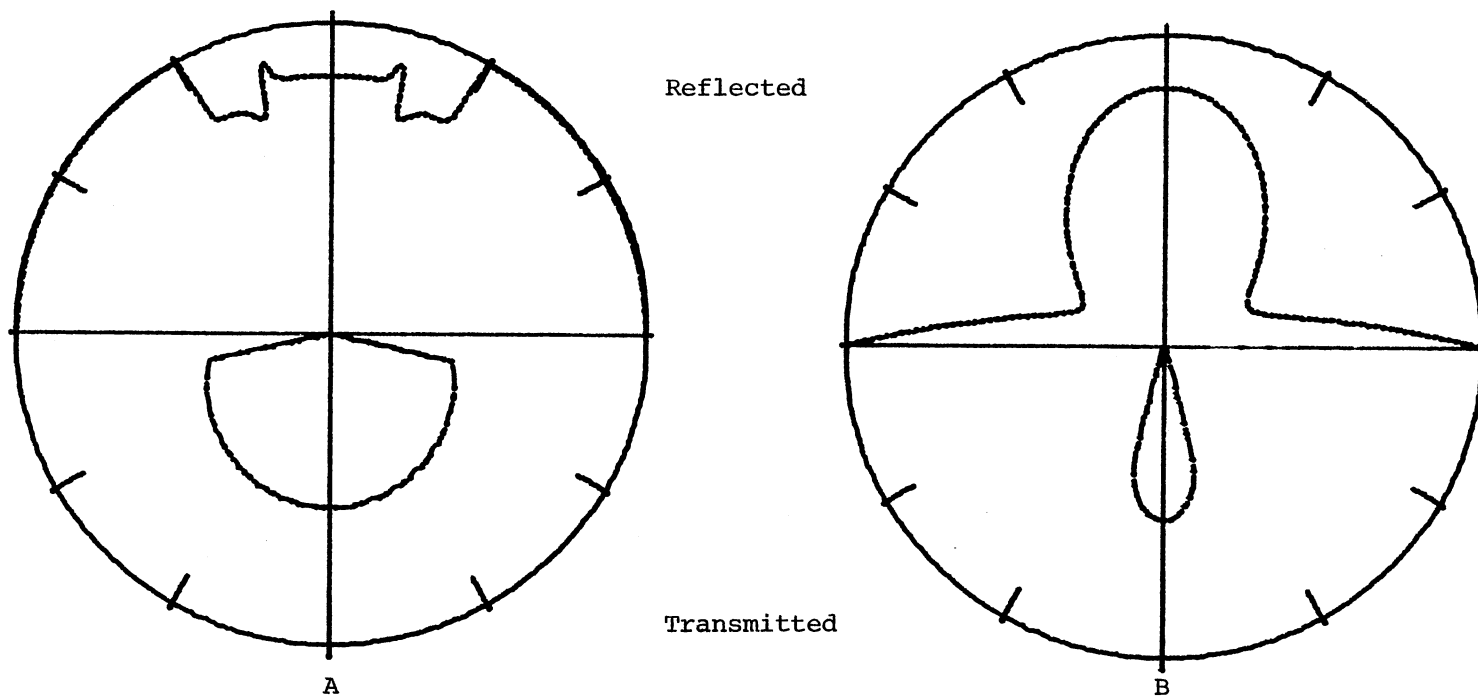


Figure 28. Polar Directivity of Reflected and Transmitted P-Wave for an Incident P-Wave on
 (A) Water/Limestone Interface and (B) Limestone/Water Interface

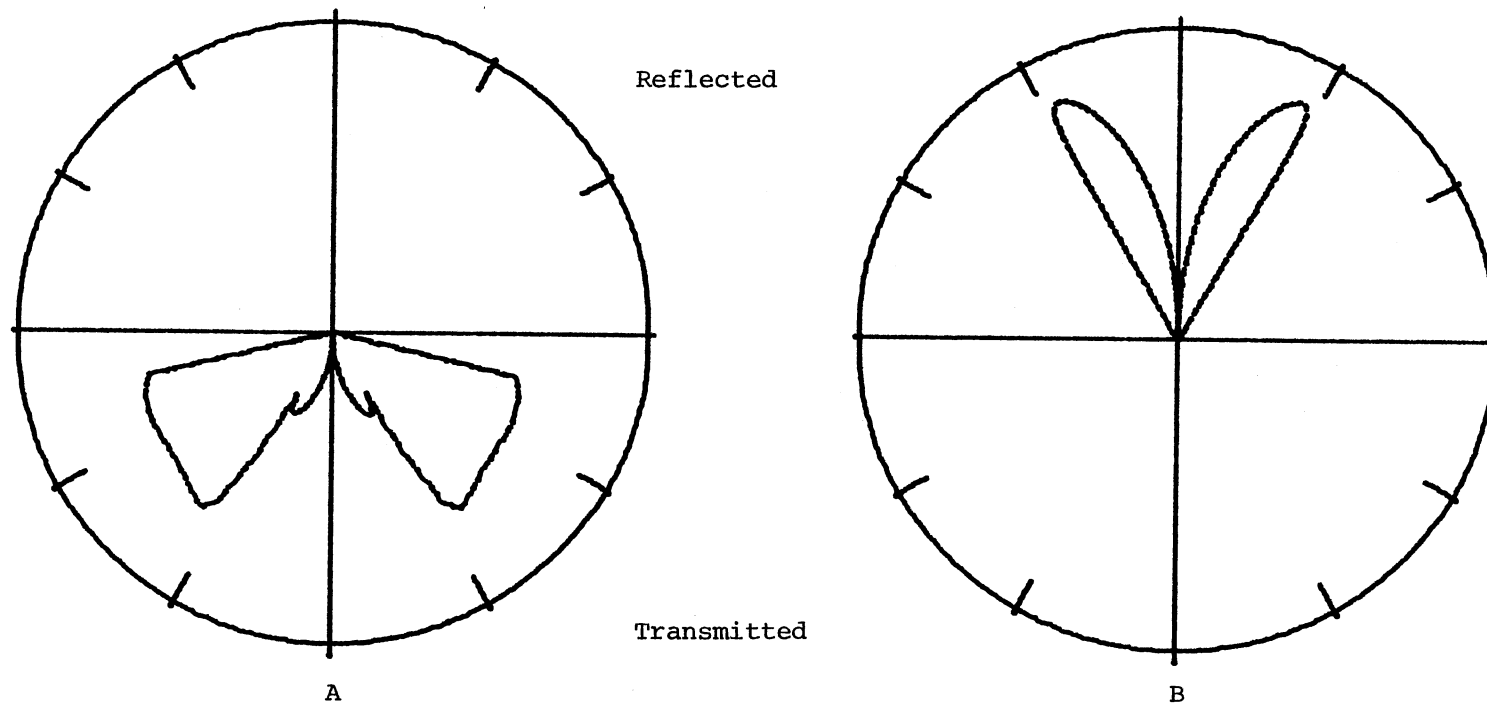


Figure 29. Polar Directivity of Reflected and Transmitted S-Wave for an Incident P-Wave on
(A) Water/Limestone Interface and (B) Limestone/Water Interface

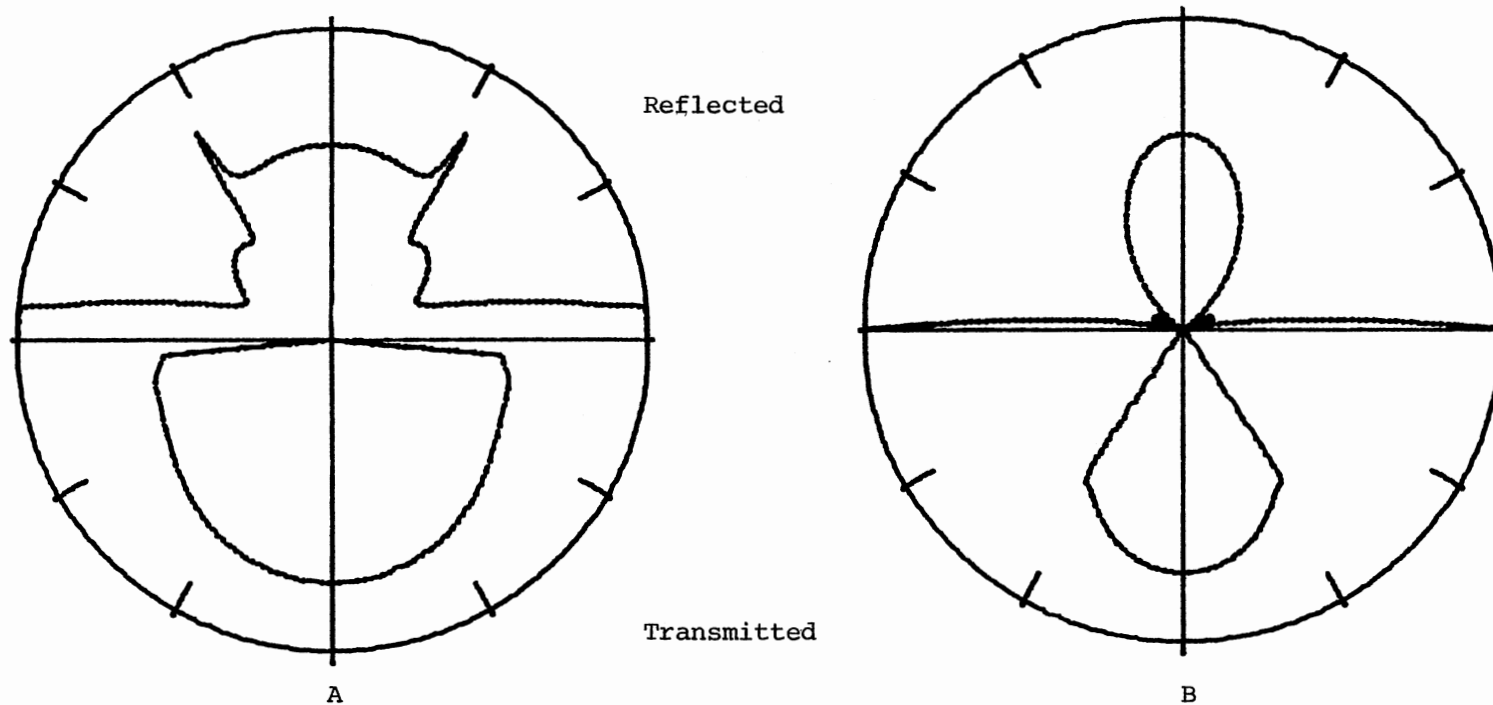


Figure 30. Polar Directivity of Reflected and Transmitted P-Wave for an Incident P-Wave on
(A) Water/Shale Interface and (B) Shale/Water Interface

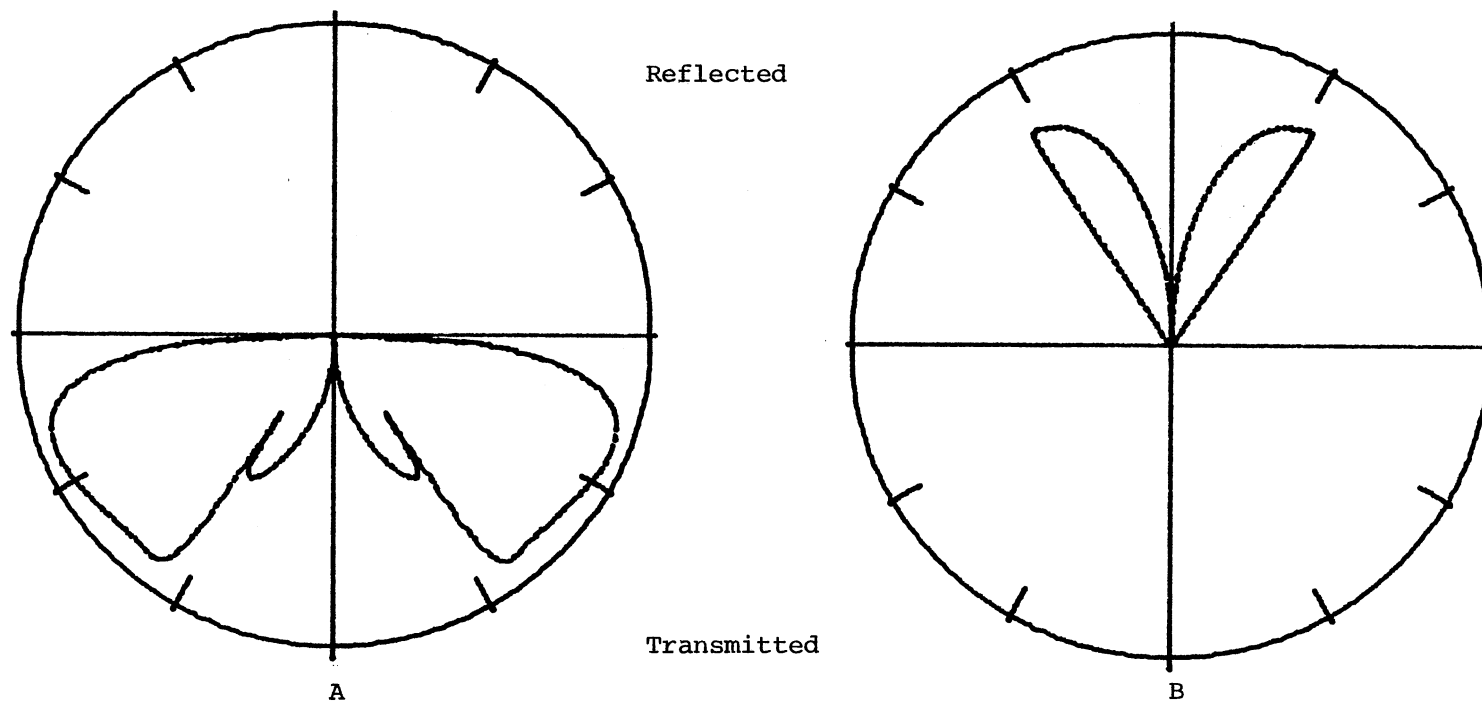


Figure 31. Polar Directivity of Reflected and Transmitted S-Wave for an Incident P-Wave on
(A) Water/Shale Interface and (B) Shale/Water Interface

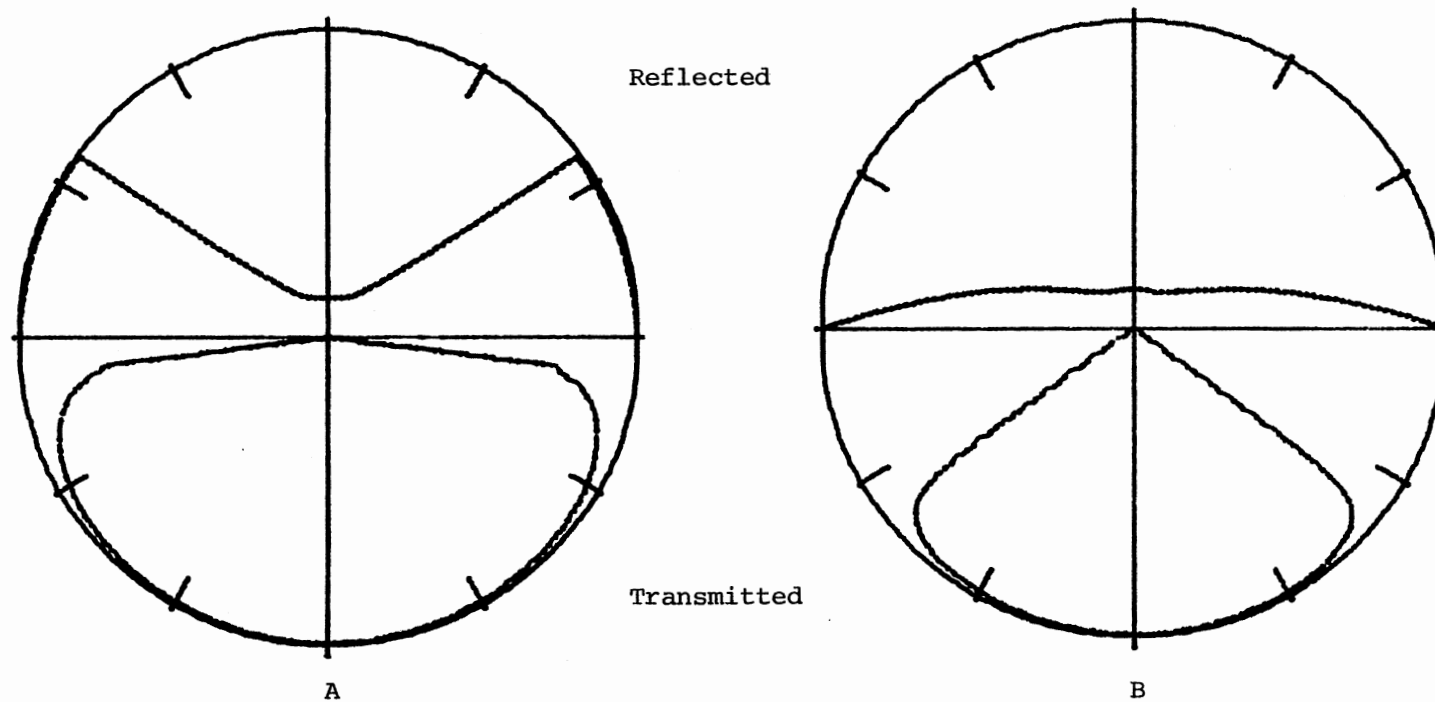


Figure 32. Polar Directivity of Reflected and Transmitted P-Wave for an Incident P-Wave on
 (A) Sandstone/Limestone Interface and (B) Limestone/Sandstone Interface

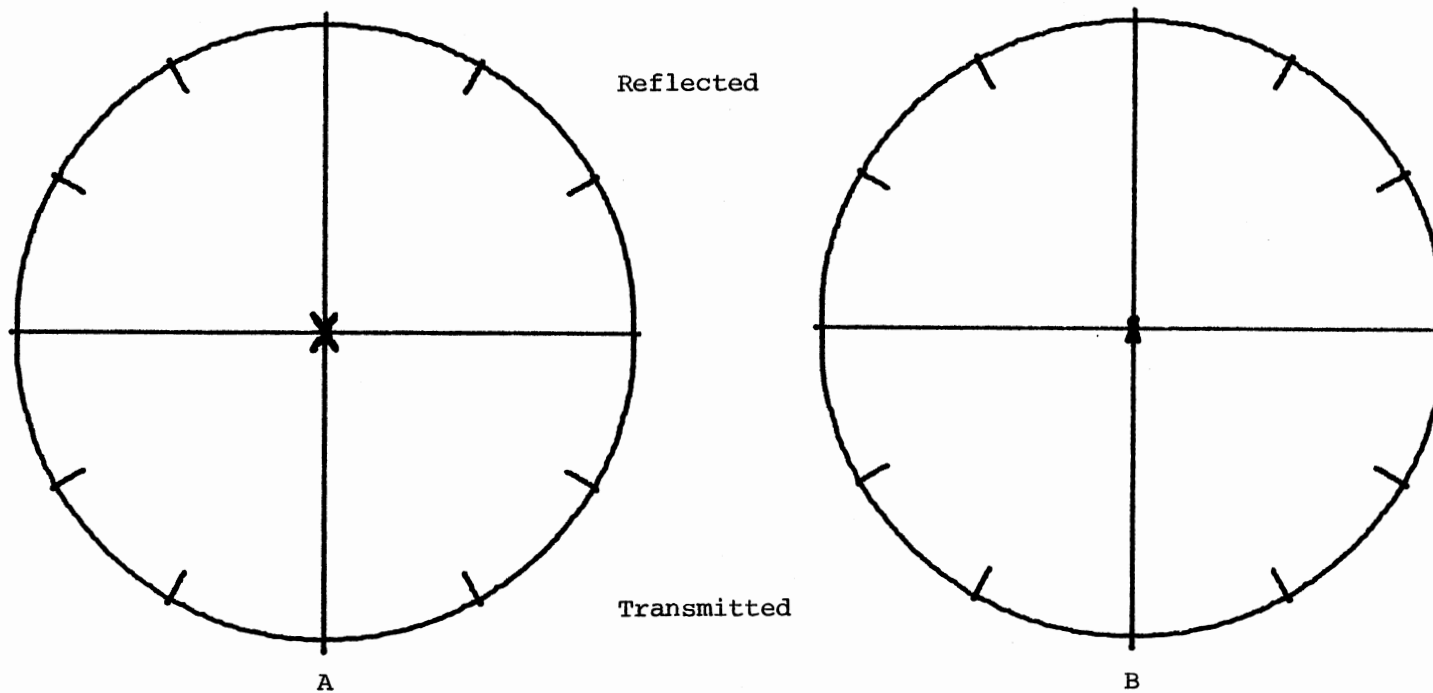


Figure 33. Polar Directivity of Reflected and Transmitted S-Wave for an Incident P-Wave on
 (A) Sandstone/Limestone Interface and (B) Limestone/Sandstone Interface

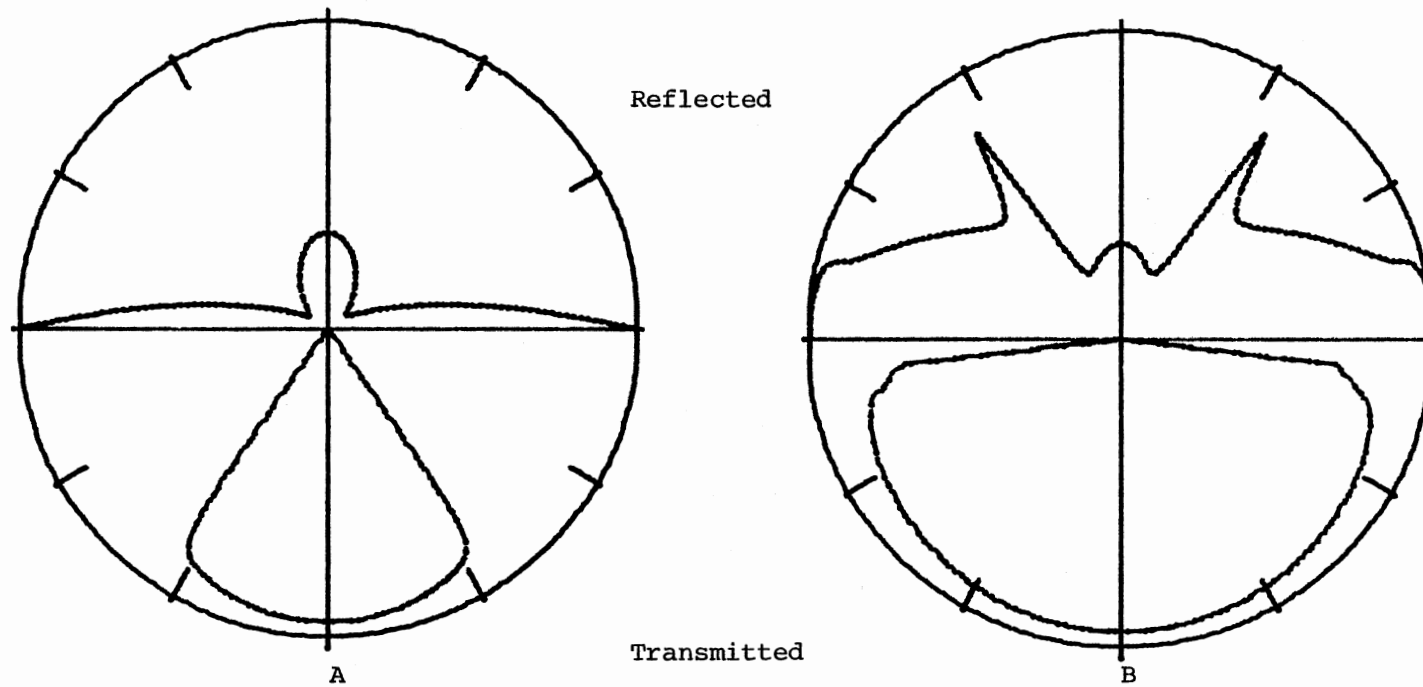


Figure 34. Polar Directivity of Reflected and Transmitted P-Wave for an Incident P-Wave on (A) Sandstone/Shale Interface and (B) Shale/Sandstone Interface

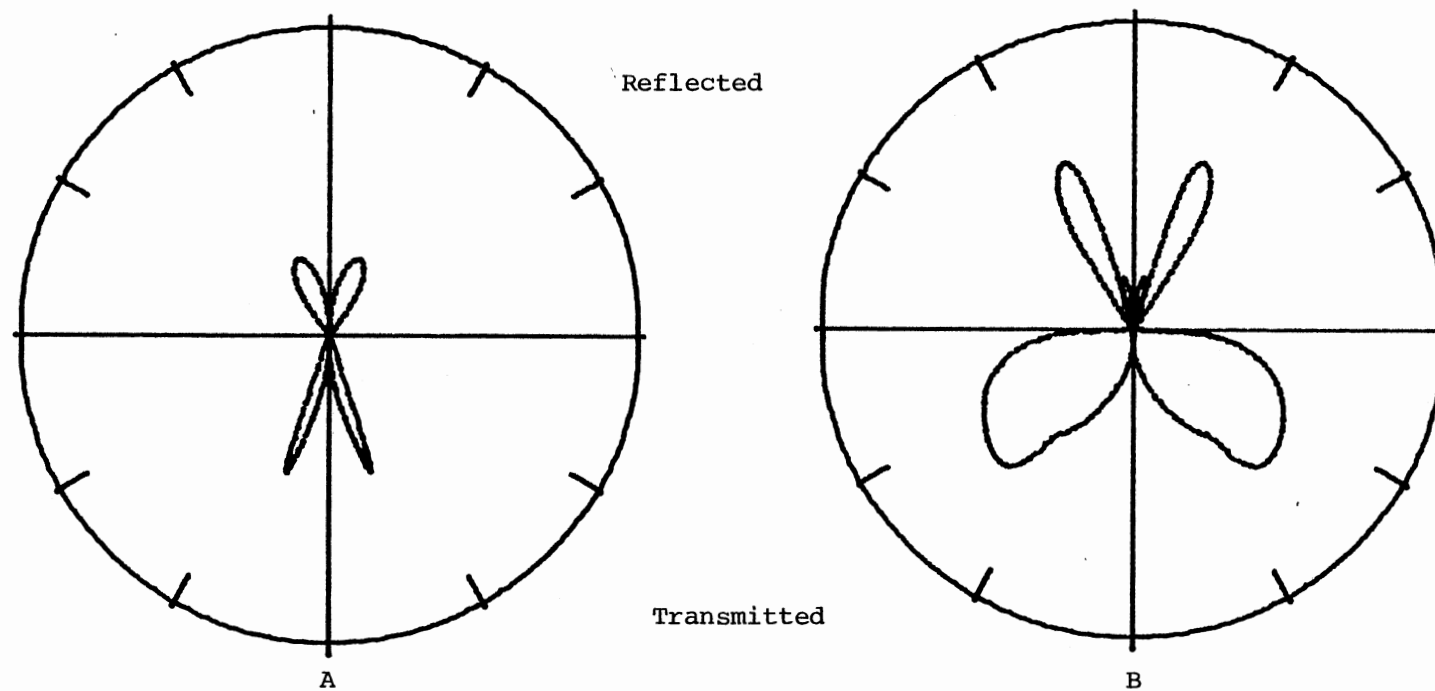


Figure 35. Polar Directivity of Reflected and Transmitted S-Wave for an Incident P-Wave on
 (A) Sandstone/Shale Interface and (B) Shale/Sandstone Interface

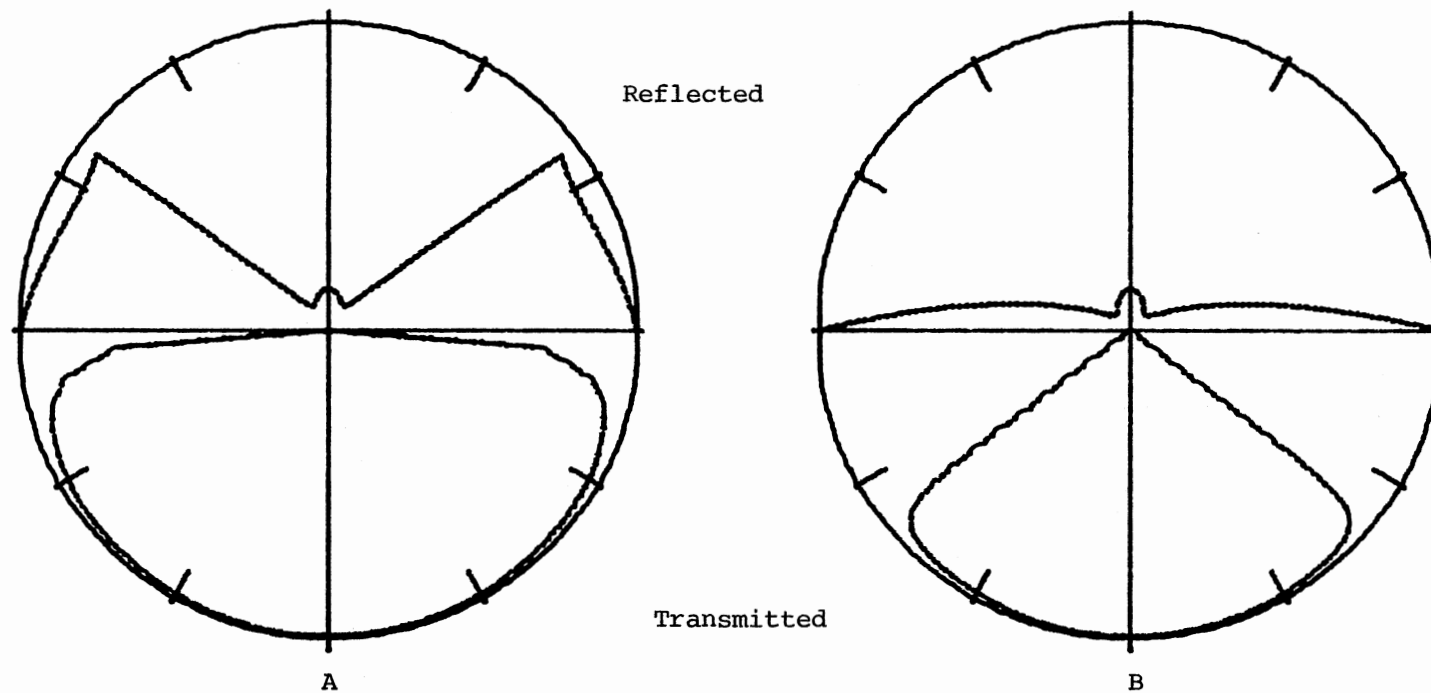


Figure 36. Polar Directivity of Reflected and Transmitted P-Wave for an Incident P-Wave on
 (A) Sandstone/Granite Interface and (B) Granite/Sandstone Interface

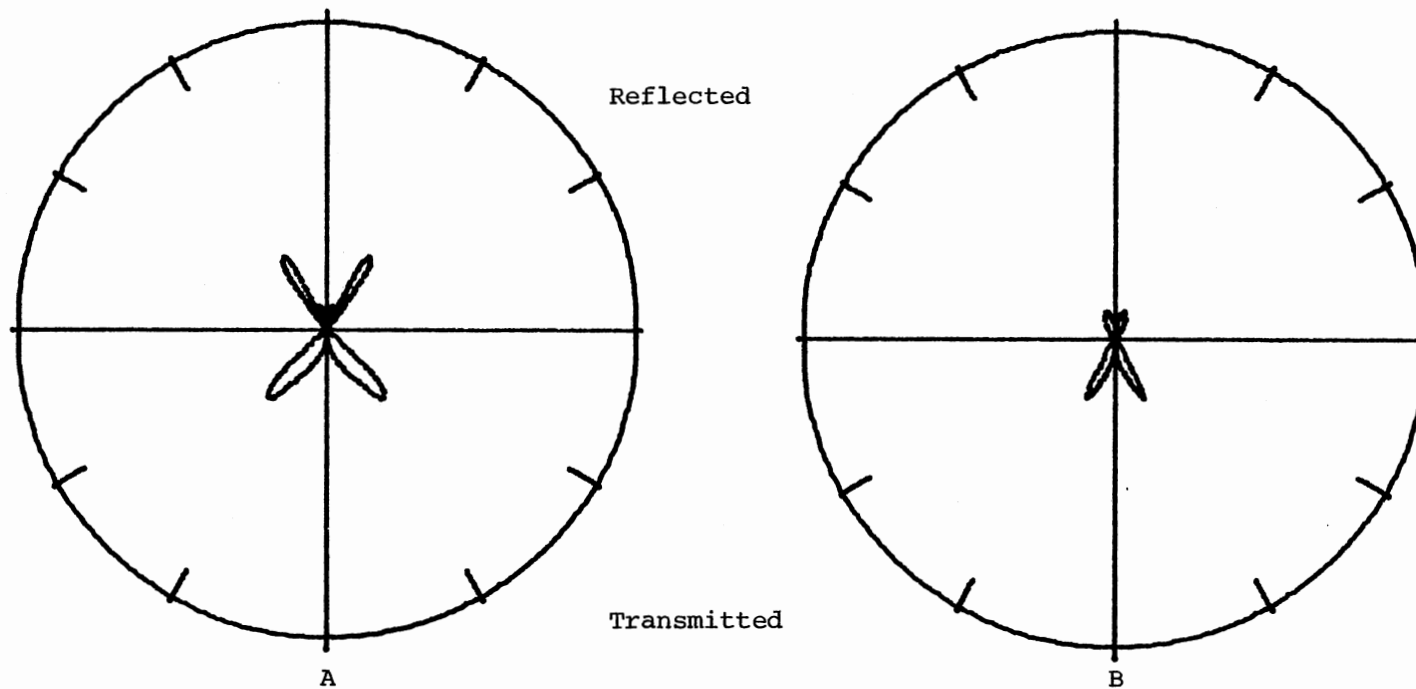


Figure 37. Polar Directivity of Reflected and Transmitted S-Wave for an Incident P-Wave on
 (A) Sandstone/Granite Interface and (B) Granite/Sandstone Interface

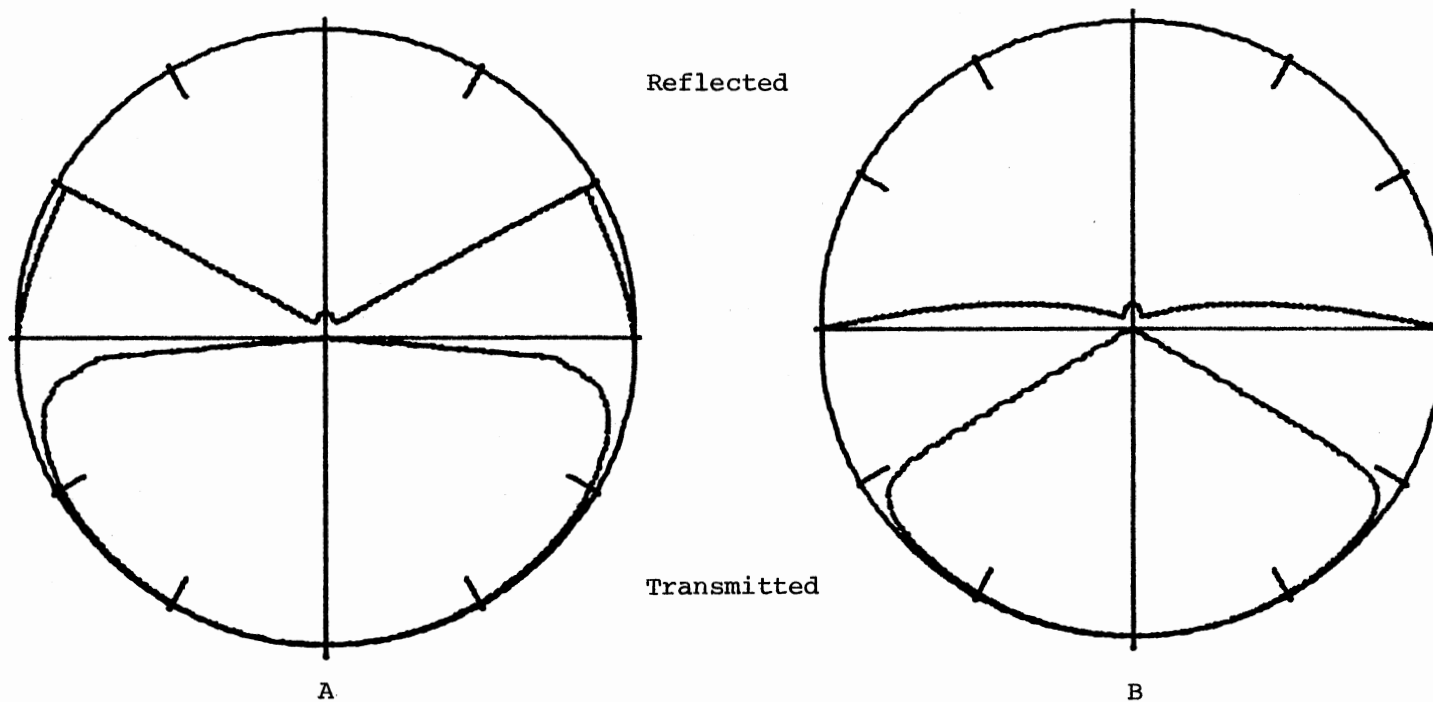


Figure 38. Polar Directivity of Reflected and Transmitted P-Wave for an Incident P-Wave on (A) Sandstone/Basalt Interface and (B) Basalt/Sandstone Interface

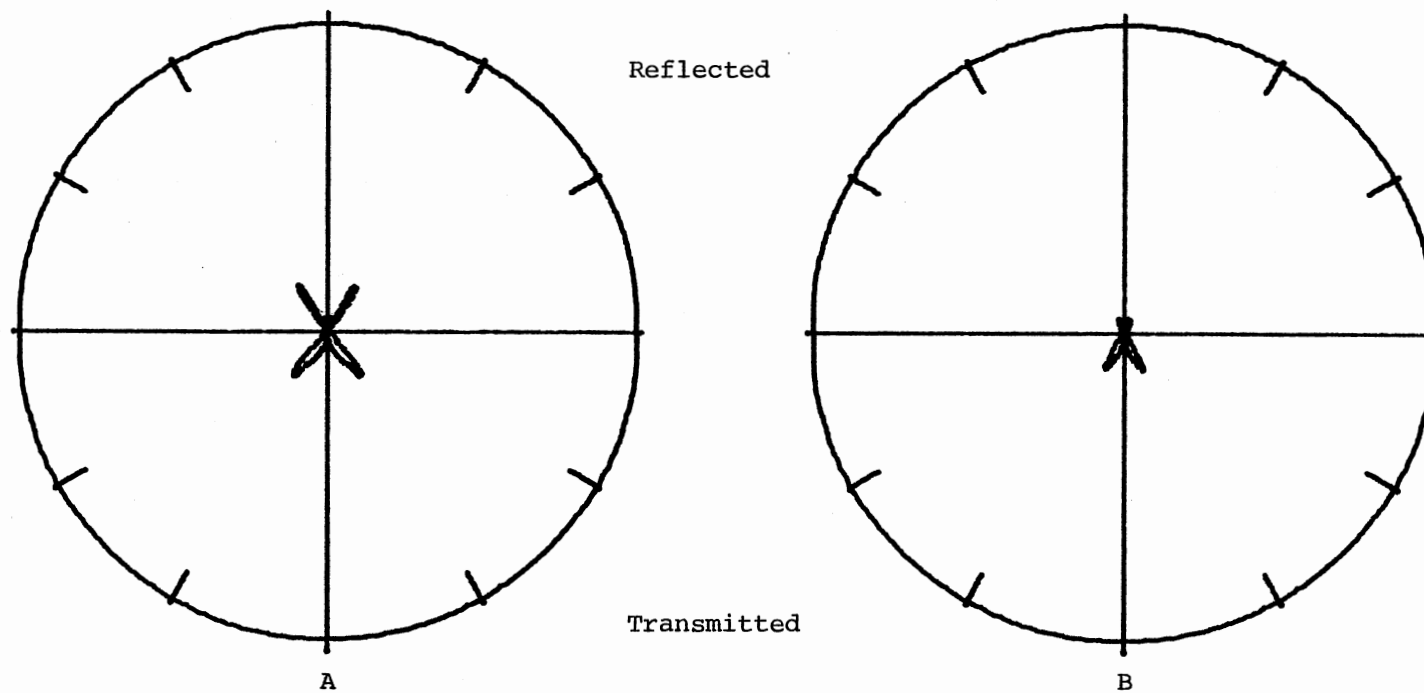


Figure 39. Polar Directivity of Reflected and Transmitted S-Wave for an Incident P-Wave on
 (A) Sandstone/Basalt Interface and (B) Basalt/Sandstone Interface

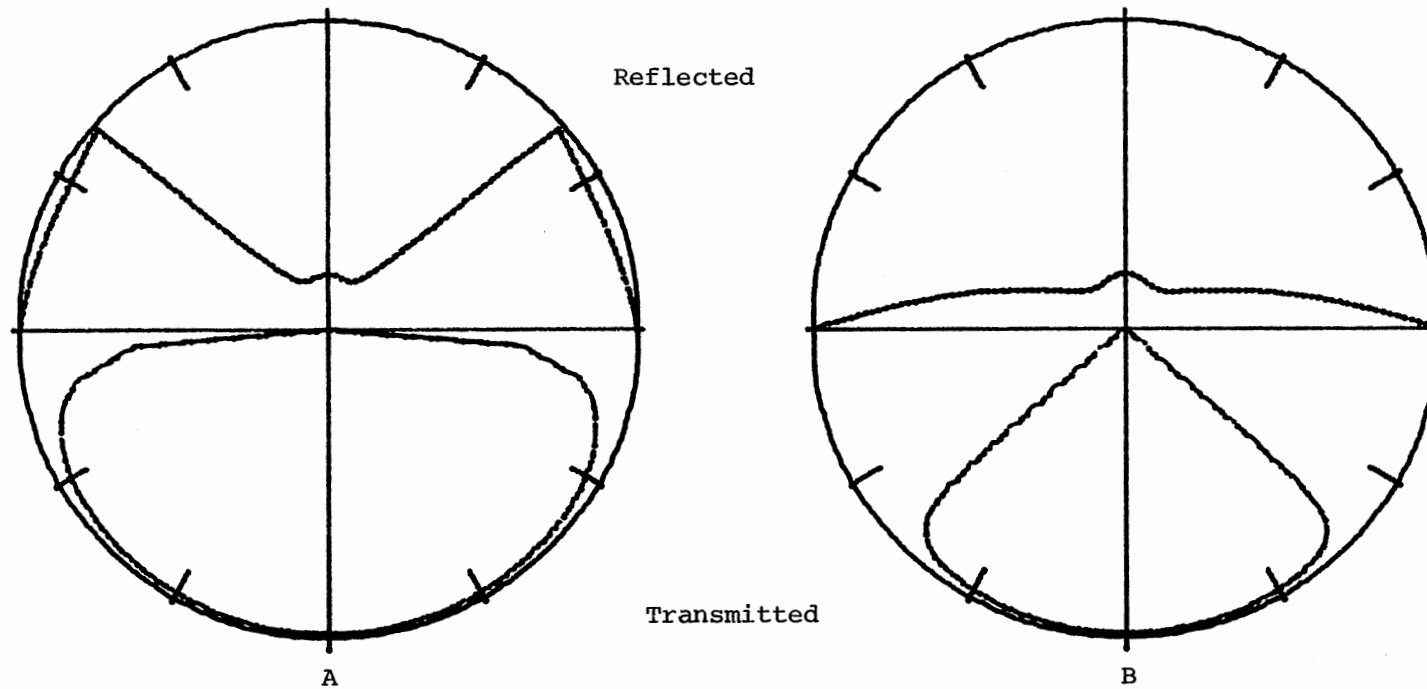


Figure 40. Polar Directivity of Reflected and Transmitted P-Wave for an Incident P-Wave on
 (A) Sandstone/Calcite Interface and (B) Calcite/Sandstone Interface

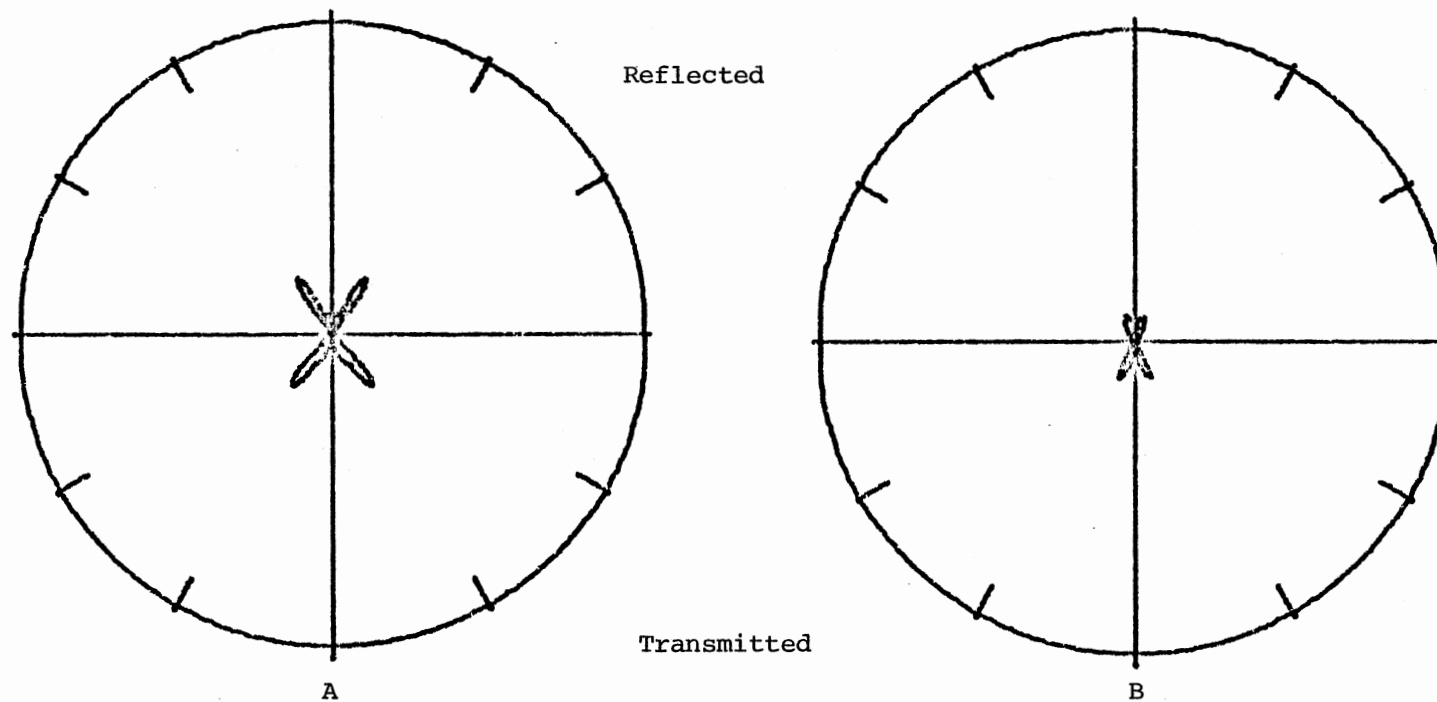


Figure 41. Polar Directivity of Reflected and Transmitted S-Wave for an Incident P-Wave on
(A) Sandstone/Calcite Interface and (B) Calcite/Sandstone Interface

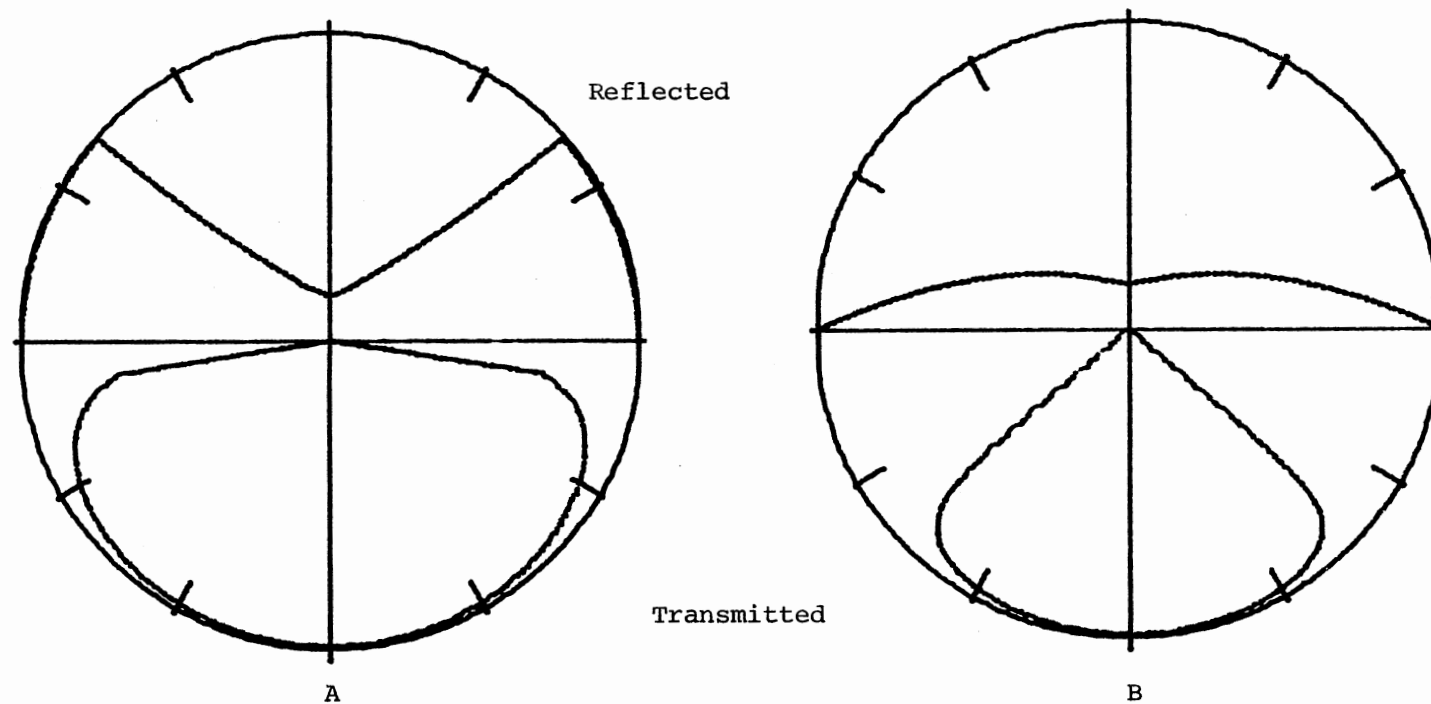


Figure 42. Polar Directivity of Reflected and Transmitted P-Wave for an Incident P-Wave on (A) Sandstone (Wet)/Limestone Interface and (B) Limestone/Sandstone (Wet) Interface

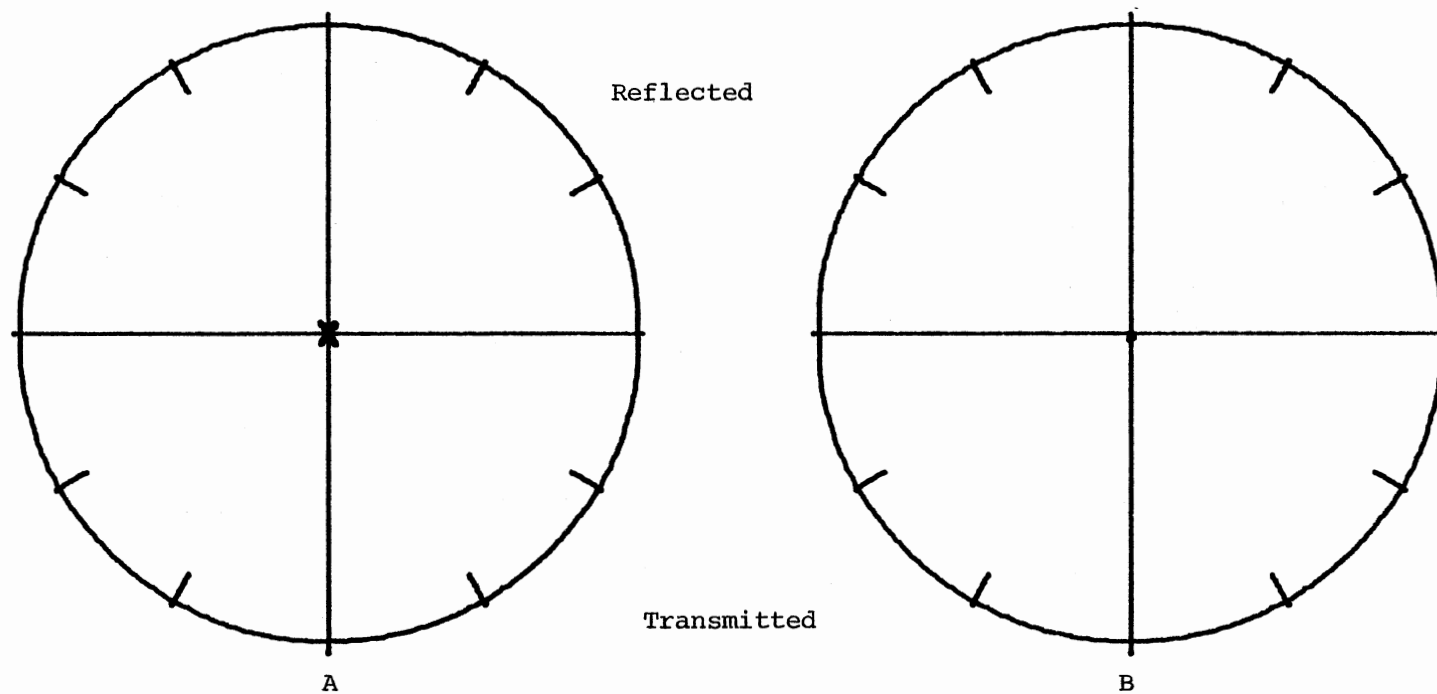


Figure 43. Polar Directivity of Reflected and Transmitted S-Wave for an Incident P-Wave on
 (A) Sandstone (Wet)/Limestone Interface and (B) Limestone/Sandstone (Wet)
 Interface

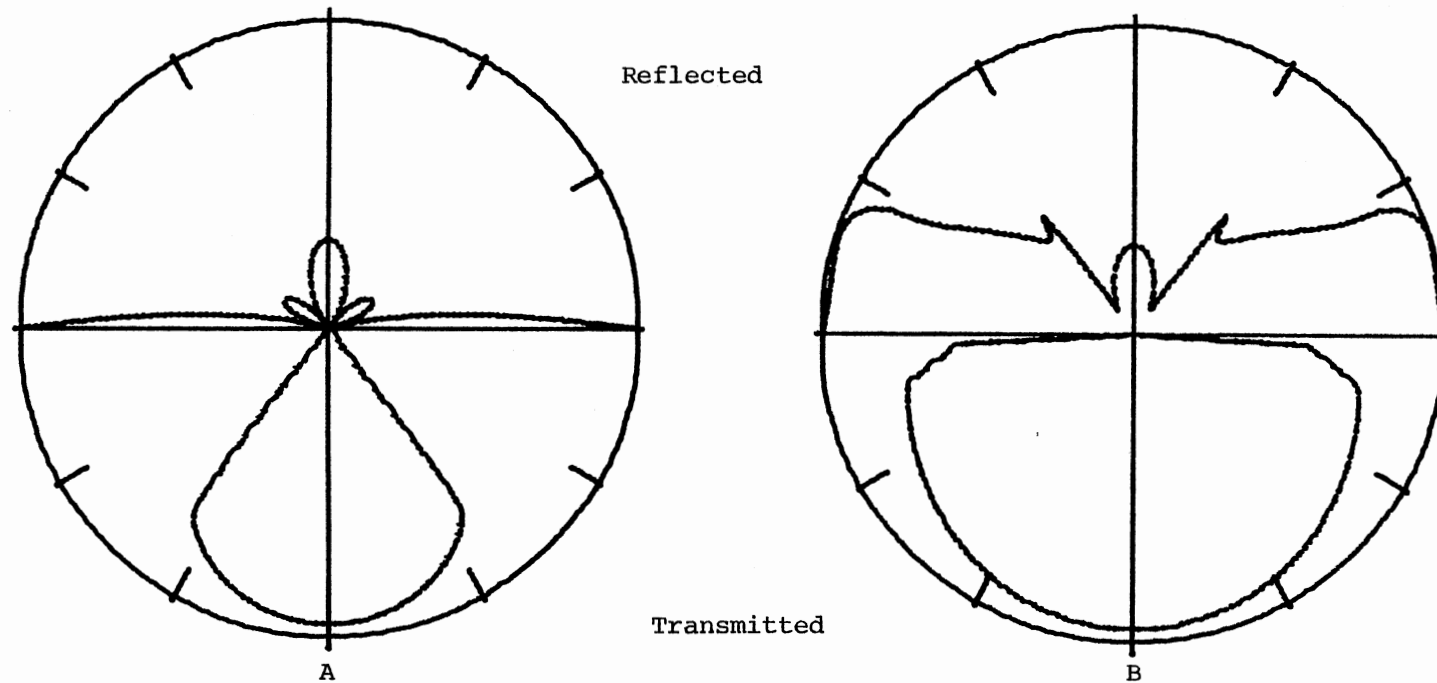


Figure 44. Polar Directivity of Reflected and Transmitted P-Wave for an Incident P-Wave on
 (A) Sandstone (Wet)/Shale Interface and (B) Shale/Sandstone (Wet) Interface

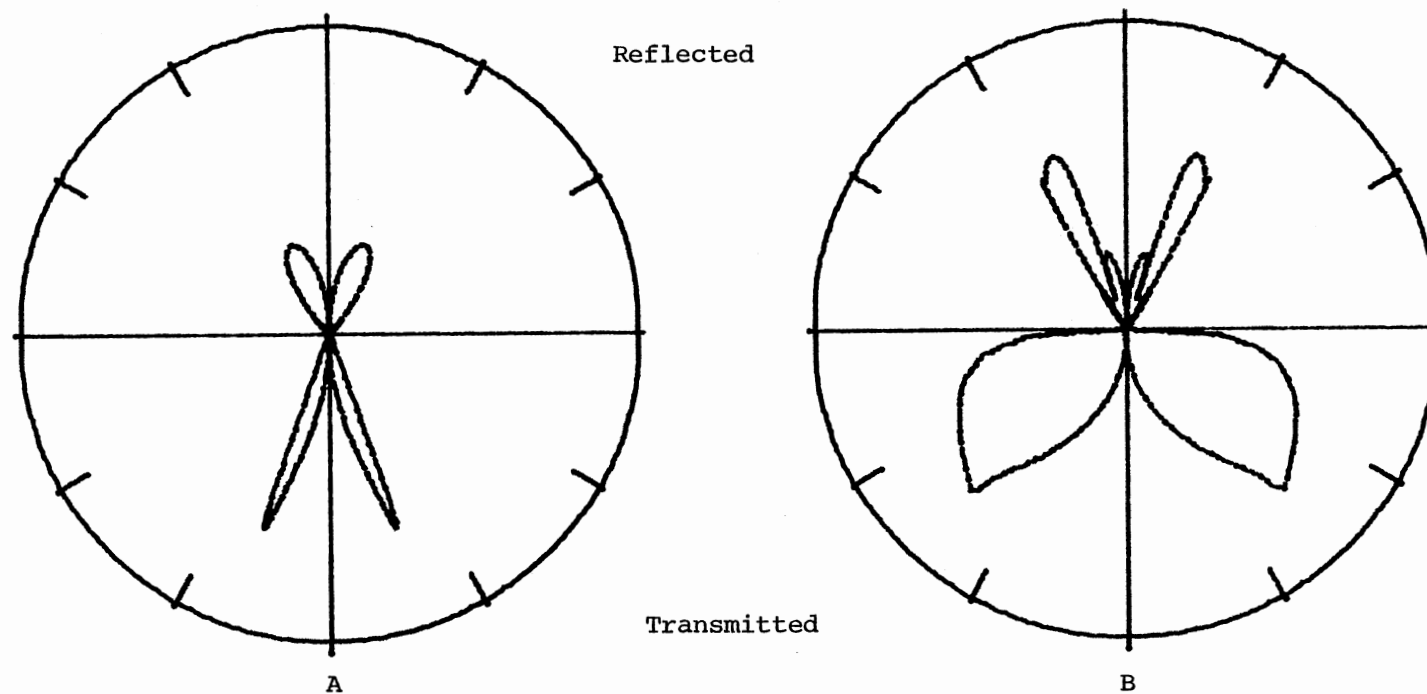


Figure 45. Polar Directivity of Reflected and Transmitted S-Wave for an Incident P-Wave on
 (A) Sandstone (Wet)/Shale Interface and (B) Shale/Sandstone (Wet) Interface

CHAPTER VI

SEISMIC DATA GATHERING METHOD AND CDP ANALYSIS

After the polar directivity of the reflected and transmitted waves is found, a further step in the analysis is considered; to apply these results to field measurements, such as common depth point (CDP) analysis. The polar plots are transformed to linear plots showing detector's response to reflected amplitudes as a function of offset; with the consideration of the spherical divergence of the amplitude as well as the polarization sensitivity of the detector. The linear plots can be compared directly with seismic measurements.

Since seismic analysis is strongly dependent on quality of data; a brief discussion of noise and noise reduction is introduced. An idea is also given about CDP gathering method, and how it is used in cancellation of multiple reflections.

The main purpose in improving the quality of seismic data is to get rid of noise which is defined as the unwanted signals that interfere with primary reflections.

Noise can be classified into two kinds. One kind is coherent or regular noise, such as surface waves and multiple reflections. The other kind is the incoherent or random noise such as scattered signals from irregularities and inhomogeneities in layers, and signals due to wind, traffic or some other sources of background noise.

Basically, there are three ways to minimize noise.

1. Developments in recording instrumentation allow frequency filtering which limits noise that has appreciable energy outside the principle frequency range of the signal. However, the spectrum of the noise often overlays the spectrum of the signal so other techniques are needed.

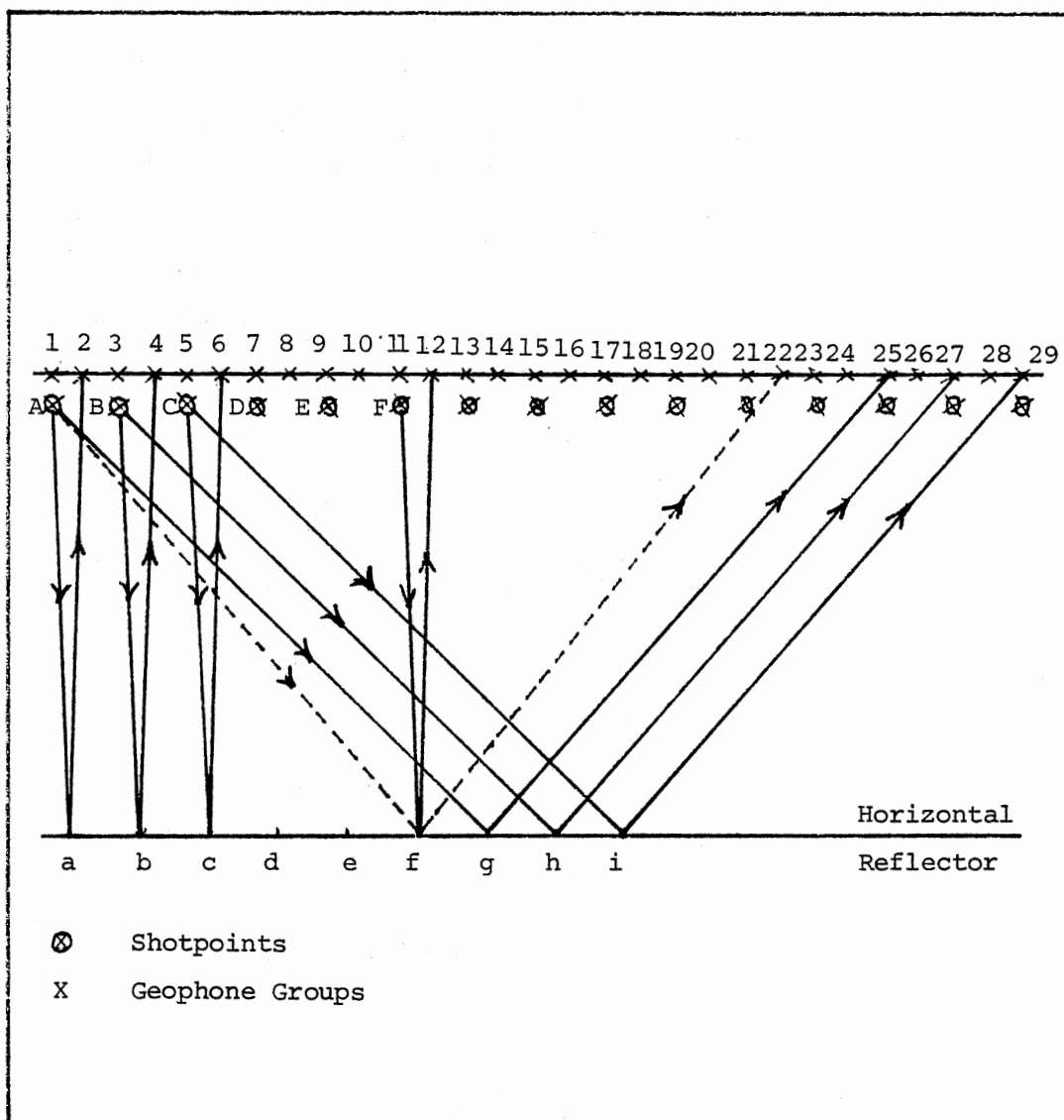
2. Set up recording arrangements that will cancel unwanted signals before they are recorded in the field. When frequency filters alone do not yield good discrimination between noise and signal then velocity discrimination is used in which multiple geophones or multiple shots are used with the proper spacing that gives the optimum cancellation; that is specially used for eliminating ground roll motion and multiple reflections.

3. Signal processing technique in which the noise is eliminated from recorded data by appropriate filtering.

Common depth point (CDP) is a seismic technique that utilizes multiple coverage of the subsurface to reduce multiple reflections. The main purpose of CDP analysis and other multi-channel techniques is to improve the signal-to-noise ratio of seismic signals. Common-depth-point shotting is illustrated in Figure 46.

We have equally spaced geophone groups which are numbered by their sequence along the seismic line instead of the trace which they represent on the seismic record. Geophone groups 1 to 24 are connected to the amplifier inputs in the recording truck and shot A is fired. If a horizontal surface is assumed, geophone 1 will record the reflection due to point a, and geophone 24 will record reflection due to geophone g. So that results in a subsurface coverage from a to g.

Geophone groups from 3 to 26 are then connected to the amplifier inputs and shot B is fired that results in a subsurface coverage from b



Source: W. M. Telford, L. P. Geldart, R. E. Sheriff and D. A. Keys,
 Applied Geophysics: New York, Cambridge University Press
 (1976), p. 302.

Figure 46. Common-Depth-Point Shooting

to h. Next, shotpoint C is fired into geophones 5 to 28 results in a coverage from C to i and so on down the seismic line. Noting that point f is the reflection point for the energy coming from shot A into geophone group 21, also it is the reflection point for energy coming from shot B into geophone group 19, from C into 17, from D into 15, from E into 13, and from F into 11.

After removal of normal movement which are discussed later in this chapter, these traces will be combined (stacked) together in a subsequent data processing operation. Thus the reflecting point f is sampled six times, and the coverage is called '6-fold' recording.

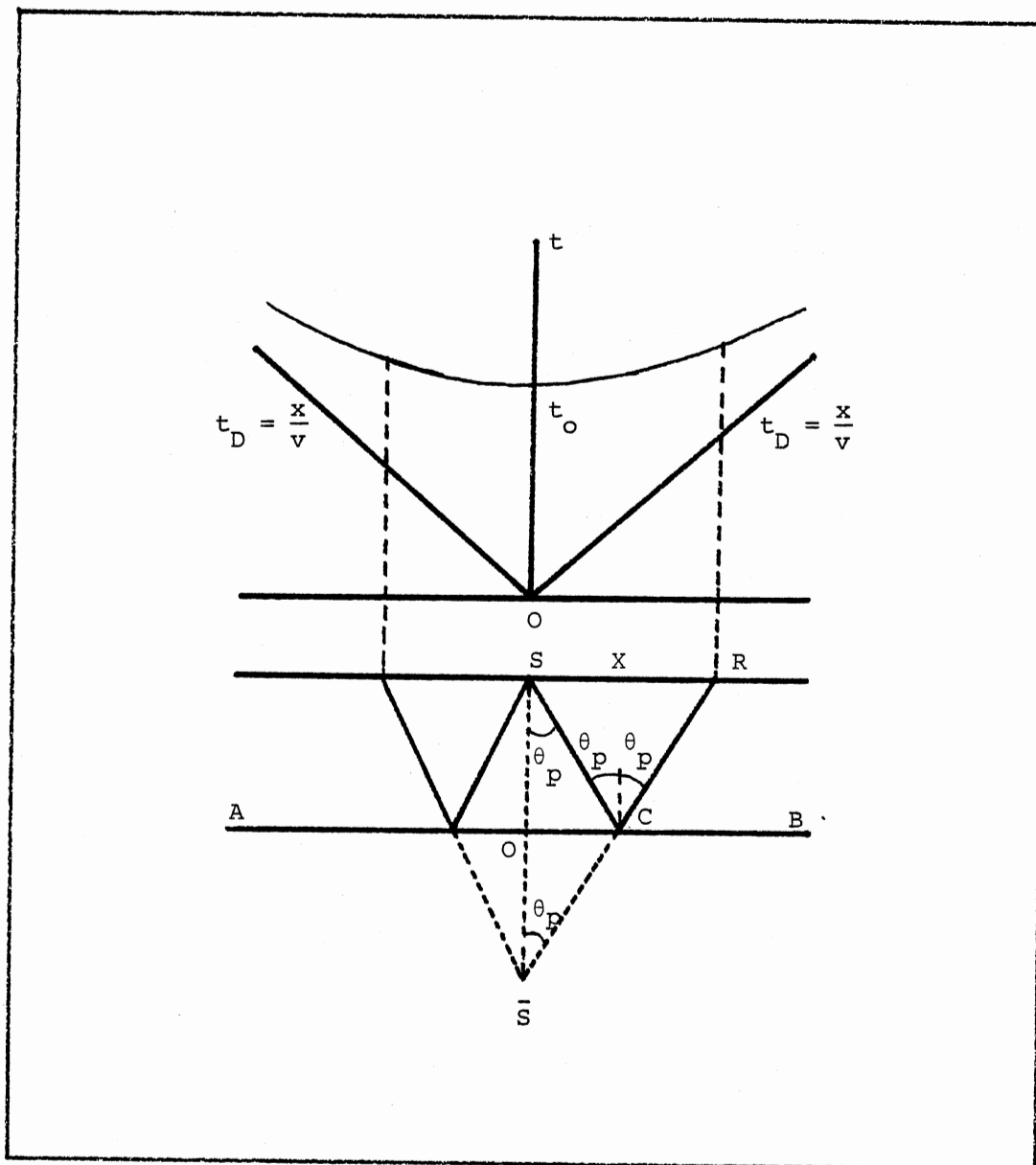
Most present-day recording uses at least 6-fold multiplicity and 12 and 24-fold multiplicity are also common, especially in marine shooting.

The Normal Moveout Correction

Normal moveout (NMO) is a term used for the extra time that a reflected signal take due to the horizontal distance from geophone to source (offset) compared with another signal that is reflected from just underneath the source; under the assumption that the reflecting surface is horizontal.

The normal moveout is easily calculated for the case of constant speed and horizontal reflecting surface, simply by referring to Figure 47.

The horizontal bed AB is at depth h below the shotpoint S. According to Snell's Law of reflection, the energy leaving S along the direction SC will be reflected along CR such that the angle of reflection equals to the angle of incidence.



Source: W. M. Telford, L. P. Geldart, R. E. Sheriff and D. A. Keys,
 Applied Geophysics: New York, Cambridge University Press
 (1976), P. 262.

Figure 47. Traveltime Curve for Horizontal Reflector

The image source \bar{S} can be located by the intersection of the extension of RC and the normal line SO. As a result the image is at the same distance below the bed as the source S is above it; keeping in mind that this is only when we are dealing with constant speed for both regions. Denoting this constant speed by V, the traveltime t for the reflected wave is $(SC + CR)/V$. However, $SC = C\bar{S}$ so that $\bar{S}R$ equals in length to the actual path SCR. Therefore $t = \bar{S}R/V$, and in terms of the offset x, we apply Pythagorean theorem to the triangle $S\bar{S}R$

$$\therefore V^2 t^2 = x^2 + 4h^2 \quad (6.1)$$

or

$$\frac{V^2 t^2}{4h^2} - \frac{x^2}{4h^2} = 1$$

which is an equation of a hyperbola with vertex at $(0, t_0)$, by substituting in the above equation for $x=0$ we have $t_0 = 2h/V$, which is the time needed for a signal reflected from point O directly below the source S. The geophone at R will also record the direct wave, so $t_D = \frac{x}{V}$ which is an equation of a straight line with slope equals the reciprocal of the velocity.

Equation (6.1) can be written as

$$\begin{aligned} t^2 &= \frac{x^2}{V^2} + \frac{4h^2}{V^2} \\ &= \frac{x^2}{V^2} + t_0^2 \end{aligned} \quad (6.2)$$

if we plot t^2 against x^2 , we obtain a straight line of slope $(1/v^2)$ and intercept t_o^2 . Then by solving for t we have

$$t = \sqrt{t_o^2 + \frac{x^2}{v^2}}$$

The normal moveout Δt_{NMO} is define by

$$\Delta t_{\text{NMO}} = t_x - t_o$$

t_x is the travel time of the reflected signal from S to R.

$$\begin{aligned} \Delta t_{\text{NMO}} &= \sqrt{t_o^2 + \frac{x^2}{v^2}} - t_o \\ &= t_o \left\{ \sqrt{1 + \frac{x^2}{t_o^2 v^2}} - 1 \right\} \end{aligned}$$

Then by using binormal expansion for the case where x is much smaller than $2h$

$$\Delta t_{\text{NMO}} = t_o \left(1 + \frac{1}{2} \frac{x^2}{(vt_o)^2} - 1 \right)$$

or

$$\Delta t_{\text{NMO}} = \frac{x^2}{2t_o v^2}$$

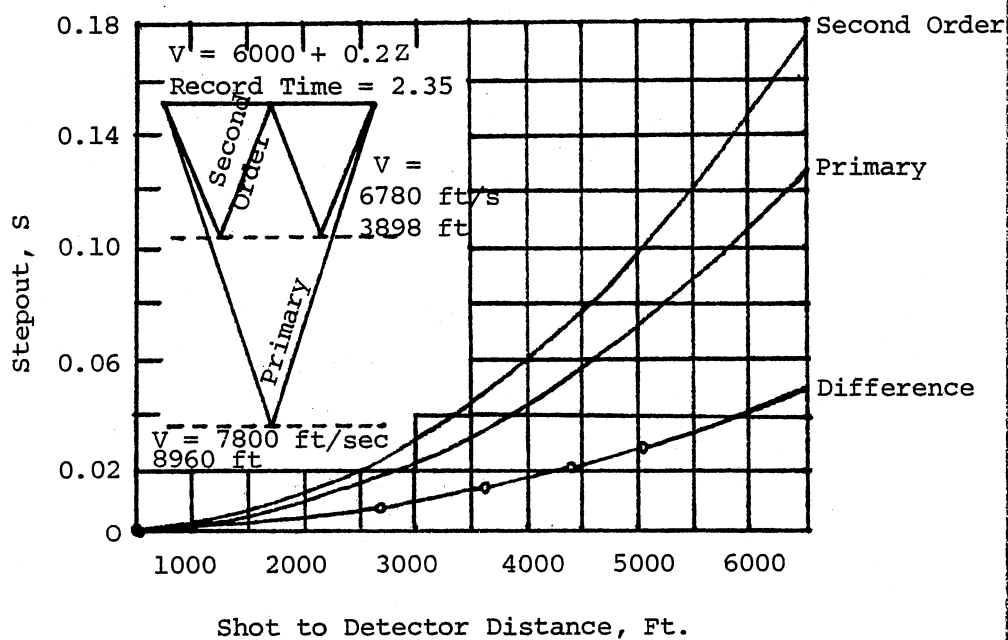
so we note that the normal moveout increases as the square of the offset x .

As we mentioned before, normal moveout must be eliminated before stacking (adding together) common-depth-point records.

Cancellation of Multiple Reflections by CDP Processing

Figure 48 illustrates a rather typical example, assuming that the shot and the near-surface velocity contrast generating the multiples are at the same level. A hypothetical velocity that increases with depth is assumed. Since the travel path of the multiple is confined to a lower velocity zone, it will exhibit the stepout shown by the upper curve of Figure 48. The deep primary reflection will follow the stepout shown in the middle curve. The lower curve shows the difference in stepout, showing the delay time of the multiple reflection from the primary one. Hence, if a number of channels with different shotpoint-to-detector distances are combined so that the primaries are in coincidence, the multiples will be out of phase as indicated by the lower curve. So, if we add traces after moveout corrections using the primary velocities, all primary reflections are in phase so they have accenuated amplitudes for such events. However, the multiples will be out of phase and they will be attenuated by adding signals for equally distributed distances. Actually, the cancellation of multiples will be more complete if the shot geophone distances were such as to allow equal time intervals between successive samples along the difference curve. The estimated distances required for a five-unit pattern array are indicated in Figure 48 by circled points numbered one through five on the lower curve.

In CDP analysis we used the image method, and we assumed that the results are identical if we let the image act as a source of spherically



Source: W. H. Mayne, "Common Reflection Point Horizontal Data Stacking Techniques," Geophysics, XXVII (1962), PP. 952-965.

Figure 48. Cancellation of Multiple Reflections by CDP Processing

symmetric radiation.

As far as the velocity analysis; by which geometric information about the subsurface structure is achieved, that assumption was valid. However, due to mode conversion, the reflected waves are not spherically symmetric, about the reflecting point, instead they have some certain directivity; so that assumption is not valid for amplitude analysis.

To be more realistic there are three different angular distributions that govern the final recorded amplitude.

1. The directivity pattern of the source itself. It is not spherically symmetric, but has some favorable directions.
2. The directivity pattern of the reflected waves, which is governed by the relative acoustic parameters of the two media.
3. The directivity pattern of the geophones which also have some favorable directions. In fact, most of geophones are sensitive to normal component of ground motion which depends on the offset of the geophones.

For simplicity we assume that the source generates spherical waves without any directivity pattern, and we consider two cases for the geophones:

- a) The land surveying case, where geophones are sensitive to the normal direction of ground motion.
- b) The marine surveying case, where hydrophones are equally sensitive to fluid pressure in all directions.

So we are left with the directivity $f(\theta)$ of the reflected waves, beside the $\frac{1}{r}$ spherical divergence of the spherical wave amplitude; where r is the traveling distance of the wave from source to the geophone.

- a) For land surveying a spherical p-wave is generated from a source S at a distance x from O , and a geophone G , which is sensitive to normal

displacement of ground motion, is detecting the reflected wave from a bed at point Q, which is at a distance h below O as shown in Figure 49.

i) The p-wave is reflected according to Snell's Law with an angle θ_p equals to the angle of incidence, and hence G is at distance x_p equals to x. The normal component of the reflected p-wave amplitude is

$$\begin{aligned} A_{Y_p}(x_p, \theta_p) &= A(x_p, \theta_p) \sin \theta_p \\ &= \frac{A_o}{2r_p} f_p(\theta_p) \sin \theta_p; \end{aligned}$$

The original amplitude of the spherical wave is A_o and $f_p(\theta_p)$ is the angular distribution of the reflected p-wave due to mode conversion at point Q, or

$$A_{Y_p}(x_p, \theta_p) = \frac{A_o}{2(h^2 + x_p^2)^{1/2}} \frac{h}{(h^2 + x_p^2)^{1/2}} f_p(\theta_p)$$

or

$$\begin{aligned} A_{Y_p} &= \frac{h}{2(h^2 + x_p^2)} f_p(\theta_p) A_o \\ &= \frac{A_o}{2h} \frac{1}{[1 + (x_p/h)^2]} f_p(\theta_p) \end{aligned}$$

or normalized to a total reflection for a source just above Q with the same height h.

$$A_{Y_o} = \frac{A_o}{2h}$$

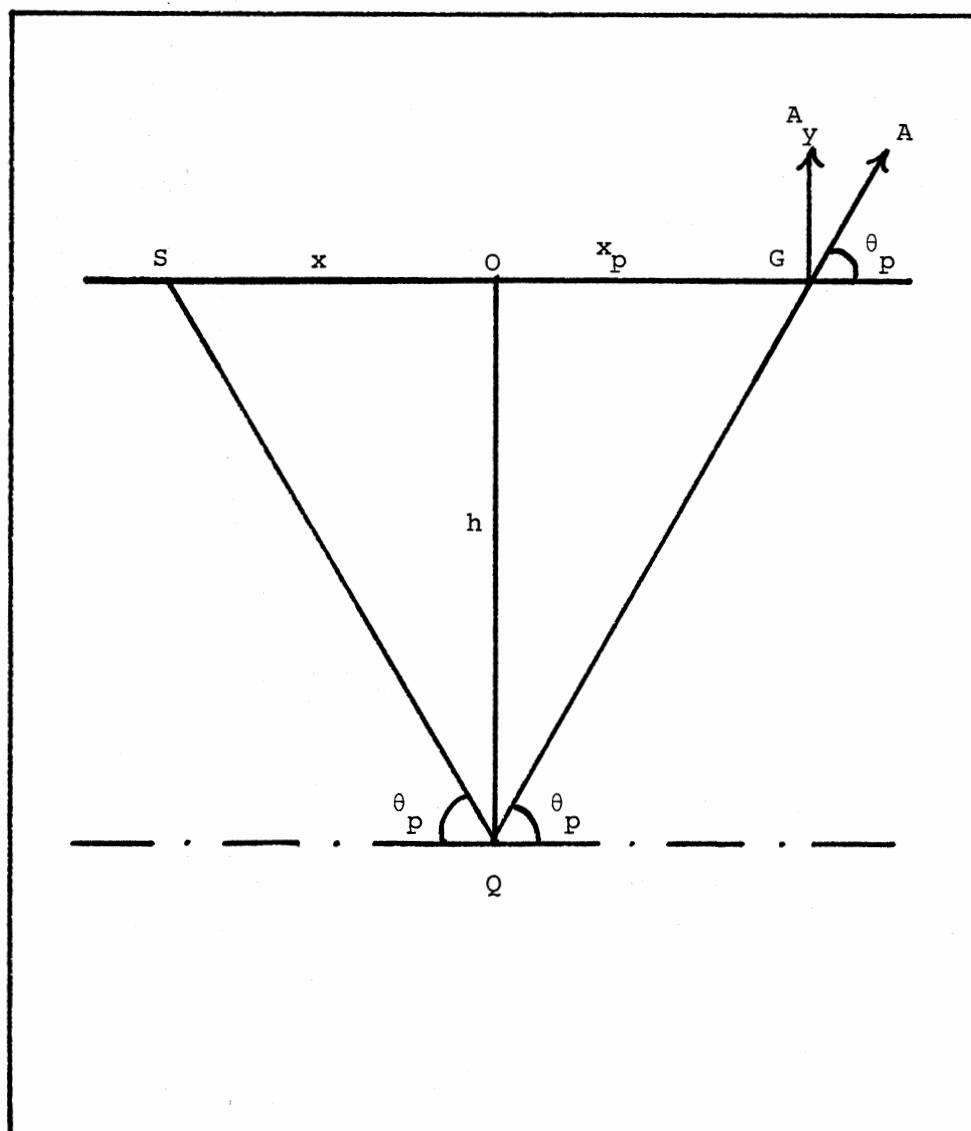


Figure 49. Geophone Response to Reflected P-Wave

$$\therefore \frac{A_y}{A_{y_0}} = \frac{1}{[1 + (x_p/h)^2]} f_p(\theta_p)$$

ii) The S-wave is reflected with an angle θ_s , so G is at a distance x_s less than x . The normal displacement of the reflected S-wave is

$$B_y(x_s, \theta_s) = B(x_s, \theta_s) \cos \theta_s$$

Since the displacement of the shear wave is transverse to the direction of propagation as in Figure 50, where $B(x_s, \theta_s) = \frac{B_0}{r} f_s(\theta_s)$; $f_s(\theta_s)$ is the directivity of the reflected S-wave at point Q.

$$\begin{aligned} \therefore B_y &= \frac{B_0}{r} f_s(\theta) \cos \theta \\ &= \frac{B_0}{(x_s^2 + h^2)^{1/2}} f_s(\theta_s) \frac{x_s}{(x_s^2 + h^2)^{1/2}} \\ &= \frac{B_0}{h} \frac{x_s}{[1 + (x_s/h)^2]} f_s(\theta_s) \end{aligned}$$

or normalized to $\frac{B_0}{h}$

$$\therefore \frac{B_y}{(B_0/h)} = \frac{x_s}{[1 + (x_s/h)^2]} f_s(\theta_s)$$

Noting that we have separated the analysis for p-wave and s-wave sense they can be detected separately due to the fact that they have different velocities and hence arrive at different times.

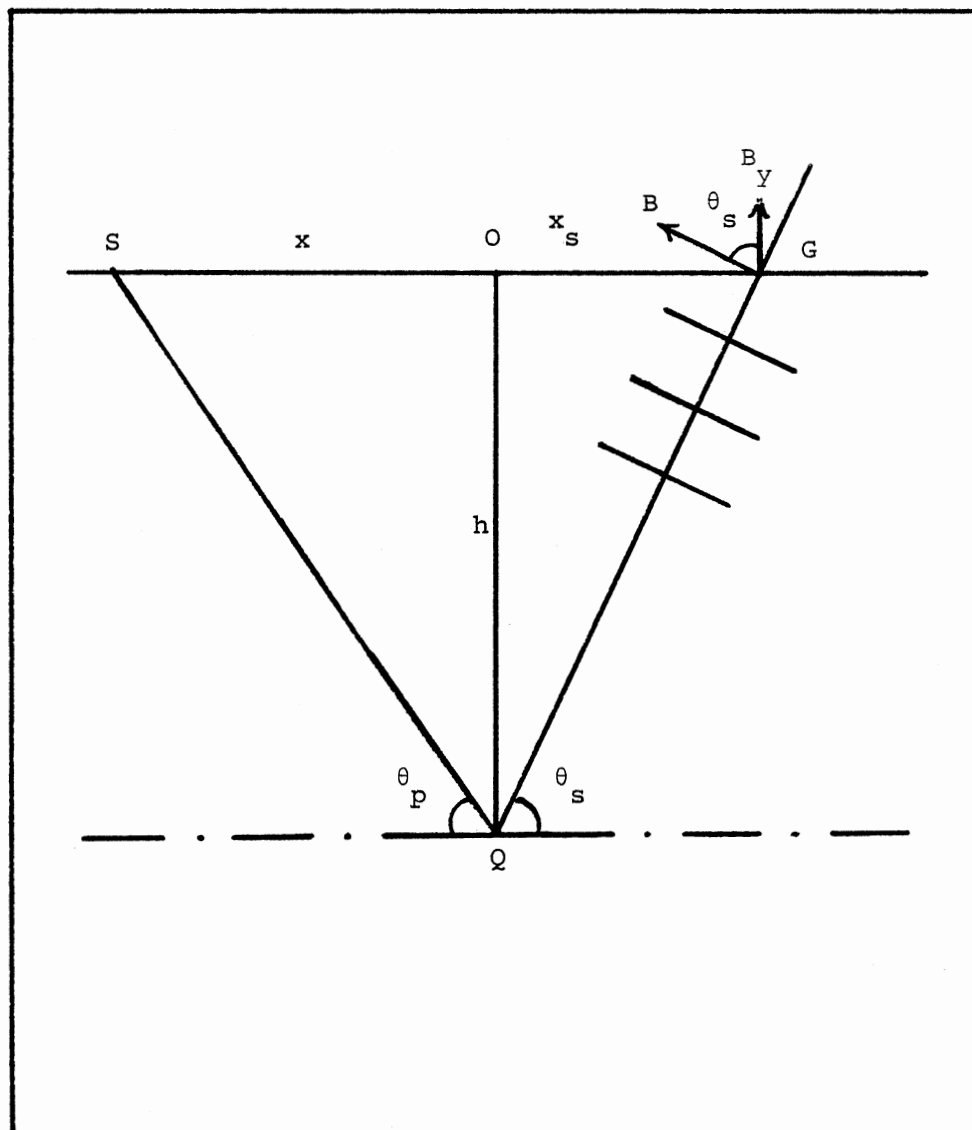


Figure 50. Geophone Response to Reflected S-Wave

b) For marine surveying consider a spherical p-wave generated from a source S at a distance x from O, and a hydrophone H, which is sensitive to fluid pressure equally in all directions, detecting the reflected p-wave from a bed at point Q. This point is at a distance h below O as shown in Figure 51.

The amplitude of the reflected p-wave is

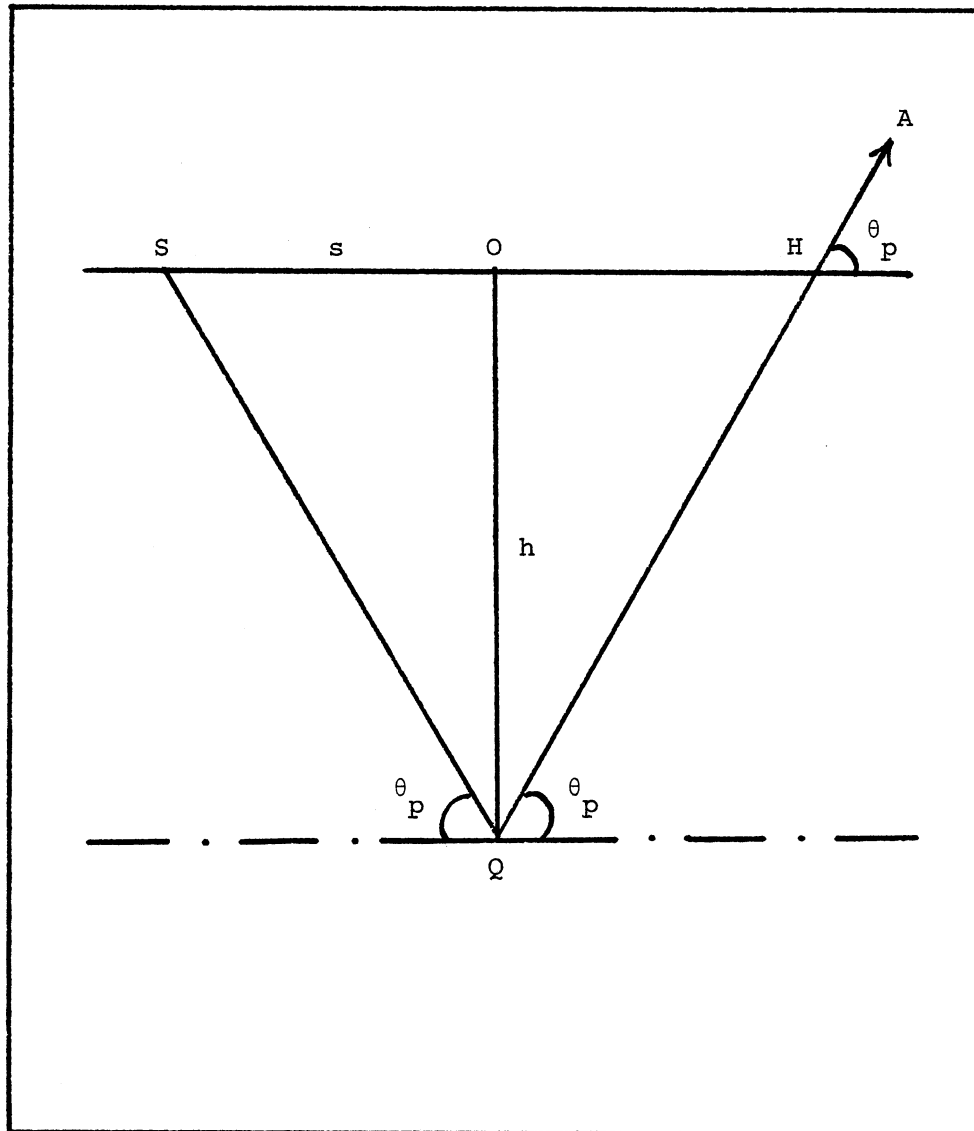
$$\begin{aligned} A_{(x_p)} &= \frac{A_o}{2r} f_p(\theta_p) \\ &= \frac{A_o}{2h} \frac{1}{[1 + (x_p/h)^2]^{1/2}} f_p(\theta_p) \end{aligned}$$

or normalized to $A_o/2h$

$$\frac{A}{(A_o/2h)} = \frac{1}{[1 + (x/h)^2]^{1/2}} f_p(\theta)$$

Acoustic Impedance and CDP Gathers

Separating the reflected p-wave from the reflected s-wave and normalizing each with its maximum amplitude leads to a plot displaying the CDP gather amplitudes as a function of offset. This curve has valuable information about the characteristic of the physical properties of the interface. The general behavior of this curve reflects the $(1/r)$ divergence of the spherical wave amplitude and the polarization sensitivity of the receiver beside the directivity pattern of the reflected wave. Hydrophone response of the reflected p-wave from fluid/solid interface is shown for air/sandstone in Figure 52, for water/sandstone in



Figuer 51. Hydrophone Response to Reflected P-Wave

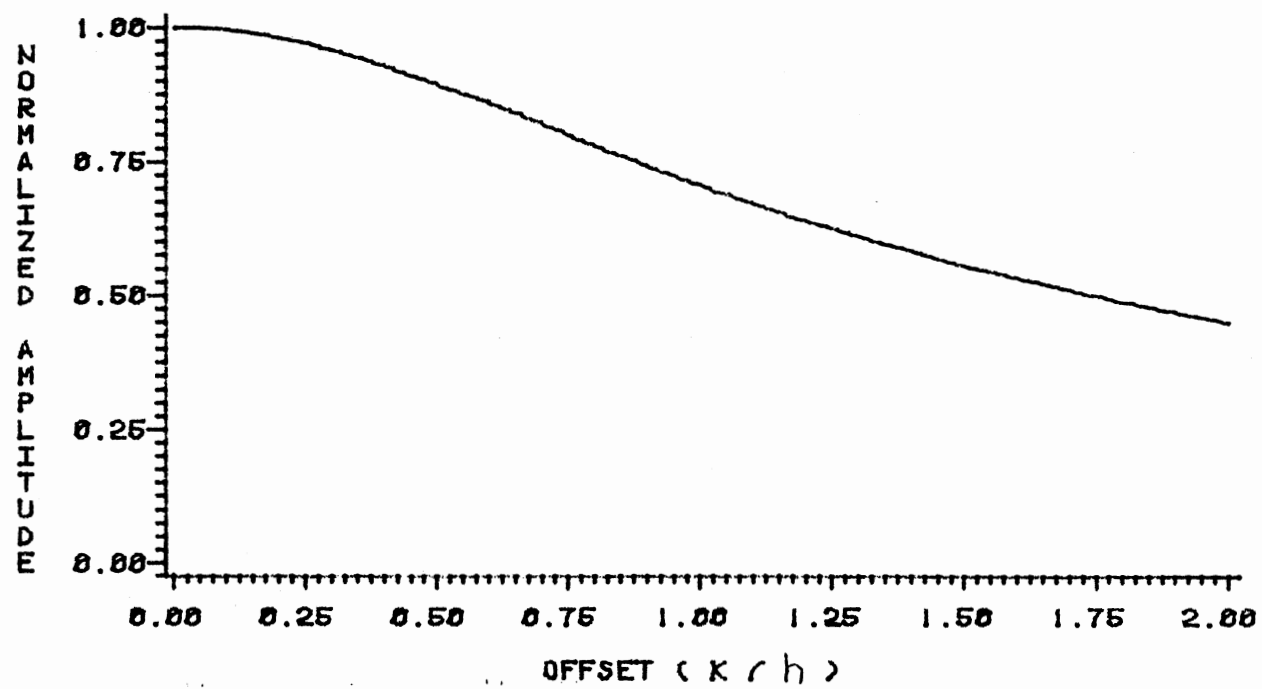


Figure 52. Hydrophone Response of a Reflected P-Wave From Air/Sandstone Interface

Figure 53, for water/limestone in Figure 54, and for water/shale in Figure 55.

The general behavior of the curve in Figure 53 reflects the $\frac{1}{r}$ divergence of the reflected wave amplitude. The offset to depth ratio is limited to 2. Beyond this direct signals and multiple reflections interfere strongly with primary reflections.

The two peaks in water/solid reflection refers to the two critical reflections at the two critical angles (p-wave and s-wave) which are discussed earlier.

Geophone response of the reflected p-wave from solid/solid interface is demonstrated for sandstone/limestone in Figure 56, for sandstone/shale in Figure 58, and for limestone/shale in Figure 60. While the geophone response of the reflected s-wave from solid/solid interface is demonstrated for sandstone/limestone in Figure 57, for sandstone/shale in Figure 59, and for limestone/shale in Figure 61.

In each case two plots are presented referring to the two ways in which a p-wave is incident at the interface. These plots show how the relative amplitudes of the reflected p-wave and s-wave depend on the acoustic properties of rock strata about a interface.

They have definite features due to mode conversion and critical reflections, which are discussed in details in the previous chapter when they were presented in the polar form.

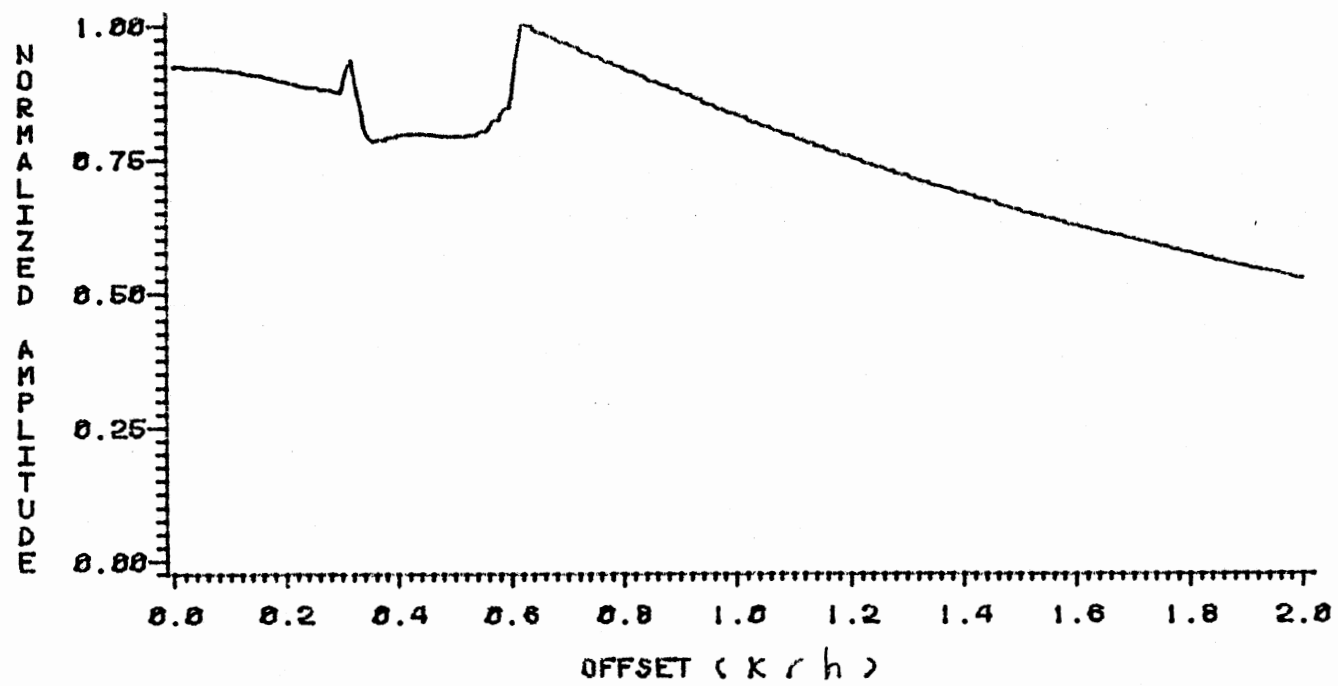


Figure 53. Hydrophone Response of a Reflected P-Wave From Water/Sandstone Interface

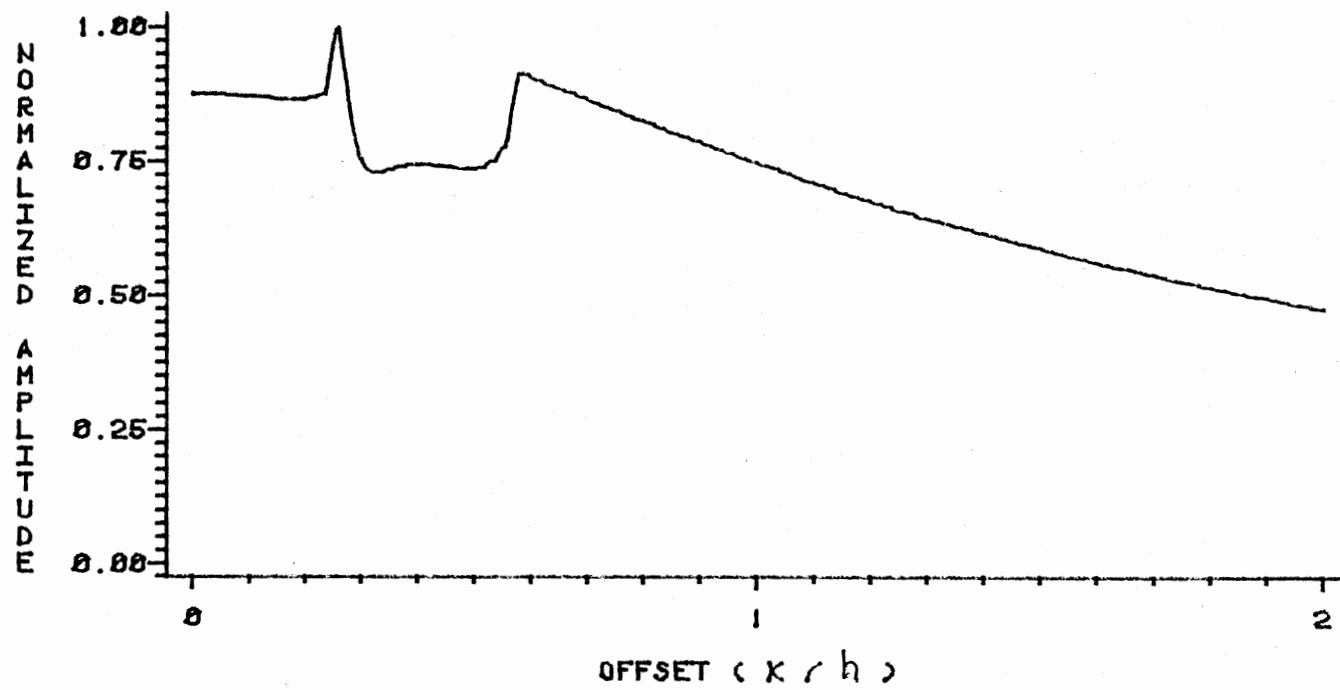


Figure 54. Hydrophone Response of a Reflected P-Wave From Water/Limestone Interface

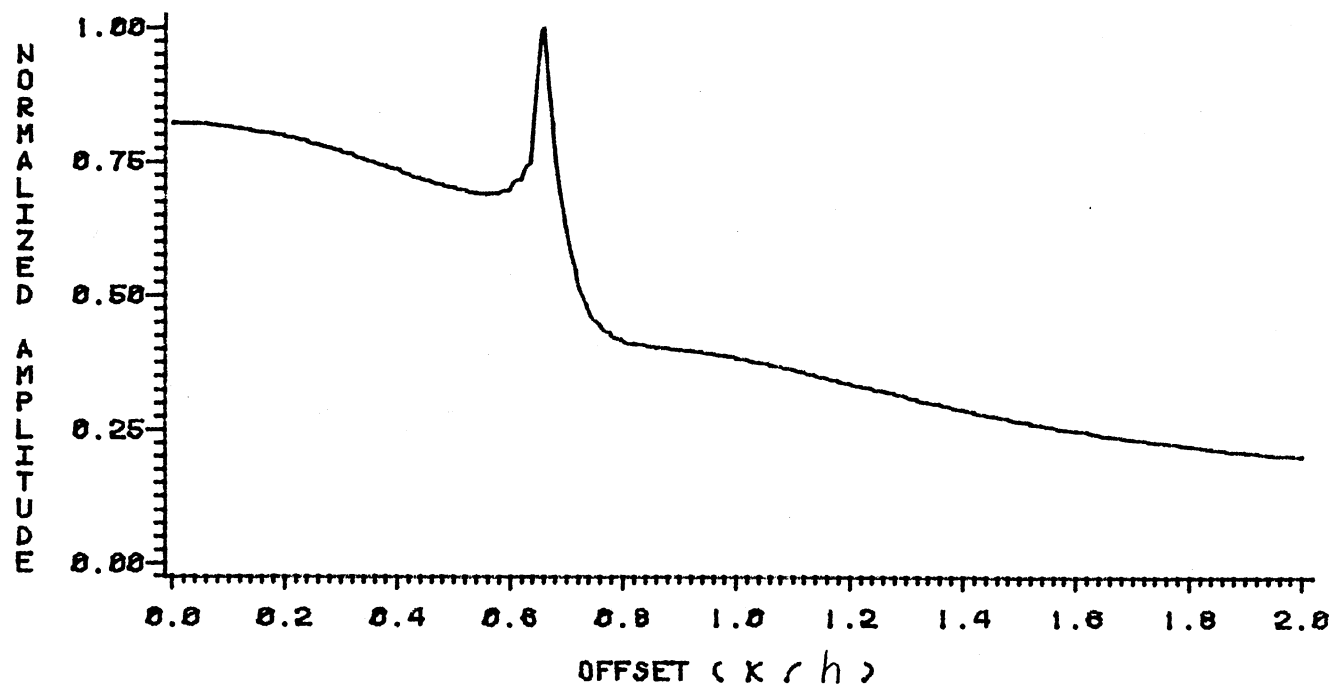


Figure 55. Hydrophone Response of a Reflected P-Wave From Water/Shale Interface

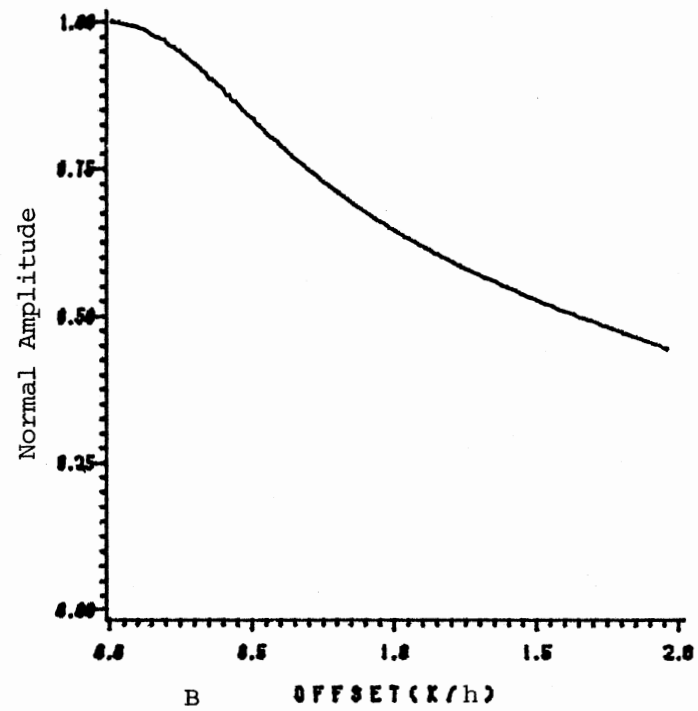
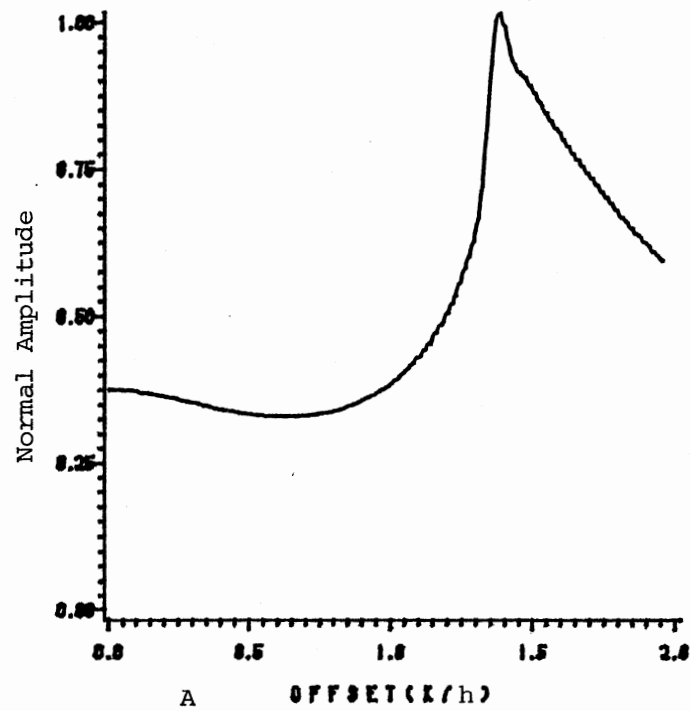


Figure 56. Geophone Response of a Reflected P-Wave for an Incident P-Wave on (A) Sandstone/Limestone Interface and (B) Limestone/Sandstone Interface

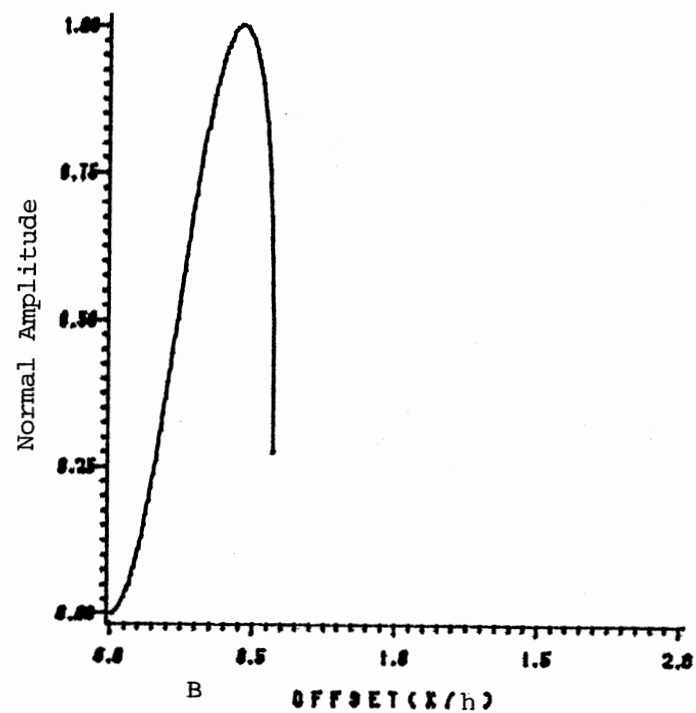
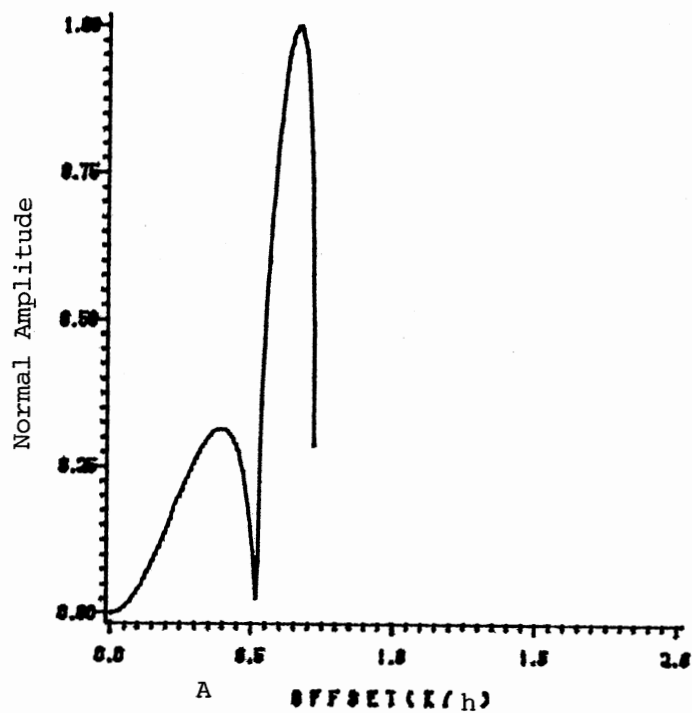


Figure 57. Geophone Response of a Reflected S-Wave for an Incident P-Wave on (A) Sandstone/Limestone Interface and (B) Limestone/Sandstone Interface

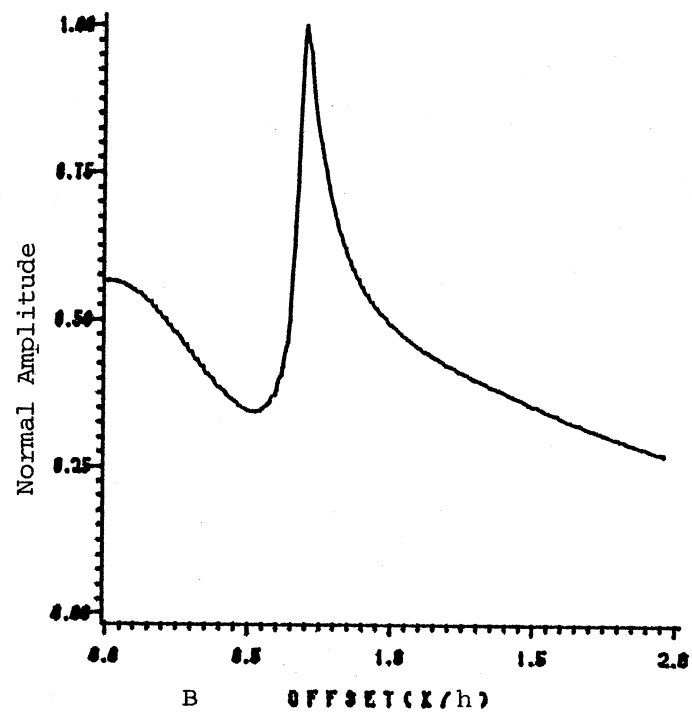
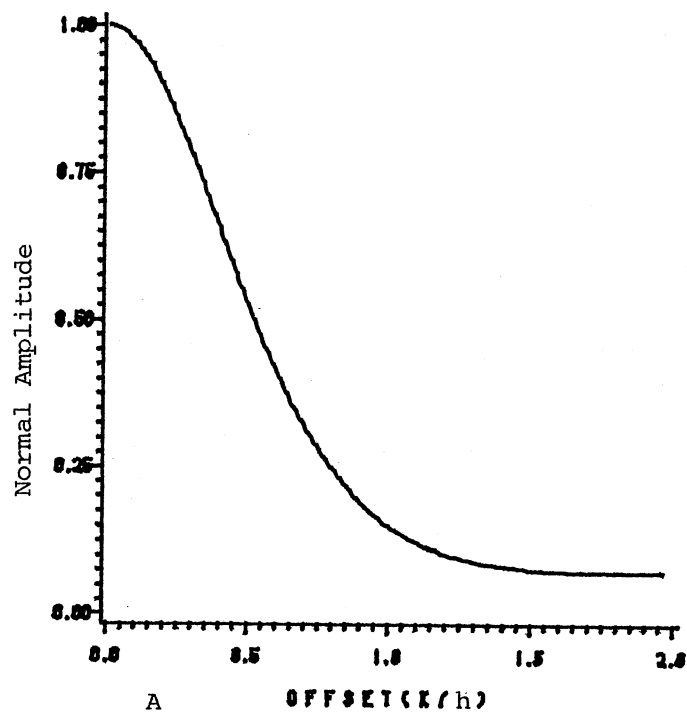


Figure 58. Geophone Response of a Reflected P-Wave for an Incident P-Wave on (A) Sandstone/Shale Interface and (B) Shale/Sandstone Interface

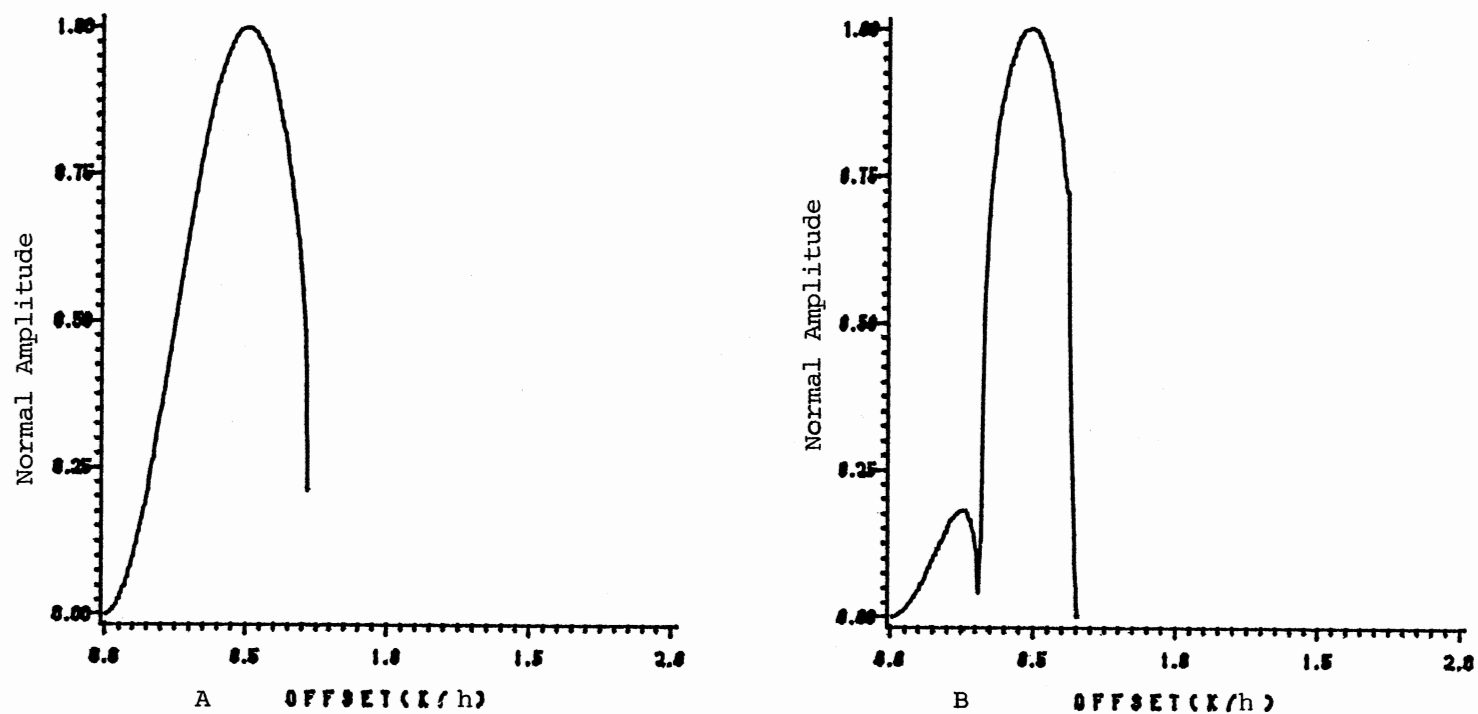


Figure 59. Geophone Response of a Reflected S-Wave for an Incident P-Wave on (A) Sandstone/Shale Interface and (B) Shale/Sandstone Interface

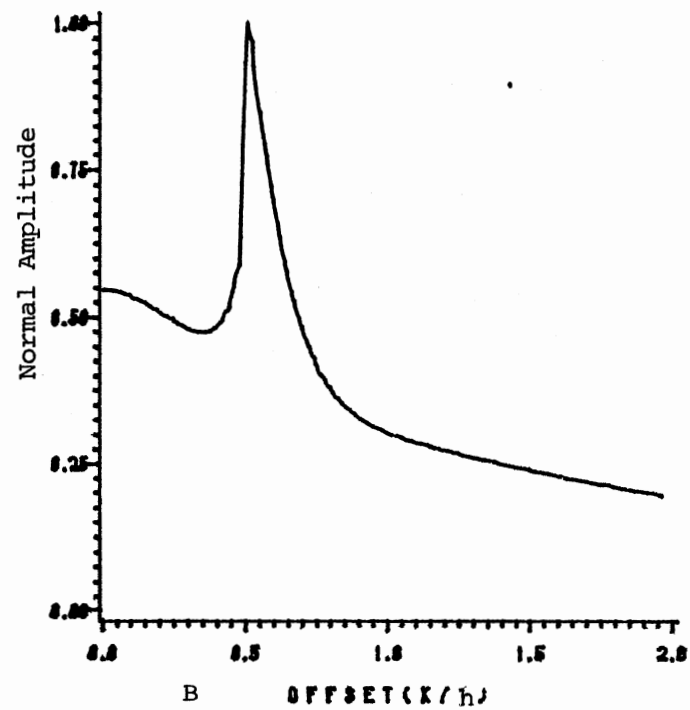
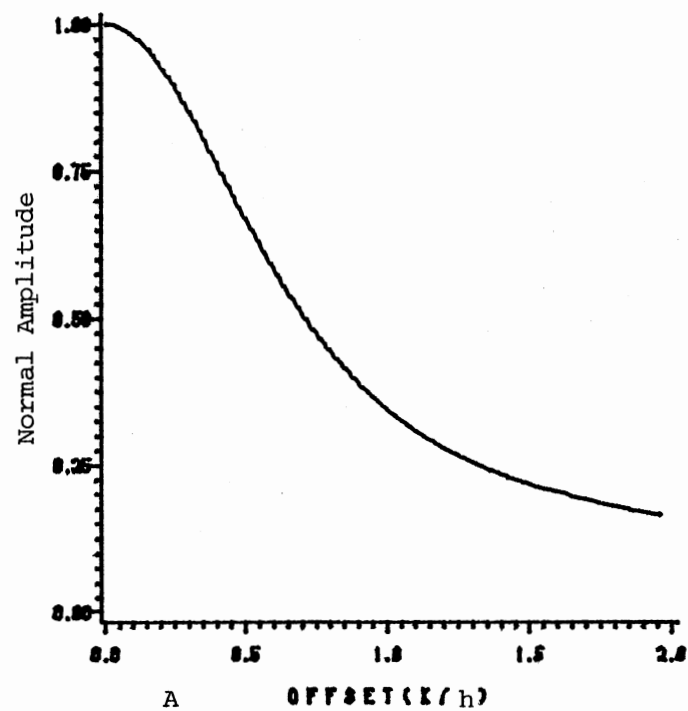


Figure 60. Geophone Response of a Reflected P-Wave for an Incident P-Wave on (A) Limestone/Shale Interface and (B) Shale/Limestone Interface

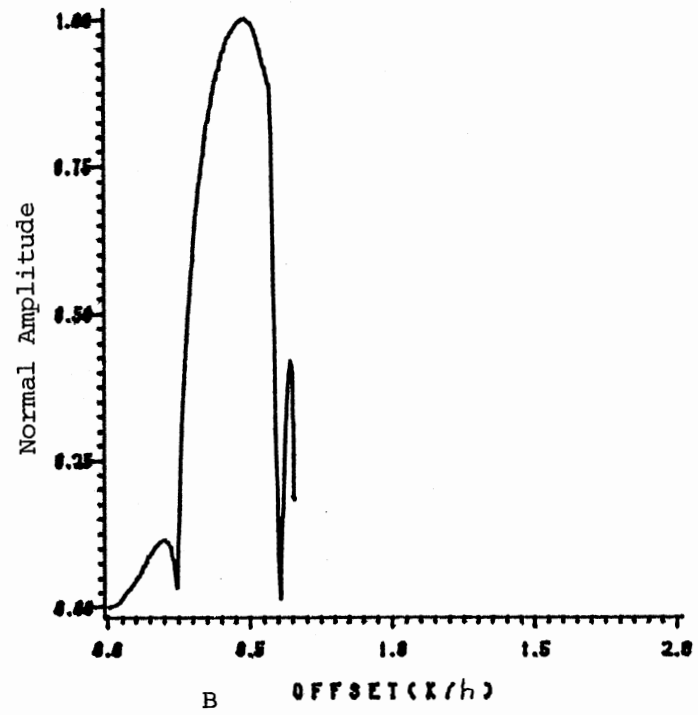
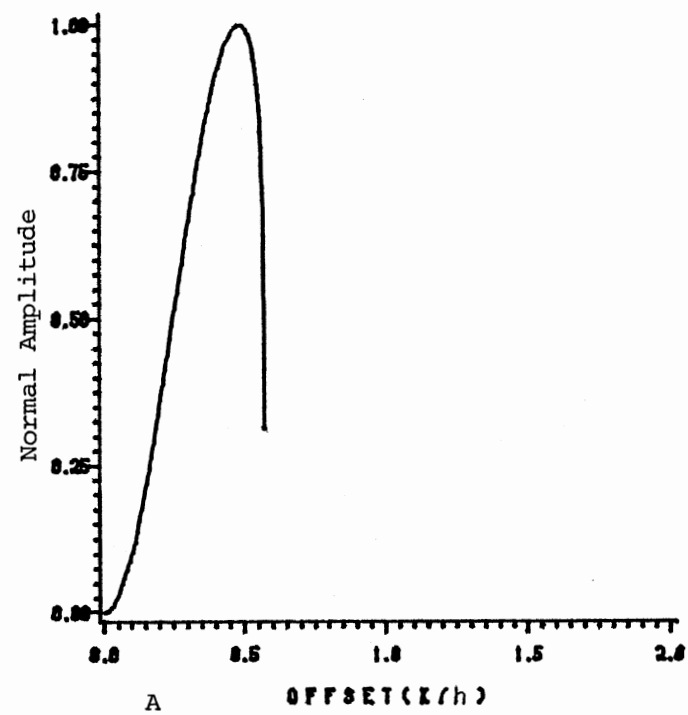


Figure 61. Geophone Response of a Reflected S-Wave for an Incident P-Wave on (A) Limestone/Shale Interface and (B) Shale/Limestone Interface

CHAPTER VII

SUMMARY AND CONCLUSIONS

Reflection of acoustic waves from plane interfaces illustrates features which are characteristic of the acoustical properties of rock strata about a certain interface. This information is contained in the relative amplitudes of the reflected waves, which has not been utilized up to this time in CDP gathering method.

The amplitudes of the reflected and transmitted waves are determined from the solution of a p-wave of unit amplitude incident on an interface of two semi-infinite media. The angular dependence of the reflected, mode converted, and transmitted waves is obtained by varying the angle of incidence from normal to grazing incidence.

There are three methods which are complementary to each other of displaying some information about the physical properties of the two media.

First, by displaying the results in polar form, these polar presentations show the directivity patterns of the reflected and transmitted plane waves. By this method the results can be recognized concisely. For the special case when we have critical angles, they provide us with definite values of the transmitted p-wave and s-wave velocities. Using the generalized Snell's Law

$$\frac{\alpha}{\cos\theta_p} = \frac{\alpha'}{\cos\theta'_p} = \frac{\beta'}{\cos\theta'_s} ,$$

at critical angles the transmitted p-wave velocity

$$\alpha' = \frac{\alpha}{\cos \theta_p^{(cp)}},$$

where $\theta_p^{(cp)}$ is the first critical angle, and the transmitted s-wave velocity

$$\beta' = \frac{\alpha}{\cos \theta_p^{(cs)}},$$

where $\theta_p^{(cs)}$ is the second critical angle. The incident p-wave velocity can be found by knowing its time of flight.

Second, by plotting the relative amplitudes which are detected by geophones or hydrophones as a function of offset of the receiver. A curve is obtained for each reflected wave, which vary significantly, due to mode conversion and total reflection, as we vary the physical properties (velocities and densities) of either side of the interface.

The general behavior of the offset curve reflects both the $(1/r)$ decrease in amplitude and the polarization sensitivity of the receiver. If the incident p-wave velocity is less than the transmitted p-wave velocity, a sharp peak is recognized showing the first critical reflection. This peak gets closer to the normal as the relative velocity of transmitted p-wave to the incident one is increased.

If the incident p-wave velocity is less than the transmitted s-wave velocity, two peaks are recognized showing the two critical reflections. These peaks also get closer to the normal as the velocities of the transmitted waves are increased with respect to the incident p-wave velocity.

The relative velocity affects the general behavior of the reflection, while the relative density affects the amount of reflection.

The mode converted s-wave with its sharp definite feature adds another dimension of knowing the acoustic properties of the two materials composing the interface. Something typical about the reflected s-wave is that it is confined to a very narrow angular region.

Third, an attempt is made to expand the directivity patterns of the reflected amplitudes as a finite expansion of some orthonormal functions, such as associated Legendre polynomials, normal Legendre functions and sinusoidal functions. The coefficients of the expansion will be dependent on the relative acoustic properties as well as the emergent angle. This method will be helpful in solving the inverse scattering problem where the relative amplitudes are known and the relative densities and velocities are needed to be found. This approach is more likely to work with non-critical cases where sharp discontinuities are avoided and fast convergence is assumed. An illustration on how to use this method is given in the Appendix. The phase shifts of the reflected waves also change sharply at critical angles where they provide a double check on the values of critical angles.

Suggestions for Further Study

This theoretical work illustrates the important information that can be extracted from the relative amplitudes of CDP gathering data. A display of the relative amplitudes as a function of offset and in a polar form, can provide a general idea about the relative acoustic properties of the reflecting surface.

The fact that a fast convergence was not achieved using Legendre

polynomials and sinusoidal functions suggests that there might be another set of orthonormal functions that will converge fast, so more theoretical work is needed to be done to solve the inverse scattering problem, and if possible to find the proper functions that will work in both critical and non-critical cases.

We limited our discussion to investigation of primary reflections and used a single image in describing the reflections. A more generalized image method should be developed to solve the more realistic problem of multiple reflections. If the time delay is involved, the multiple image method could be used to generate synthetic seismograms which could be compared directly with field measurements.

Finally, we have dealt with a horizontal interface, but when the reflecting surface is inclined, it will affect our analysis, so it may be possible to use the location of the maxima of the reflected s-wave as an indication of that inclination of the reflecting bed. This inclination or dip is a valuable parameter in petroleum exploration to indicate migration directions.

All of these methods can be integrated to give a comprehensive idea about the structure of the subsurface formation, to identify the bed rocks, and finally to locate oil or gas reservoirs.

A SELECTED BIBLIOGRAPHY

1. Carmichael, Robert S. CRC Handbook of Physical Properties of Rocks.
1st Ed. Boca Raton, Florida: CRC Press, Inc., 1982, pp. 195-200.
2. Clay, C. S. and H. McNell. "An Amplitude Study of Seismic Model."
Geophysics, 20, 4 (Oct. 1955), pp. 766-773.
3. Ergin, K. "Energy Ratio of the Seismic Waves Reflected and Refracted
at a Rock-Water Boundary." *Bulletin of the Seismological
Society of America*, 42, 4 (Oct. 1952), pp. 349-372.
4. Ewing, W. M., and W. S. Jardefzky. Elastic Waves in Layered Media.
1st Ed. New York: McGraw-Hill Book, Inc., 1957, pp. 74-81.
5. Friedlander, F. G. "On the Total Reflection of Plane Waves." *The
Quarterly Journal of Mechanics and Applied Mathematics*, 1,
(Dec. 1948), pp. 376-384.
6. Fu, C. Y. "Studies on Seismic Waves: I. Reflection and Refraction
of Plane Waves." *Geophysics*, 11, 1 (Jan. 1946), pp. 1-23.
7. Goodier, J. N., and R. E. D. Bishop. "A Note on Critical Reflec-
tions of Elastic Waves at Free Surfaces." *Journal of Applied
Physics*, 23, 1 (Jan. 1952), pp. 124-126.
8. Gutenberg, B. "The Amplitudes of Waves to be Expected in Seismic
Prospecting." *Geophysics*, 1, (July 1936), pp. 252-256.
9. Jardefzky, W. S. "Remarque on Critical Reflections of Elastic Waves
at Free Surfaces." *Journal of Applied Physics*, 23, 11 (Nov.
1952), pp. 1279-1280.
10. Jeffreys, H. "The Reflection and Refraction of Elastic Waves."
*Royal Astronomical Society, Monthly Notices, Geophysical Sup-
plement*, 1, (June 1926), pp. 321-334.
11. Knott, C. G. "Reflection and Refraction of Elastic Waves, With
Seismological Application." *Philosophical Magazine*, 48,
(July 1899), pp. 64-97.
12. Koefoed, O. "On the Effect of Poisson's Ratios of Rock Strata on
the Reflection Coefficients of Plane Waves." *Geophysical
Prospecting*, 3, (Dec. 1955), pp. 381-387.

13. Kolsky, H. Stress Waves in Solids. 1st Ed. New York: Dover Publications, Inc., 1963, pp. 1-40.
14. Love, A. E. H. The Mathematical Theory of Elasticity. 4th Ed. New York: Dover Publications, 1944, pp. 97-103.
15. Mayne, W. H. "Common Reflection Point Horizontal Data Stacking Techniques." *Geophysics*, 27, 6, Part II (Dec. 1952), pp. 927-938.
16. Muskat, M. and M. W. Meres. "Plane Waves in Elastic Media." *Geophysics*, 5, 2 (April 1940), pp. 115-148.
17. Nakil, A. M. "Wavelet Maps: A New Analysis Tool for Reflection Seismograms." *Geophysics*, 35, 3 (June 1970), pp. 447-460.
18. Richards, T. C. "Motion of the Ground on Arrival of Reflected Longitudinal and Transverse Waves at a Wide-Angle Reflection Distances." *Geophysics*, 26, 3 (June 1961), pp. 277-297.
19. Stoneley, R. "Elastic Waves at the Surface of Separation of Two Solids." *Royal Society Proceedings*, 106, (Oct. 1924), pp. 416-428.
20. Telford, W. M., L. P. Geldart, R. E. Sheriff, D. A. Keys. Applied Geophysics. 1st Ed. Cambridge: Cambridge University Press, 1976, pp. 250-304.

APPENDIX A

ORTHOGONAL EXPANSION

A set of orthogonal functions, $\{f_i(x)\}$, are used to expand a given function;

$$y(\vec{\alpha}, x) = \sum_{i=1}^{N_{\alpha}} \alpha_i f_i(x),$$

where N_{α} is the number of independent functions needed for the expansion. This orthogonal set is used to fit a tabulated data set having N_x points $(x_i, y_o(x_i))$.

Let us define a set $\{y_{oi} | i=1, 2, \dots, N_x\}$; where N_x is number of data points. Such that

$$y_o(x_1) \equiv y_{o1}, y_o(x_c) \equiv y_{o2}, \dots, y_o(x_{N_x}) = y_{oN_x}$$

For a given choice of $\vec{\alpha}$ the error between tabulated data and fitting function is defined as

$$D^2(\vec{\alpha}) = \sum_{i=1}^{N_x} \{y(\vec{\alpha}, x_i) - y_{oi}\}^2$$

Demand that $\vec{\alpha}$ chosen, $\vec{\alpha} = \vec{\alpha}_o$, so that $D^2(\vec{\alpha}_o)$ is an extremum.

$$\left. \frac{\partial D^2(\vec{\alpha})}{\partial \alpha_j} \right|_{\vec{\alpha}=\vec{\alpha}_o} = 0$$

$$\therefore \sum_{i=1}^{N_x} \{y(\vec{\alpha}, x_i) - y_{oi}\} \frac{\partial y(\vec{\alpha}, x_i)}{\partial \alpha_j} \bigg|_{\vec{\alpha}=\vec{\alpha}_o} = 0$$

$$\sum_{i=1}^{N_x} \{y(\vec{\alpha}_o, x_i)\} f_j(x_i) = \sum_{i=1}^{N_x} y_{oi} f_j(x_i)$$

or

$$\sum_{i=1}^{N_x} \left\{ \sum_{k=1}^{N_\alpha} \alpha_k f_k(x_i) \right\} f_j(x_i) = \sum_{i=1}^{N_x} y_{oi} f_j(x_i)$$

$$\sum_{k=1}^{N_\alpha} \left\{ \sum_{i=1}^{N_x} f_k(x_i) f_j(x_i) \right\} \alpha_{ok} = \sum_{i=1}^{N_x} y_{oi} f_j(x_i)$$

Define A_j and g_j as

$$A_{jk} = \sum_{i=1}^{N_x} f_k(x_i) f_j(x_i); k, j=1, 2, \dots, N_\alpha$$

$$g_j = \sum_{i=1}^{N_x} y_{oi} f_j(x_i); j=1, 2, \dots, N_\alpha$$

The above equations become

$$\sum_{k=1}^{N_\alpha} A_{jk} \alpha_{ok} = g_j$$

or in matrix notation

$$A \vec{\alpha}_o = \vec{g}$$

$$\vec{\alpha}_o = A^{-1} \vec{g}$$

Three different sets are used for the orthogonal expansion. These sets are seniosoidal functions, Legendre polynomials, and associated Legendre functions. When we used the first seven terms of any set to

fit a tabulated data set, $\{\theta_i, \xi_i(\theta_i)\}$, of the reflected p-wave amplitude as a function of the angle of incidence; the results were as follows:

1. The case, when there is no critical reflection; sinusoidal and Associated Legendre functions gave better fits than that using the Legendre polynomials.

2. When there exists some critical reflections, more terms are needed for the expansion of any set, to get acceptable fit for most data points.

3. It is very difficult, with a reasonable number of terms, to fit all data points including points at which critical reflections occur, which are of major interest for us.

4. With that many number of terms needed for the expansion to fit all cases we found it impractical to relate each term of the expansion to the relative acoustic properties of strata about the interface.

APPENDIX B

LEGENDRE POLYNOMIALS

Generating formula for the Legendre polynomials is

$$P_n(x) = \frac{1}{2^n n!} \frac{d^n}{dx^n} \{ (x^2 - 1)^n \}$$

where $x = \cos \theta$.

The first five terms of $P_n(x)$ are:

$$P_0(x) = 1$$

$$P_1(x) = x$$

$$P_2(x) = \frac{1}{2} (3x^2 - 1)$$

$$P_3(x) = \frac{1}{2} (5x^3 - 3x)$$

$$P_4(x) = \frac{1}{8} (35x^4 - 30x^2 + 3)$$

and
$$P_5(x) = \frac{1}{8} (63x^5 - 70x^3 + 5x) .$$

The Legendre Polynomials, $P_n(x)$, are orthogonal on the interval $-1 \leq x \leq 1$, that is

$$\int_{-1}^1 P_n(x) P_m(x) dx = \frac{2}{2n+1} \delta_{mn} .$$

APPENDIX C

ASSOCIATED LEGENDRE FUNCTIONS

Generating Formula:

$$P_L^m(x) = \frac{(-1)^m}{2^\ell \ell!} (1-x^2)^{m/2} \frac{d^{\ell+m}}{dx^{\ell+m}} (x^2-1)^\ell$$

where $x = \cos\theta$ and ℓ is a positive integer. The first few terms of Associated Legendre Functions are:

$$P_0^0(x) = 1$$

$$P_1^0(x) = x$$

$$P_1^1(x) = -(1-x^2)^{1/2}$$

$$P_2^0(x) = \frac{1}{2}(3x^2-1)$$

$$P_2^1(x) = -3x(1-x^2)^{1/2}$$

$$P_2^2(x) = 3(1-x^2)$$

$$P_3^0(x) = \frac{1}{2}(5x^3-3x)$$

$$P_3^1(x) = -\frac{1}{2}(1-x^2)^{1/2} (15x^2-3)$$

$$P_3^2(x) = 15x(1-x^2)$$

$$P_3^2(x) = -15(1-x^2)^{3/2}$$

For fixed m the function $P_\ell^m(x)$ forms an orthogonal set in the index ℓ on the interval $-1 \leq x \leq 1$.

$$\int_{-1}^1 P_\ell^m(x) P_{\ell'}^m(x) dx = \frac{2}{2\ell+1} \frac{(\ell+m)!}{(\ell-m)!} \delta_{\ell\ell'}$$

In general $\{P_\ell^m\}$ does not form an orthogonal set of functions. When we use them for the expansion we have to remove the degeneracy first. Lower order terms can be written as a linear combination of higher order terms in the following manner:

$$P_0^0(x) = \frac{1}{2}(2P_2^0(x) + P_2^2(x)),$$

$$P_1^0(x) = \frac{1}{6}(6P_3^0(x) + P_3^2(x)),$$

$$P_1^1(x) = \frac{1}{12}(2P_3^1(x) + P_3^3(x)).$$

When we used the first seven independent terms of Associated Legendre polynomials ($L = 2, M = 0,1,2, L = 3, m = 0,1,2,3$) we eliminated the lowest order terms ($L=0, L=1$) by using the above linear combinations.

APPENDIX D

SYMBOLS

\bar{A}	=	Vector potential field
A_i	=	Amplitude of incident p-wave
A_r	=	Amplitude of reflected p-wave
A_t	=	Amplitude of transmitted p-wave
α	=	Speed of incident p-wave
α'	=	Speed of transmitted p-wave
B_i	=	Amplitude of incident s-wave
B_r	=	Amplitude of reflected s-wave
B_t	=	Amplitude of transmitted s-wave
β	=	Speed of incident s-wave
β'	=	Speed of transmitted s-wave
C	=	Phase velocity along interface
$\delta_r^{(p)}$	=	Phase shift of reflected p-wave
$\delta_r^{(s)}$	=	Phase shift of reflected s-wave
ϵ	=	Strain
ψ	=	Scalar potential field
γ	=	Skin depth
\vec{K}_p	=	Wave vector of incident p-wave
\vec{K}'_p	=	Wave vector of transmitted p-wave
\vec{K}_s	=	Wave vector of incident s-wave

\vec{K}'_s = Wave vector of transmitted s-wave

λ = Lamé constant

ρ = Density

η_r = Square root energy of reflected s-wave

η_t = Square root energy of retransmitted s-wave

ξ_r = Square root energy of reflected p-wave

ξ_t = Square root energy of transmitted p-wave

\bar{S} = Displacement

σ = Poisson's ratio

σ_{ij} = Stress

θ_p = Incident angle of p-wave

θ'_p = Refracted angle of p-wave

$\theta_p^{(cp)}$ = Critical angle of transmitted p-wave

$\theta_p^{(cs)}$ = Critical angle of transmitted s-wave

θ_s = Incident angle of s-wave

θ'_s = Refracted angle of s-wave

μ = Shear modulus

ω = Angular frequency

Z = Acoustic impedance

VITA

Hamzah Abdulgader AlMoghrabi

Candidate for the Degree of

Master of Science

Thesis: REFLECTION AND REFRACTION OF ACOUSTIC WAVES AT A PLANE INTER-
FACE

Major Field: Physics

Biographical:

Personal Data: Born in Khulais, Hejaz, Saudi Arabia, May 13,
1955.

Education: Graduated from Al Shati High School, Jeddah, Saudi
Arabia, in May 1972; received the Bachelor of Science degree
in physics from the University of Petroleum and Minerals,
Dahran, Saudi Arabia, in May 1977; completed the requirements
for the Master of Science degree in physics at Oklahoma State
University in July 1983.

Professional Experience: Teaching Assistant, Physics and Mathe-
matics Department, College of Architecture, King Faisal Uni-
versity, 1977-1979; Research Assistant, Physics Department,
Oklahoma State University, 1983.

Professional Organizations: Member Society of Exploration Geo-
physicists, and The American Physical Society.